CHAPTER 5 ELECTROCHEMICAL PROPERTIES OF $CoCl_2(PPh_3)_2$

This chapter dwells on characterization of the synthesized $CoCl_2(PPh_3)_2$ in a mixture of acetonitrile and pentanol (1:1), using both electrochemical (cyclic voltammetry (CV) and chronoamperometry) and spectroscopic (UV-Vis and NMR spectroscopy) techniques. CV was used to identify different species formed in solution, to investigate the electrocatalytic properties of the complex $CoCl_2(PPh_3)_2$ by titration with PPh_3, for quantitative analysis, and development of internal standards. Chronoamperometry was used to determine number of electrons and physical parameters (i.e. electrochemical surface area (A) of the working electrode and diffusion coefficient of ferrocene in a mixture of acetonitrile and pentanol (1:1)). UV-Vis and NMR spectroscopy were used to characterize and investigate the electrocatalytic properties of the complex $CoCl_2(PPh_3)_2$ by titrating with PPh_3.

Typical experimental conditions of CV were as follows, unless otherwise stated:

- Platinum (Pt) and glassy carbon (GC) disks were used as working electrodes (WE).
- A mixture of acetonitrile and pentanol in a 1:1 volume ratio was used as a background solvent.
- Tetrabutyl ammonium hexafluorophospate ($TBAPF_6$) was used as a supporting electrolyte at a concentration of 0.05 M.
- An analyte concentration of 7.7×10^{-4} mol/l was employed.
- The scan rate was 50 mV/s.
- CV's were recorded starting from 0 to more positive potentials.
- Only the third (or last) CV scan was used for analysis.
- All measurements were made at room temperature.

5.1 ANODIC VOLTAMMETRIC STUDIES OF $CoCl_2(PPh_3)$

The main aim of the research project was towards on-line monitoring of cobalt organometallic compounds, using electrochemical techniques in non-aqueous solutions. Most of this organometallic compounds are very sensitive to air and moisture. First, we had to understand their electrochemical behaviour by conducting experiments in an open cell. In order to do this a cobalt organometallic compound that was stable to some extend when exposed to moisture was chosen as a model compound. $CoCl_2(PPh_3)_2$ complex was found to satisfy the above criteria. The anodic electrochemical behaviour of $CoCl_2(PPh_3)_2$ was never studied before using electrochemical techniques. Most work on this compound involved studies by polarography and inorganic techniques. A thorough study was conducted to determine the electrochemical properties of $CoCl_2(PPh_3)_2$ in batch solutions to identify species present in solution during its oxidation. We synthesized this compound and characterized it using elemental analysis and infrared spectroscopy (the results obtained are presented in Experimental Section, Chapter 3).

The anodic voltammetric study of $CoCl_2(Ph_3)_2$ was conducted in a mixture of acetonitrile and pentanol (1:1). Most electrochemical measurements are performed in non-aqueous solvents like acetonitrile, CH_2Cl_2, THF, DMF, etc. They are not normally conducted in alcohols because supporting electrolytes cannot dissolve in alcohols. Pentanol, as an alcohol, was added as one of the background solvents because there was a need to work in the presence of alcohols to become closer to industrial samples that contained alcohols. Electron transfer processes of a certain compound may differ depending on the type of working electrode (WE) material used. First we had to search for an electrode material which would allow the study of electrochemical oxidation of $CoCl_2(PPh_3)_2$ free of complications from surface interactions.

5.1.1 Examination of Different Working Electrode Materials That Could be Used for Anodic Voltammetric Studies of $CoCl_2(PPh_3)_2$

Platinum (Pt) and glassy carbon (GC) disks WE were chosen since they were the most useful and convenient materials for anodic studies. Their influence on the background current curves obtained in a mixture of acetonitrile and pentanol (1:1) were evaluated using cyclic voltammetry (CV) [Figure 5.1]. This experiment allowed us to identify any impurities present in solution, i.e. oxidation or reduction of electrolyte components or the electrode

material itself, as this can cause havoc in the interpretation of results obtained in the presence of an electroactive species. The experiment then defined the accessible potential window, in which the observable electrode reactions should yield voltammetric signals to allow analysis without interference of background contributions.

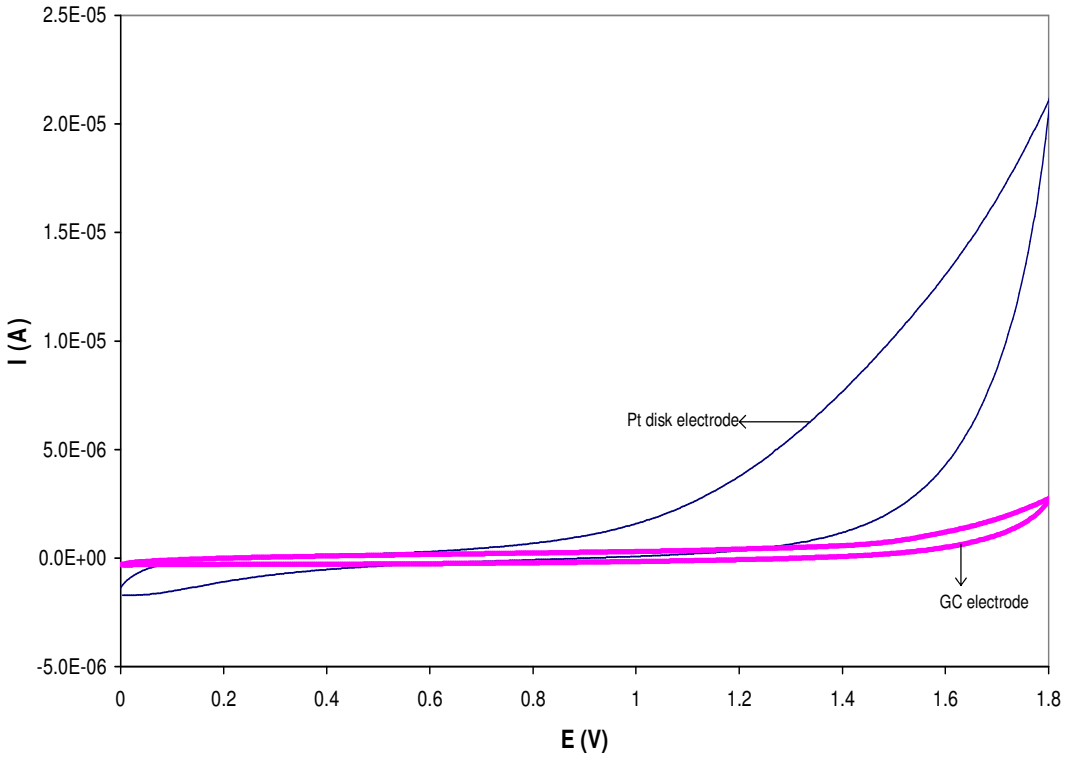

Figure 5.1 Influence of Pt and GC disk WE on the background current CV curve that defines the accessible potential window in a mixture of acetonitrile and pentanol.

The background current curve obtained at a Pt disk WE showed electrochemical activity at E above 1.2 V (Figure 5.1). An increase in background current could have arisen due to oxidation of either the solvent or the anion of the supporting electrolyte (or both) resulting in formation of one or several new compounds. $TBAPF_6$ has been used widely as a supporting electrolyte for the electrochemical studies at a Pt disk WE and it was not oxidized in various non-aqueous solvents, including acetonitrile and alcohols. This then leaves the background solvent as a possible cause of an increase in background current at high potentials above 1.2 V.

Acetonitrile (with $TBAPF_6$) undergoes electrochemical oxidation at E_p = 3.6 V (versus saturated calomel electrode (SCE)), whilst alcohols undergoes electrochemical oxidation at E_p = > 2.5 V in acetonitrile at a Pt electrode [66]. In this study a current increase was observed very early inside the potential window of the two solvents used. It must be noted that the potential window for non-aqueous solvents depends on the solvent purity and especially on the amount of traces of water [1]. It is well-known that water is the most common impurity or contaminant in non-aqueous solvents. Therefore, an increase in background current at potentials above 1.2 V might have arisen due to oxygen evolution from traces of water present. Traces of water were always present in the solvents used even after purification since a simple distillation procedure was conducted (see Experimental Section, Chapter 3).

Gold [66] demonstrated that on raising the potential in solutions containing acetate in aqueous solutions on a Pt electrode, PtO and adsorbed oxygen began to cover the surface and oxygen evolution took place in the range between 1.2 – 1.8 V. A further increase in the potential brought about a change in the oxide composition to a higher oxide (PtO_2) [66]. He also found that a similar surface modification of platinum took place in non-aqueous solvents that favour surface oxide formation, considering the fact that water is easily present at the 1 mM level in such solvents [66]. Therefore, the accessible potential window in this study, in a mixture of acetonitrile and pentanol (1:1) at a Pt disk WE was determined in the positive potential to be from 0 to + 1.2 V.

To prove that an increase in background current at more positive potentials arisen due to traces of moisture present in the background solvents, we compared the background curves that contained different amounts of water after distillation (Figure 5.2). We found the shape and the increase in current of the background curves to depend on the amount of water present.

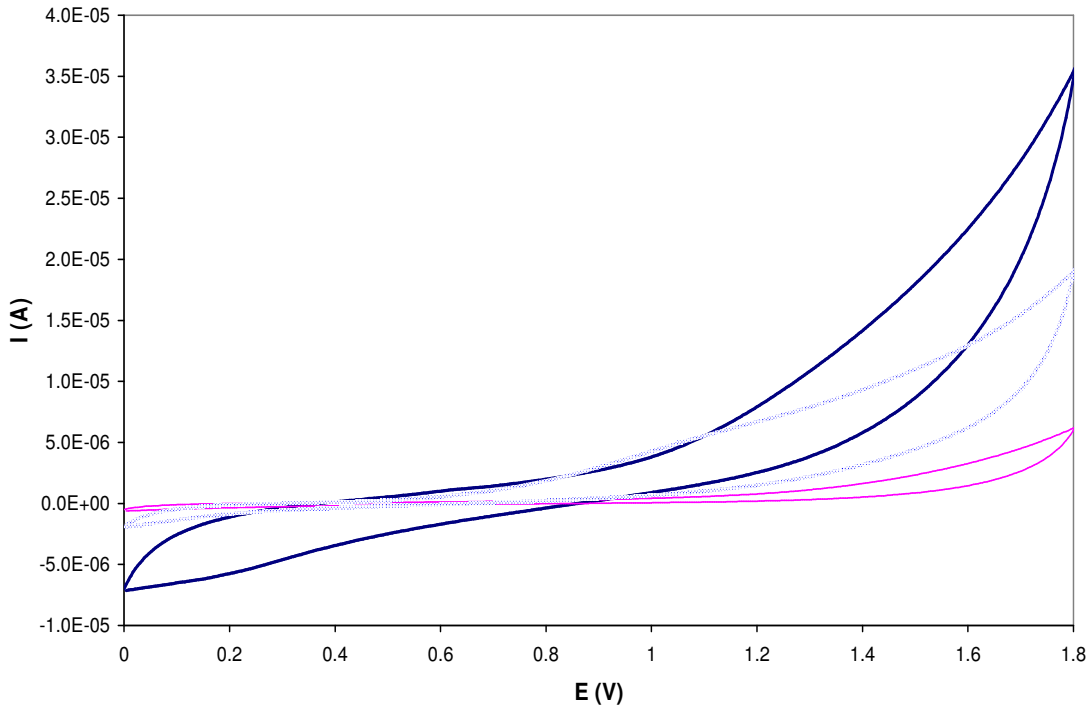

Figure 5.2 Influence of moisture on the background current CV curves obtained at a Pt disk WE. The amounts of water present were as follows: 210 (—), 455.5 (….) and 895.3 (—) ppm.

The background curve obtained at a GC disk WE on the other hand displayed a wide region (between 0 and + 1.8 V) in which 'no' current flowed through the electrolyte solution, except for a very minute residual current due mostly to non-faradaic processes (i.e. processes not involving electrochemical transformations) [Figure 5.1]. This means none of the possible reactants in the system, i.e. the solvent molecule or the anion of the supporting electrolyte is electroactive at this potential range. From these results we decided that GC disk will be a suitable WE material to be used for the analysis of $CoCl_2(PPh_3)_2$ in a mixture of acetonitrile and pentanol (1:1) that contained traces of water.

CV of $CoCl_2(PPh_3)_2$ at a GC disk WE is shown in Figure 5.3. CV of $CoCl_2(PPh_3)_2$ revealed two well-defined oxidation peaks labelled peak 1(a) at E_p = 0.85 V and peak 2(a) at E_p = 1.20 V which had a coupled reduction peak 3(a) at E_p = 1.0 V in the reverse scan, when the potential is switched at 1.5 V (Figure 5.3, dotted-line curve). On repeating the scan and increasing the switching potential to more positive (E_λ = 1.9 V), oxidation peak 1(a) shifted to more positive potential (peak 1(b)), peak 2(a) flattened, and the overall background current increased tremendously at more positive potentials (Figure 5.3, solid-line curve).

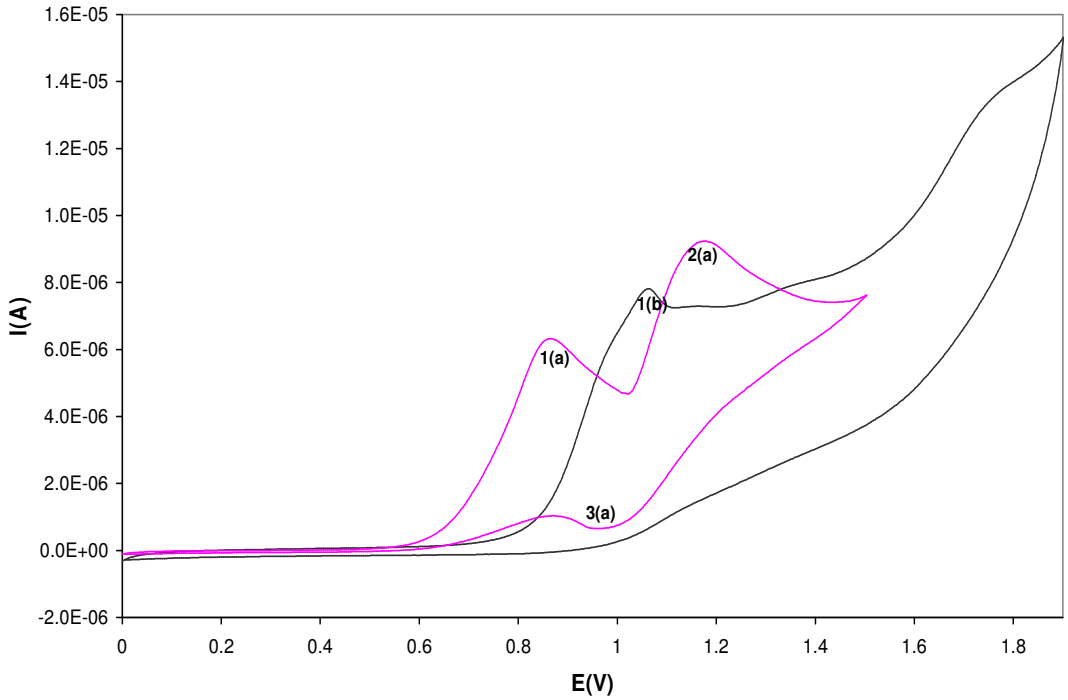

Figure 5.3 CV curves obtained in solutions containing $CoCl_2(PPh_3)_2$ at a GC disk WE at a potential range (a) 0 to 1.15 V (—) and (b) 0 to 1.9 V (—).

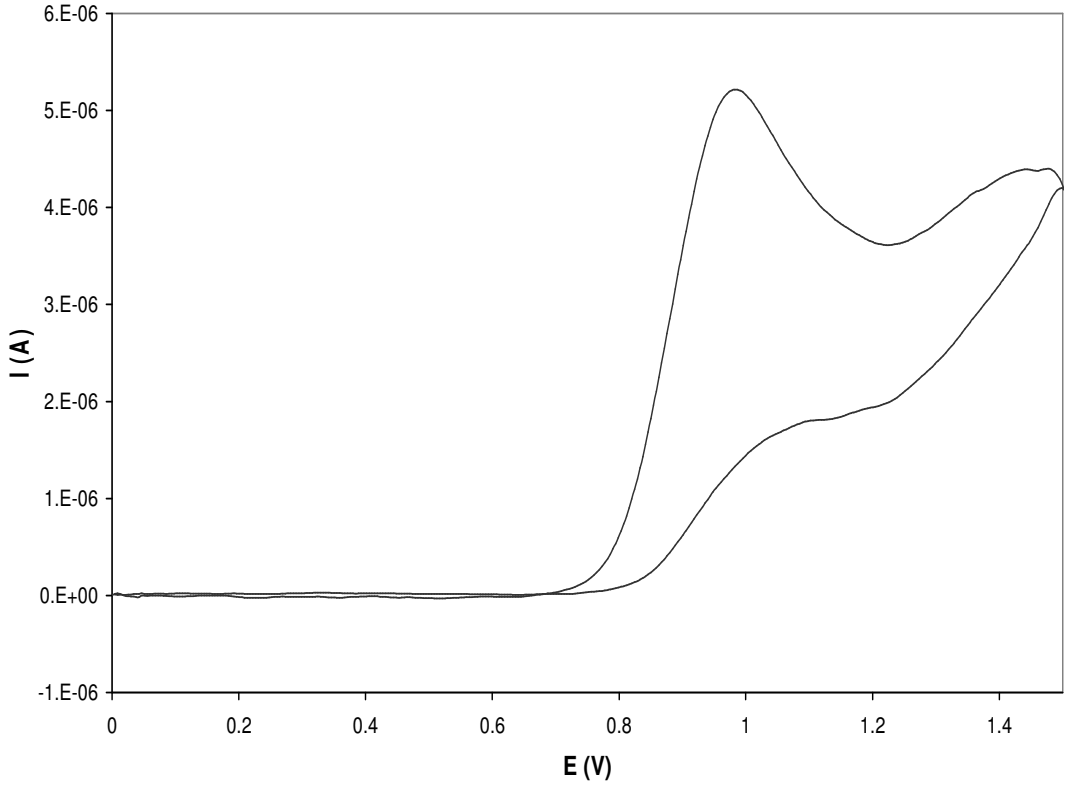

Figure 5.4 CV curve of $CoCl_2(PPh_3)_2$ obtained after 1 minute of recording CV in Fig. 5.3 using the same solution.

Unfortunately the activity of the WE could not be maintained for more than a few CV cycles in solutions containing $CoCl_2(PPh_3)_2$ as shown in Figure 5.3 (potentials range up to 1.9 V). The measurement was repeated in the same solution for a shorter potential range; the oxidation peak 2 and its coupled reduction peak 3 disappeared (Figure 5.4). A decrease in peak current for the oxidation process at more positive potentials (~ 1.2 V) was attributed to deactivation of the GC disk WE surface, probably by oxidation or by surface interaction with other species in solution.

CV was also recorded using $CoCl_2$ as an electroactive species at a GC disk WE (Figure 5.5), since it was one of the starting materials used during synthesis of $CoCl_2(PPh_3)_2$. CV of $CoCl_2$ showed two overlapping ill-defined oxidation peaks at E_p ~ 1.10 and 1.25 V. On extending the potential to more positive, the oxidation peaks shifted to more positive potentials and the overall background current at higher potentials increased.

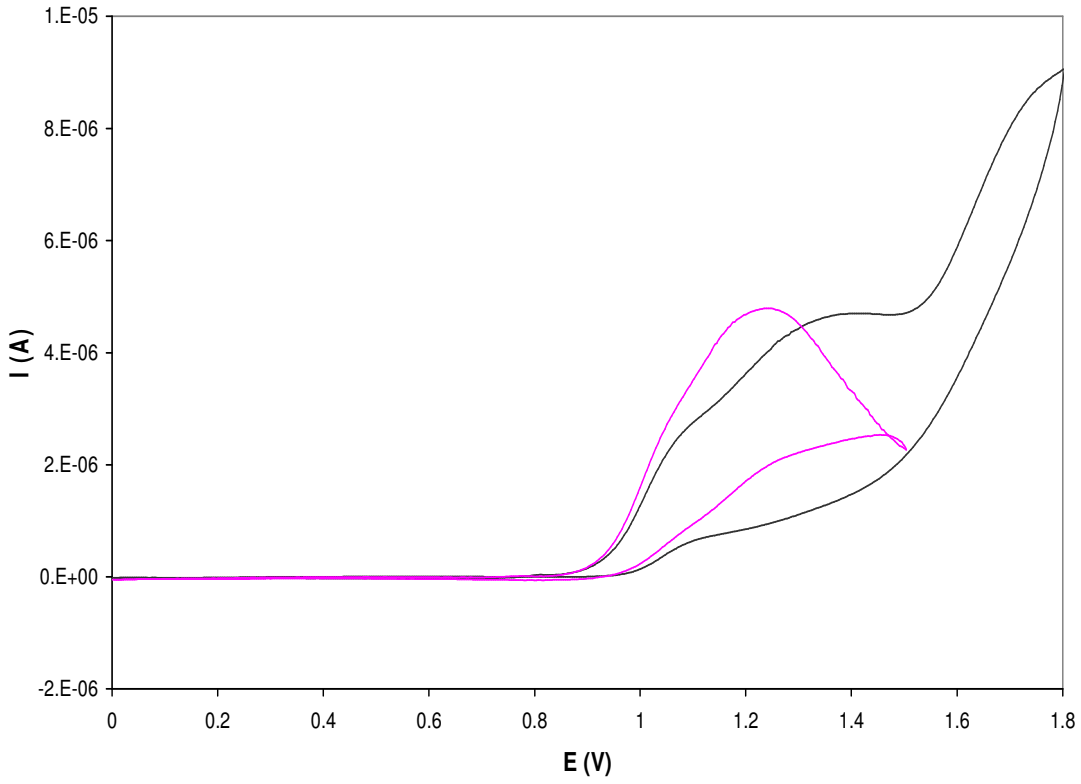

Figure 5.5 CV curves obtained in solutions containing $CoCl_2$ at a GC disk WE at a potential range (a) 0 to 1.15 V (—) and (b) 0 to 1.8 V (—).

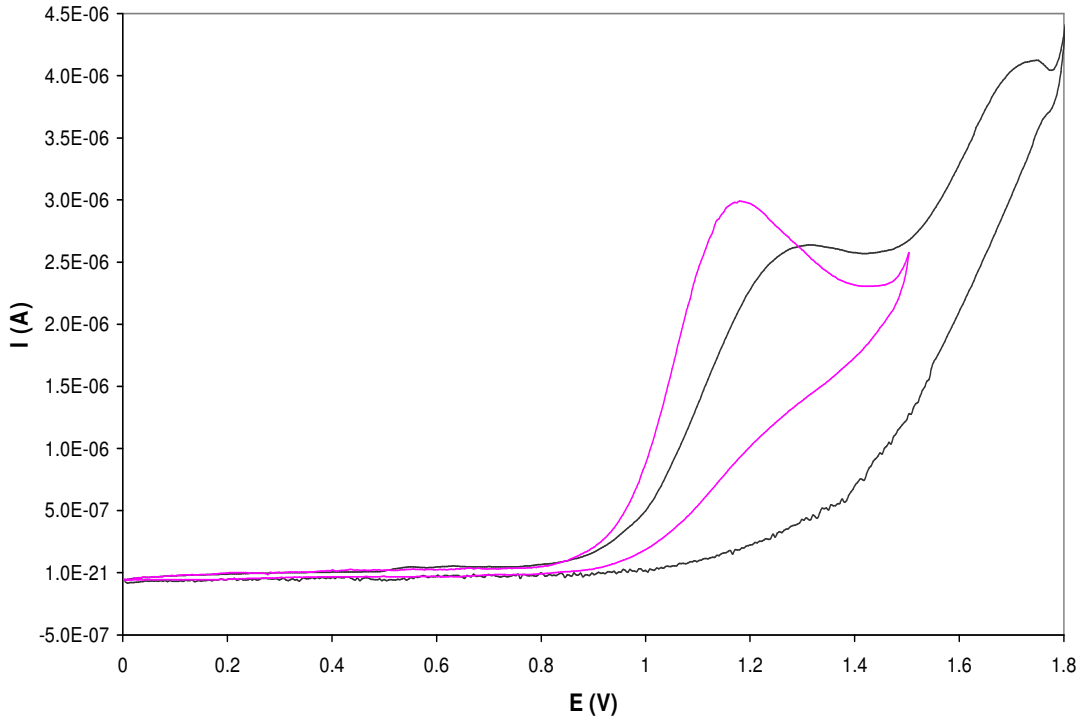

Figure 5.6 CV curves obtained in solutions containing TEACl at a GC disk WE at a potential range (a) 0 to 1.15 V (—) and (b) 0 to 1.8 V (—).

The same experiment was also performed using tetraethyl ammonium chloride (TEACl) at a GC disk WE (Figure 5.6), since it contained chloride as the only electroactive species present to see the effect of chloride on GC electrode. CV of TEACl showed a well-defined diffusion controlled oxidation peak at E_p = 1.10 V, which shifted to more positive potentials and became broad when the GC WE was exposed to higher potential of 1.8 V and the overall background current at higher potentials increased.

CV was also recorded using PPh_3 as an electroactive species at a GC disk WE (Figure 5.7), since it was one of the starting materials used during synthesis of $CoCl_2(PPh_3)_2$. The CV of PPh_3 showed one diffusion controlled oxidation peak at E_p = 0.90 V and no shift in potential was observed when the switching potential was extended to 1.8 V. No increase in current was observed at high potentials when the potential was scanned to 1.8 V. The oxidation peak at 0.90 V in PPh_3 solutions was identical to the one at 0.85 V obtained in $CoCl_2(PPh_3)_2$ solutions. Since in both solutions this oxidation peak was not affected by an increase in potential, it was related to either oxidation of cobalt or PPh_3 from the complex.

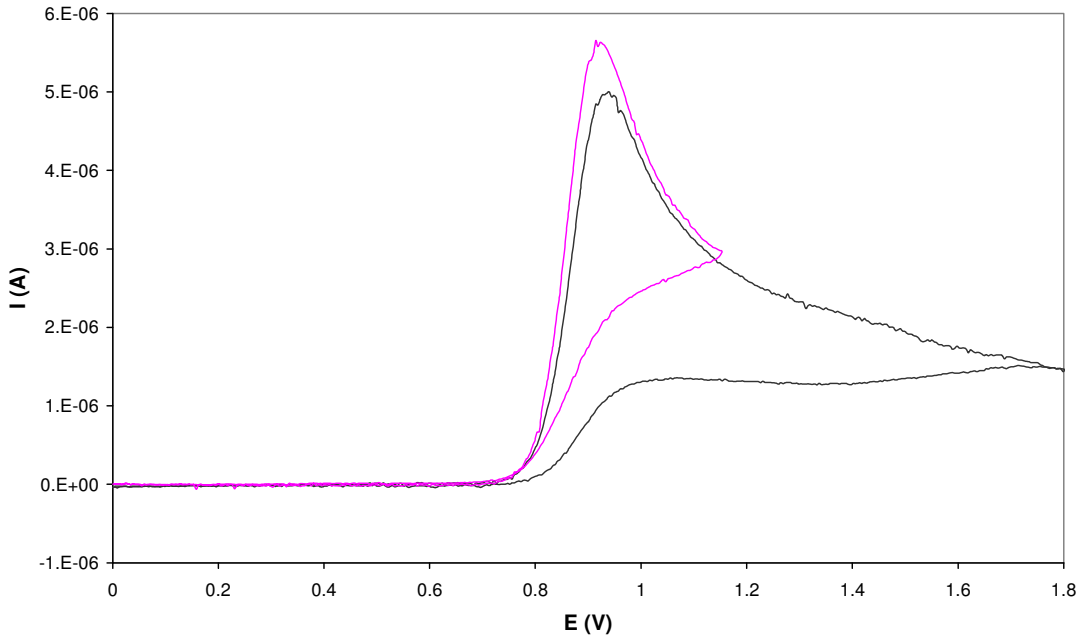

Figure 5.7 CV curves obtained in solutions containing PPh_3 at a GC disk WE at a potential range (a) 0 to 1.15 V (—) and (b) 0 to 1.8 V (—).

From the above results we attributed an overall increase in background current observed in solutions containing $CoCl_2(PPh_3)_2$, $CoCl_2$ or TEACl to generation of chlorine at the GC WE surface. The oxidized chloride in turn modified the GC disk WE surface. However, PPh_3 generated a good irreversible diffusion controlled signal at a GC disk WE, as it did not contain chloride ions.

In conclusion, it appears that a decrease in activity of GC WE shown from voltammograms of $CoCl_2(PPh_3)_2$ was due to the adsorption of a chloride ion or of small amounts of unknown side products produced during oxidation of $CoCl_2(PPh_3)_2$ at the WE surface. However, from the CV's measured in solutions containing PPh_3, the peak heights were reproducible from run to run for several cycles without loss of a GC WE activity. It appears that one will not be able to use GC disk WE for monitoring or studying the electrochemistry of compounds that contains chloride, because chloride modified the GC WE surface. However, GC WE can be recommended for monitoring of compounds that do not oxidize it, for example PPh_3. Moreover, the use of GC WE in chloride containing medium, i.e. in solutions containing $CoCl_2(PPh_3)_2$ at potentials below chloride oxidation (i.e. below, 1.2 V) should be considered. GC appeared to be an excellent WE to use for electrochemical studies in non-

aqueous solutions containing traces of water since it had the largest available potential window in comparison to Pt WE.

Gold disk electrode was also examined as a possible WE material to be used for the anodic voltammetric studies of $CoCl_2(PPh_3)_2$. A background current curve obtained at a gold disk WE is shown in Figure 5.8. A diffusion controlled peak was observed at E_p = 1.20 V, which might have arisen due to oxidation of aldehydes formed from a reaction of an oxygen radical generated from H_2O with pentanol or simply due to formation of gold oxide. The above suggestion was not confirmed since any literature on oxidation of aldehydes or of gold oxide was not conducted to check at which potential were they oxidized. Since $CoCl_2(PPh_3)_2$ showed oxidation peaks at potentials below and around 1.2 V at a GC disk WE, it follows that it might not be possible to study the electrochemical behaviour of this complex using gold disk as a WE.

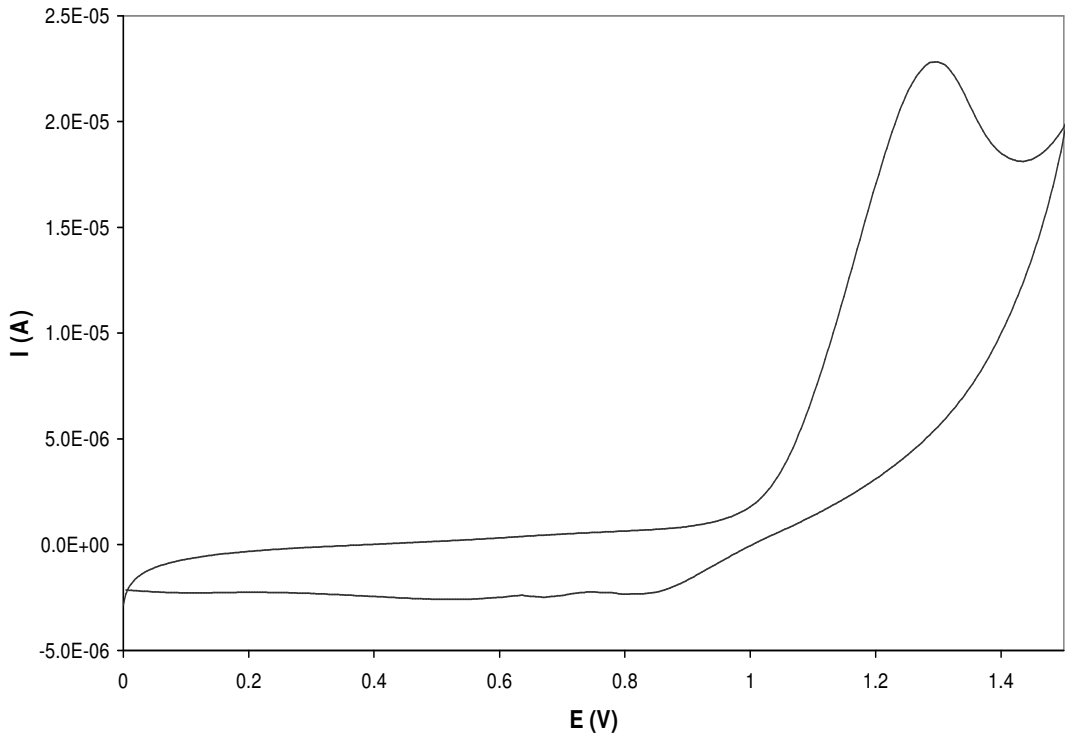

Figure 5.8 Background current CV curve that defines the accessible potential window at a gold disk WE.

In order to prove the above statement we recorded a CV curve of $CoCl_2(PPh_3)_2$ at a gold disk WE (Figure 5.9). There was a tremendous increase of background current at potentials

above 1.2 V and the oxidation peak observed from the CV of the background current curve disappeared. In conclusion, gold disk cannot be used as a WE for studying the electrochemical behaviour of compounds that are oxidized at more positive potentials than 1.20 V in a mixture of acetonitrile and pentanol.

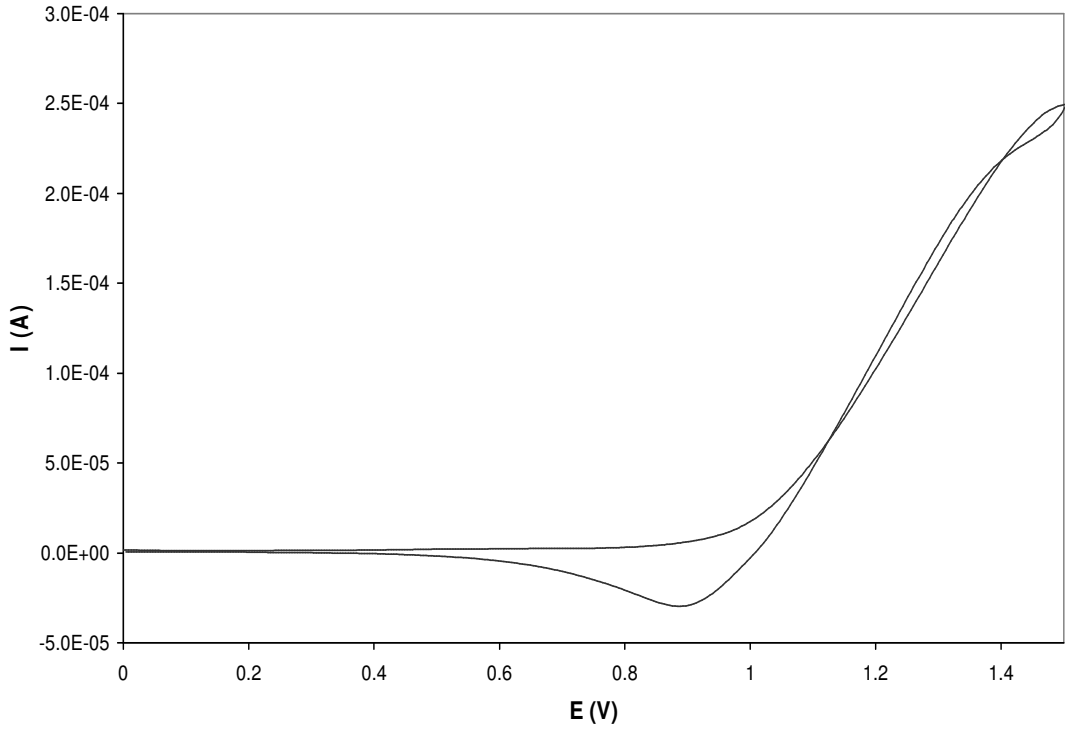

Figure 5.9 CV curves obtained in solutions containing $CoCl_2(PPh_3)_2$ at a gold disk WE.

Since we exhausted all the electrode materials that we had, we decided to go back to examine the anodic voltammetric behaviour of $CoCl_2(PPh_3)_2$ in a mixture of acetonitrile and pentanol (1:1) at a Pt disk WE (Figure 5.10). CV of $CoCl_2(PPh_3)_2$ showed two well-defined oxidation peaks labelled peak 1 and 2 when the potential was scanned up to 1.15 V (insert in Figure 5.10). On scanning to more positive potential of 1.8 V, another irreversible oxidation peak labelled peak 4 was observed with a very large current (Figure 5.10). A large peak current observed from oxidation peak 4 might have arisen due to a catalytic reaction of some species present in $CoCl_2(PPh_3)_2$ solution with traces of water present in the background solvents. The oxidation peaks 1 and 2 were reproducible and well-defined, only the oxidation peak 4 varied slightly from different experiments due to different amounts of water present.

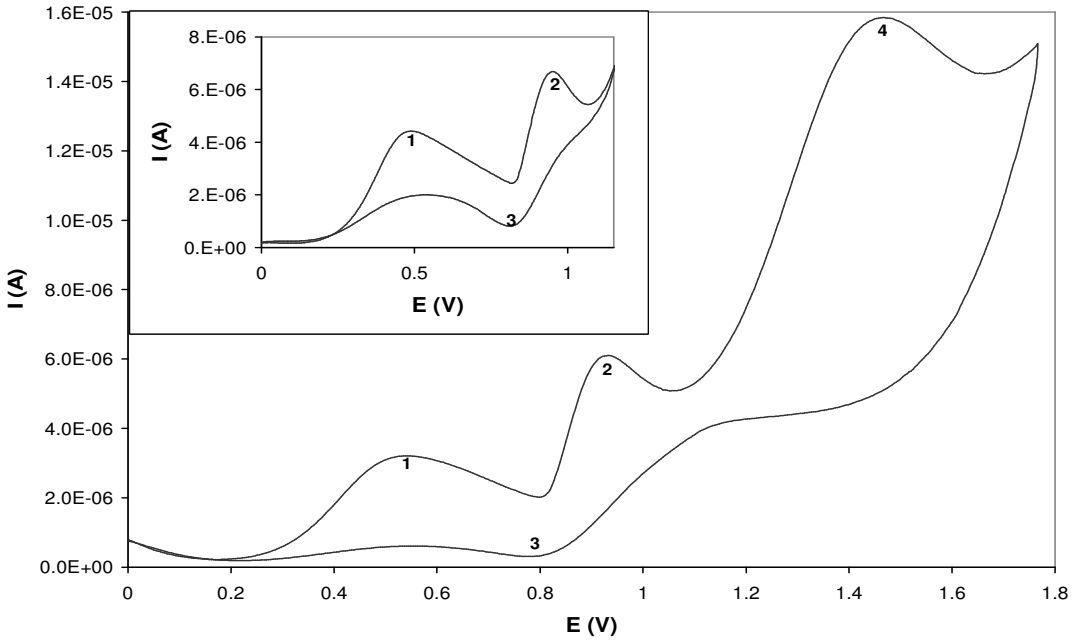

Figure 5.10 CV curves obtained in solutions containing $CoCl_2(PPh_3)_2$ at a Pt disk WE. CV curve obtained at short potential range up to 1.15 V is shown as an insert.

From these results we decided to use Pt disk WE for studying the anodic voltammetric behaviour of $CoCl_2(PPh_3)_2$ even if the background current curve showed electrochemical activity at potentials above 1.2 V because of traces of H_2O present. From the CV curve of $CoCl_2(PPh_3)_2$ shown in Figure 5.10 it appeared that we can still analyse its electrochemical properties at a Pt disk WE even in the presence of traces of H_2O.

5.1.2 Identification of Redox Peaks Observed From CV Curves of $CoCl_2(PPh_3)_2$

This section deals with assignment of the three oxidation peaks observed from the CV curve of $CoCl_2(PPh_3)_2$ at a Pt disk WE. In order to do this we examined the CV curve of $CoCl_2$ and that of PPh_3 individually and added together, as they were the starting materials during synthesis of this complex, $CoCl_2(PPh_3)_2$.

CV curves of $CoCl_2$ in Figure 5.11 revealed an irreversible diffusion controlled oxidation peak labelled peak 1 at E_p = 0.95 V, with the corresponding reduction peak labelled peak 1' at E_p = 0.70 V and an oxidation peak 2 which had a very large current (about 5 times higher than current of peak 1) at E_p = 1.50 V.

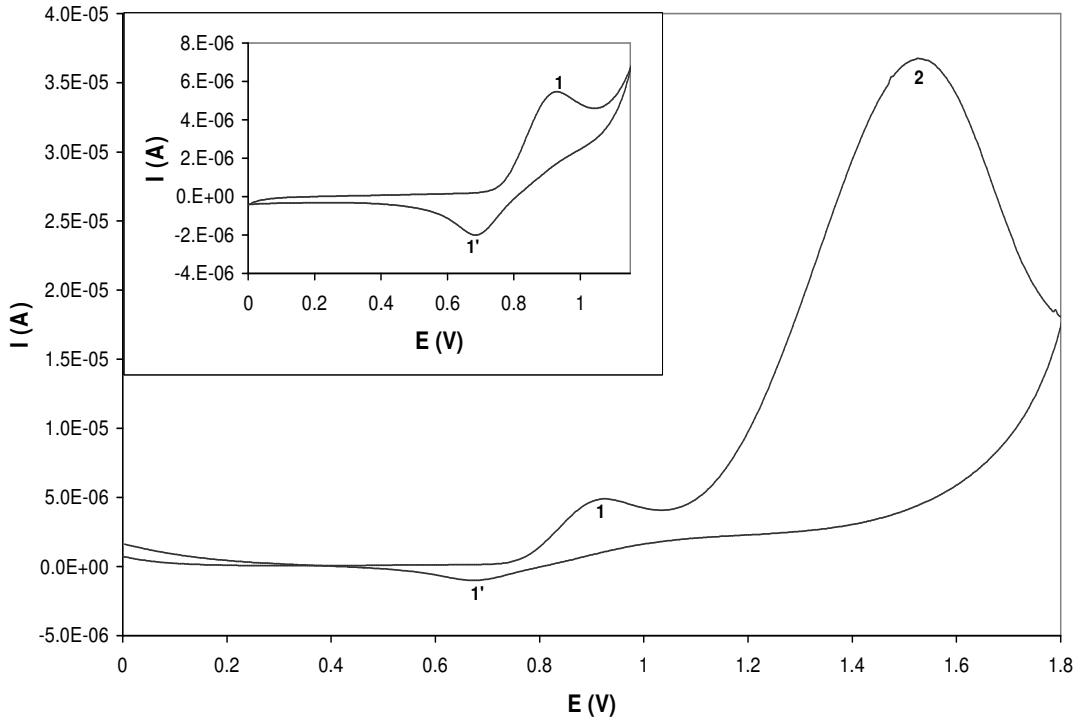

Figure 5.11 CV curves obtained in solutions containing $CoCl_2$ at a Pt disk WE. CV curve obtained at short potential range up to 1.15 V is shown as an insert.

The oxidation peak 2 and 4 of $CoCl_2(PPh_3)_2$ (Figure 5.10) and oxidation peak 1 and 2 of $CoCl_2$ (seen in Figure 5.11) were observed at similar positions and had similar shapes. The current of the oxidation peak 2 obtained from $CoCl_2$ solutions was much higher and shifted to more positive potentials as compared to that of oxidation peak 4 obtained from $CoCl_2(PPh_3)_2$ solutions. The shift may be due to a greater degree of solvation of the chloride ions when different amounts of water are present in the background solutions, or due to the fact that the catalytic reaction of chloride takes place more rapidly with increase in amount of water.

The two background curves obtained before measurement of the CV curve of $CoCl_2(PPh_3)_2$ and that of $CoCl_2$ are shown for comparison in Figure 5.12 to confirm the above point that the increase in current for the oxidation peak at E_p ~ 1.40 V arisen due to different amounts of water present in the background solutions. The background solvent used during measurement of $CoCl_2$ contained more moisture as the solvents were exposed to moisture when they were added to the cell before measurement. Whilst with $CoCl_2(PPh_3)_2$ the solvents were collected under argon using schlenk tubes. A background current obtained

before measurement of $CoCl_2$ was higher than the one obtained before measurement of $CoCl_2(PPh_3)_2$ at potentials above 1.2 V.

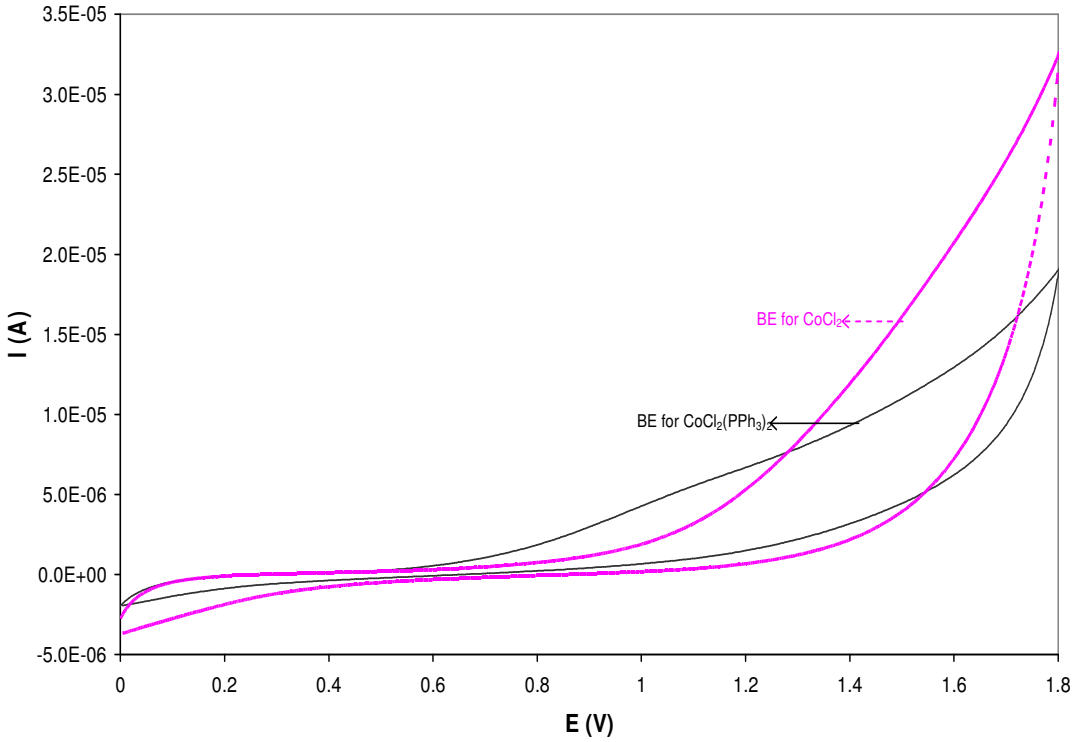

Figure 5.12 Influence of water on the background current CV curves obtained before CV measurements of $CoCl_2(PPh_3)_2$ and $CoCl_2$ at a Pt disk WE.

These show that the current of an oxidation peak 2 was enhanced by an increased amount of water in the background solutions. From these data we concluded that the oxidation peak 2 (from a CV of $CoCl_2$) and 4 (from a CV of $CoCl_2(PPh_3)_2$) arisen due to a catalytic reaction of chloride with water present in the background solvent. Therefore, the peak intensity depends on the amount of water present.

CV curves of PPh_3 are shown in Figures 5.13 and they revealed only one oxidation peak labelled peak 1 at E_p = 1.05 V. No coupled reduction peak was observed from the voltammograms and no further oxidation peaks were observed on scanning to more positive potentials. CV of PPh_3 was also reported by Hershberger and co-workers [42] who found PPh_3 to be oxidized irreversibly with one-electron transfer to PPh_3^+ at ~ 1.3 V in acetonitrile.

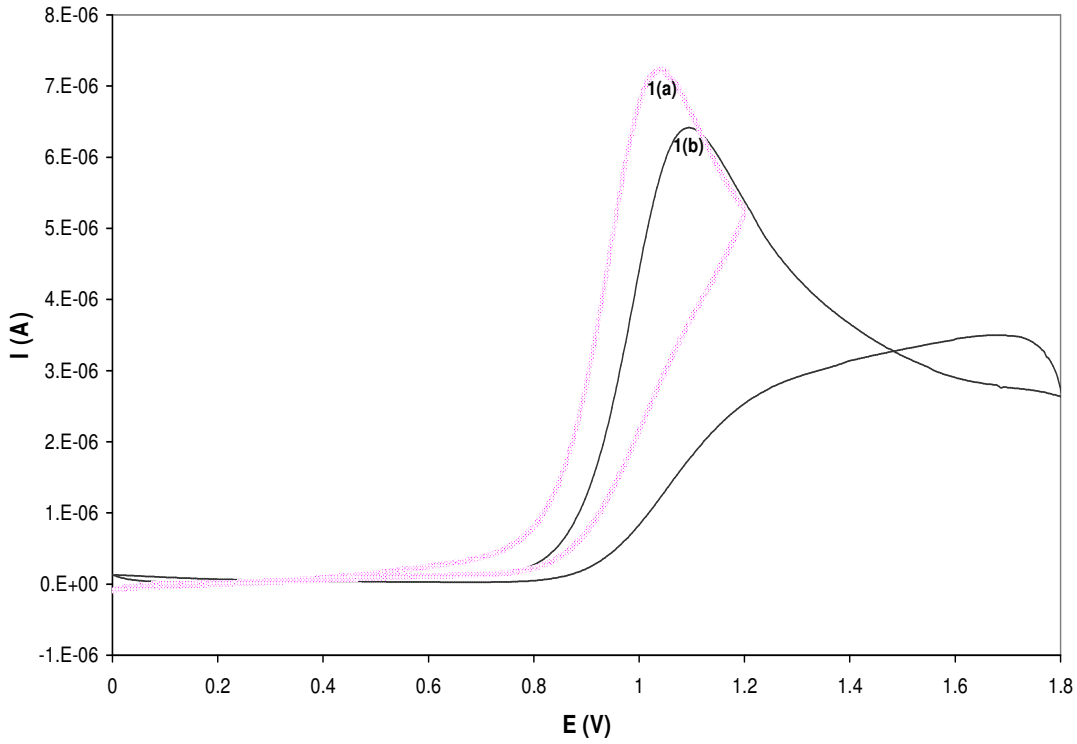

Figure 5.13 CV curves obtained in solutions containing 1.54×10^{-3} mol/l PPh_3 at a Pt disk WE at a potential range (a) 0 to 1.15 V (….) and (b) 0 to 1.8 V (—).

In the absence of chloride ions, a large oxidation peak at ~ 1.40 V was not observed and there was no enhancement of current at more positive potentials, which showed the absence of a catalytic effect. This proves that the oxidation peak observed at E_p ~ 1.40 V observed from the CV's of $CoCl_2$ and $CoCl_2(PPh_3)_2$ arisen due to a catalytic reaction of chloride with water present in the background solvent, as it was only observed from CV's of the compounds containing chloride.

In order to assign the oxidation peak 1 of the complex $CoCl_2(PPh_3)_2$, we synthesized the complex electrochemically by first recording the CV with only $CoCl_2$ present in solution and then adding two equivalent moles of PPh_3. CV curve of $CoCl_2$ is shown in Figure 5.14 (solid-line curve) and reveals the presence of one oxidation peak at $E_p = 0.95$ V, which has a coupled reduction peak at $E_p = 0.70$ V when the scan is reversed at 1.15 V.

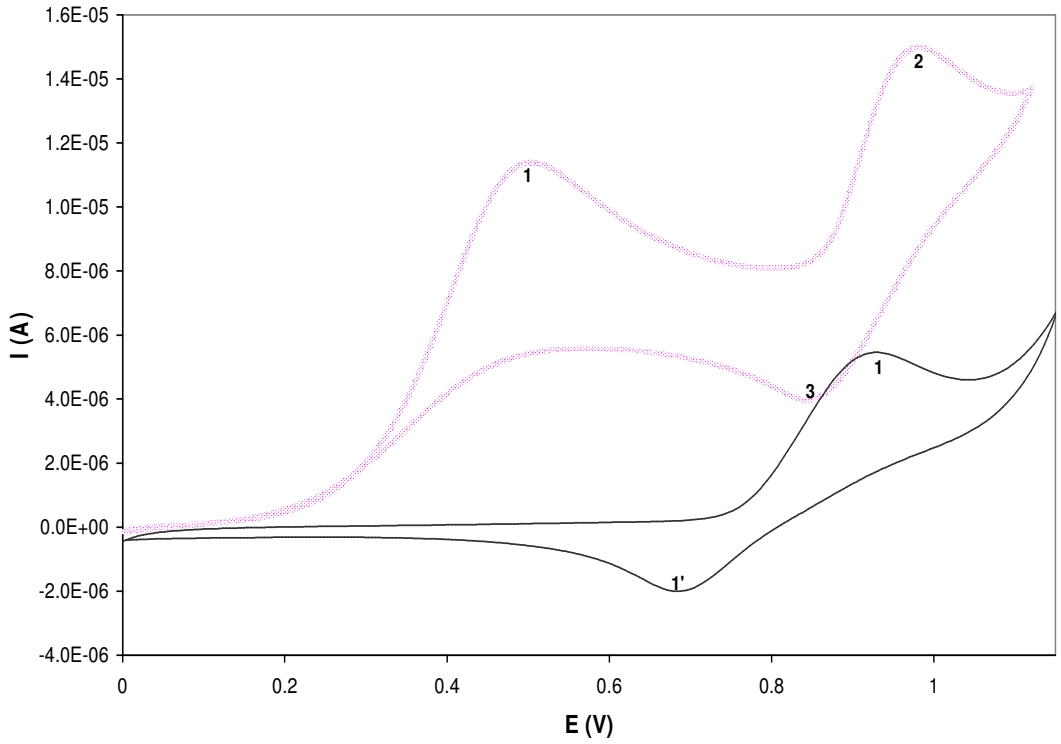

Figure 5.14 Effect of added PPh_3 on the CV curve of $CoCl_2$. CV curves of a 7.7×10^{-4} mol/l $CoCl_2$ before (—) and after (....) addition of 1.54×10^{-3} mol/l (2 equiv) of PPh_3 in a mixture of acetonitrile and pentanol (1:1) are presented.

Addition of two equivalent moles of PPh_3 resulted in an appearance of another irreversible oxidation peak labelled peak 1 at a less positive potential of ~ 0.50 V (Figure 5.14, dotted-line curve). This peak was not observed before from the CV curve of a free PPh_3, or that of $CoCl_2$. Since it only appeared after mixing of the two starting materials, it was assigned to oxidation of Co^{II} to Co^{III} from the complex, $CoCl_2(PPh_3)_2$. It can be seen from Figure 5.14 that peak 1 observed from the CV of $CoCl_2$ remained at the same position after addition of PPh_3 (now labelled peak 2, on the dotted-line curve). Its coupled reduction peak 1' shifted to more positive potentials (now labelled peak 3) and the electrode process at E_p = 0.95 V became partially reversible. The above results showed that the CV peak of $CoCl_2$ observed in the absence of a PPh_3 ligand was modified in the presence of this ligand and a new peak due to the reaction product (i.e. $CoCl_2(PPh_3)_2$) appeared at a more positive potential. This behaviour is characteristic of electrocatalysis as discussed in Chapter 1 section 1.4 that the CV wave normally observed in the absence of the ligand (i.e. PPh_3 in this case) can be modified in the presence of this ligand and a new wave due to the reaction product will appear.

At this stage we managed to assign the oxidation peak 1 and 4 observed from the CV of $CoCl_2(PPh_3)_2$. Assignment of the oxidation peak 2 was a bit difficult since the CV curves of both $CoCl_2$ and PPh_3 showed an oxidation peak around the same potential (~ 1.0 V). But from analysis of the CV curves of $CoCl_2$ before and after addition of PPh_3 it was shown that PPh_3 reacted completely with $CoCl_2$ to form a complex $CoCl_2(PPh_3)_2$. From this result we immediately assumed that the oxidation peak 2 of $CoCl_2(PPh_3)_2$ did not arise from PPh_3 oxidation but rather from oxidation of a chloride ligand present in the complex. Firstly we attempted to assign an oxidation peak 1 observed from a CV curve of $CoCl_2$. To our knowledge there was no literature available on anodic voltammetric studies of $CoCl_2$, so we looked at some literature on anodic voltammetric studies of chloride and compared the results with those obtained from CV of $CoCl_2$.

The electrochemical behaviour of the chloride/chlorine system has been previously studied at the rotated platinum microelectrodes in acetonitrile solutions using LiCl as a chloride source [67]. Voltammetric studies demonstrated that the electrode reaction gave two anodic waves, at 1.1 V and 1.7 V. The following overall reactions were postulated, $3Cl^- \leftrightarrow Cl_3^- + 2e^-$ and $2Cl_3^- \leftrightarrow 3Cl_2 + 2e^-$, for the first and second wave, respectively. The Cl^-/Cl_2 couple was also studied in acetone and nitromethane and only one anodic and one cathodic wave was found and the total electrochemical reaction was given as $2Cl^- \leftrightarrow Cl_2 + 2e^-$ [68]. The second anodic wave occurred at 1.9 V in nitromethane and at 1.8 V in acetone. It was attributed to oxidation of the background current.

Chloride oxidation was also reported to occur as a one-step process in dimethylformamide (DMF) [69] and dimethylsulphoxide (DMSO) [70]. Sereno et al [71] decided to investigate this electrode reaction thoroughly in acetonitrile. Since acetonitrile can be considered as an aprotic solvent with similar properties to nitromethane and DMF, there was no valid reason to justify a different behaviour for its electrode process [71]. They found that chloride undergone a two-electron exchange per mol to chlorine and only one anodic and one cathodic wave was found using LiCl as a chloride source at a platinum rotating disk electrode.

From the above results we decided to investigate first the electrochemical behaviour of $CoCl_2$ at a Pt disk WE in acetonitrile. A CV curve of $CoCl_2$ in acetonitrile is shown in Figure 5.15. The voltammogram revealed only one broad oxidation peak at E_p = 1.1 V and

one reduction peak at E_p = 0.65 V. No additional oxidation or reduction peaks were observed when scanning to more positive or less negative potentials.

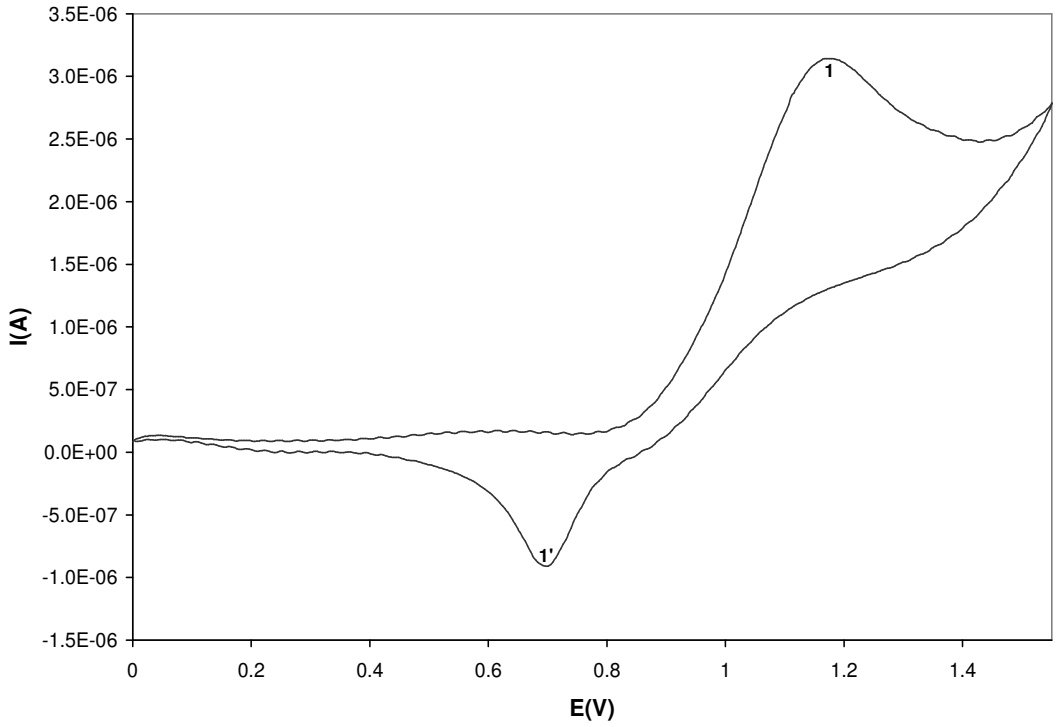

Figure 5.15 CV curves obtained in solutions containing $CoCl_2$ in acetonitrile at a Pt disk WE.

From these results we suggested that the oxidation peak 1(a) obtained from the CV of $CoCl_2$ (Figure 5.15) in acetonitrile arose due to overlap between cobalt and chloride oxidation. This result was related to some literature studies on reduction of cobalt bromide, where Co^{II} and bromide were found to be reduced at the same potential giving rise to one reduction peak [14]. Furthermore, the oxidation peak 2 at 1.5 V obtained from CV of $CoCl_2$ in a mixture of acetonitrile and pentanol (1:1) was not observed in acetonitrile even when the potential was scanned further to 1.8 V. This might have arisen due to the fact that most of the water that was responsible for an increase in current of the background current curves at potentials above 1.2 V, in a mixture of acetonitrile and pentanol was from pentanol. It appeared that it was more difficult to remove traces of water from pentanol than from acetonitrile. When the amount of water was measured individually, pentanol after distillation still contained about 1500 ppm of water whilst acetonitrile after distillation contained only about 200 ppm of water. This proves the above suggestion that most of the

water came from pentanol and maybe pentanol in the presence of water undergone oxidation easier.

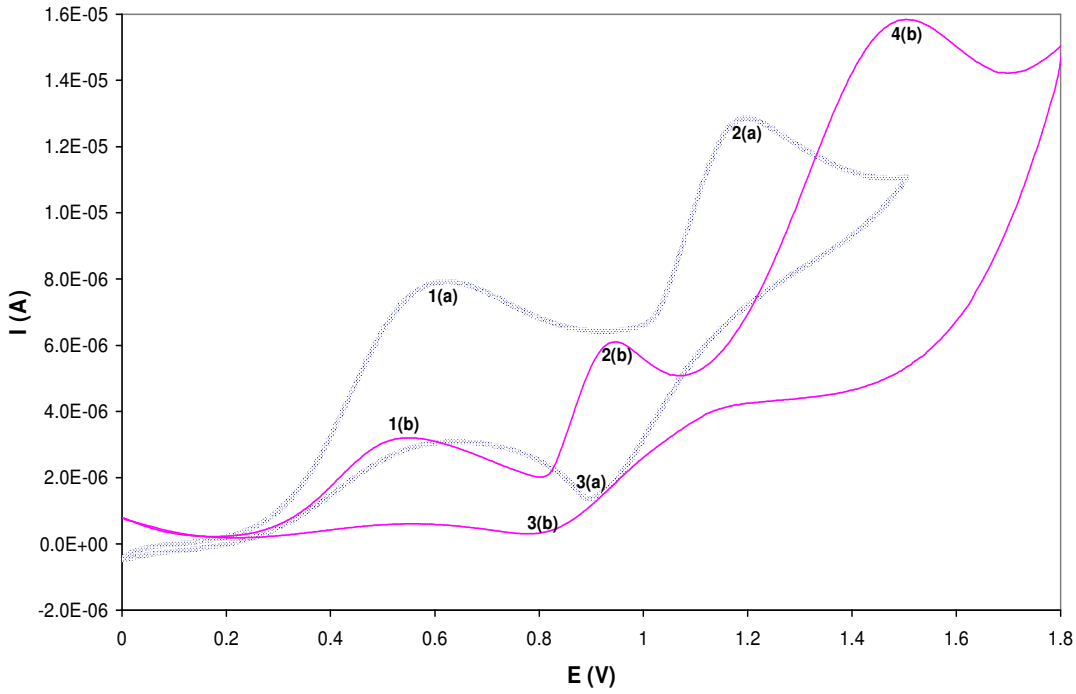

Figure 5.16 CV curves obtained in solutions containing $CoCl_2(PPh_3)_2$ in acetonitrile (....) and in a mixture of acetonitrile and pentanol (—) at a Pt disk WE.

We also investigated the electrochemical behaviour of $CoCl_2(PPh_3)_2$ in acetonitrile solutions at a Pt disk WE (Figure 5.16) and only two oxidation peaks were observed at E_p = 0.6 V and 1.2 V and one reduction peak at E_p = 0.9 V. The oxidation peak 4 previously observed from the voltammogram of $CoCl_2(PPh_3)_2$ in a mixture of acetonitrile and pentanol solution (Figure 5.16, solid-line curve) was not observed in acetonitrile solution. The oxidation peak 2 at E_p = 1.2 V agreed in position to the one obtained in solutions containing $CoCl_2$ in acetonitrile, which suggests that it might also have arisen due to oxidation of only a chloride ligand (Figure 5.17) since cobalt is oxidized already at less positive potentials in this complex, $CoCl_2(PPh_3)_2$. Surprisingly, the oxidation peak 1 obtained in $CoCl_2$ solutions was about a factor of 2 times less than the oxidation peak 2 of $CoCl_2(PPh_3)_2$ (even if concentration of both analytes were equal). This might have arisen due to different amounts of water present in acetonitrile. To verify this we compared the two background current CV curves obtained in acetonitrile before measurement of the curves in Figure 5.18 (Figure 5.18).

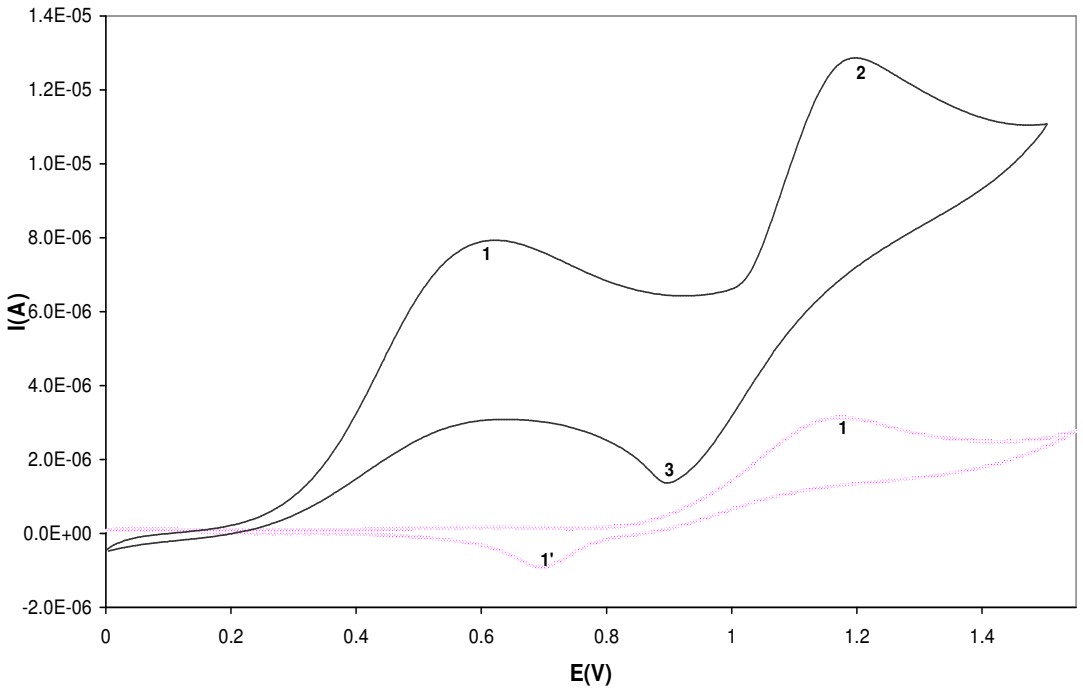

Figure 5.17 Comparison of the CV curves of $CoCl_2(PPh_3)_2$ (—) and $CoCl_2$ (....) obtained in acetonitrile.

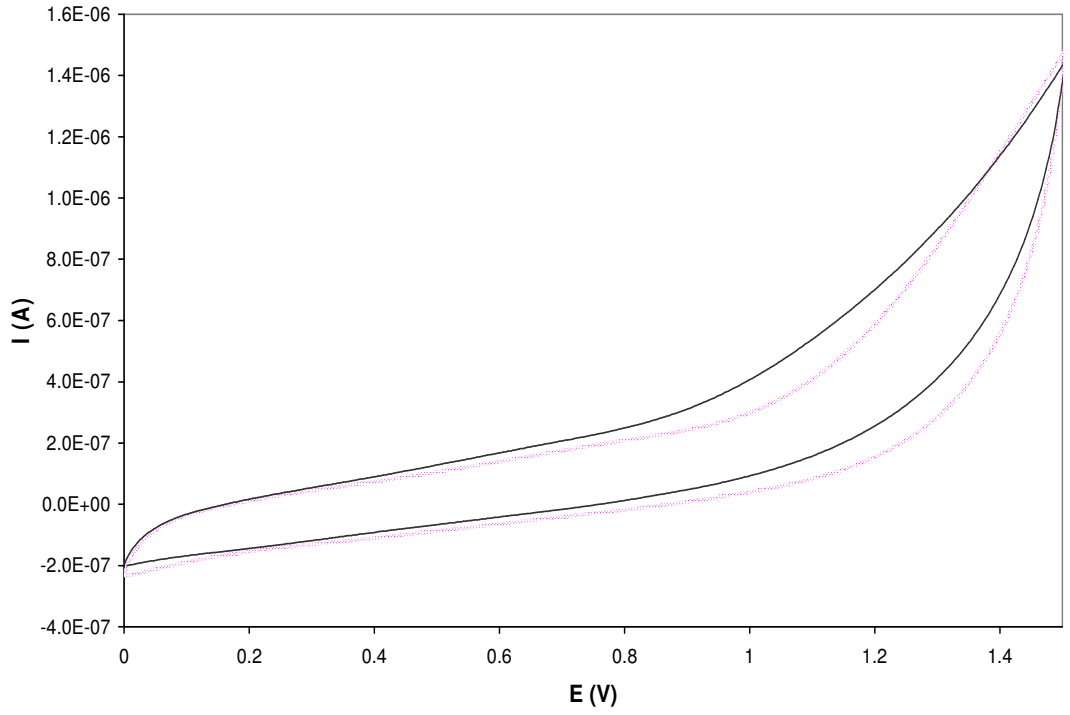

Figure 5.18 Comparison of the background current CV curves recorded in acetonitrile before measurements of the CV curves of $CoCl_2(PPh_3)_2$ (—) and that of $CoCl_2$ (....).

The two background current voltammograms in Figure 5.18 were similar and had the same current and shape. This shows that an increase in peak current for oxidation peak 2 from $CoCl_2(PPh_3)_2$ solutions did not arise because of traces of water present in acetonitrile. We concluded that an increase might have arisen due to just error in concentration measurement. From the above results we concluded that the oxidation peak 2(a) in solutions containing $CoCl_2(PPh_3)_2$, arisen due to oxidation of a chloride ligand.

The oxidation peak at E_p ~ 1.4 V was only observed from the voltammograms of compounds containing chloride in a mixture of acetonitrile and pentanol and it was assigned to a catalytic reaction of chloride with water present in the background solvents. We decided to investigate this further since traces of water were also present in acetonitrile solutions. Figure 5.19 shows comparison of the background current CV curve obtained in acetonitrile (bold solid-line curve) and that obtained in a mixture of acetonitrile and pentanol (solid-line curve). A large increase in current was observed from 1.2 V on the voltammogram recorded in a mixture of acetonitrile and pentanol, whilst no increase in current was observed in solutions containing only acetonitrile (Figure 5.19). These account for a large catalytic oxidation peak current observed in voltammograms of compounds containing chloride in acetonitrile/pentanol solvent mixtures.

Since the oxidation peak at ~ 1.40 V was observed only on CV's of compounds containing chloride in acetonitrile/pentanol solvent mixtures, it was assigned to a catalytic reaction of chloride with traces of water present in the solvent solution mixture (most likely from alcohols). The same behaviour was observed from the voltammograms of LiCl in nitromethane and acetone [68]. In conclusion, the electrode reaction occurring at E_p ~ 0.95 V in $CoCl_2(PPh_3)_2$ was complicated by a catalytic reaction occurring at E_p ~ 1.4 V which caused a diffusion current enhancement. From the above it follows that the mechanistic studies of organometallic compounds containing chloride i.e. $CoCl_2(PPh_3)_2$, should be investigated in acetonitrile solutions in the absence of pentanol and water. But monitoring should be possible in a mixture of acetonitrile and pentanol since one can apply a potential of 0.50 V for studies involving $CoCl_2(PPh_3)_2$ without interference of chloride and water oxidation.

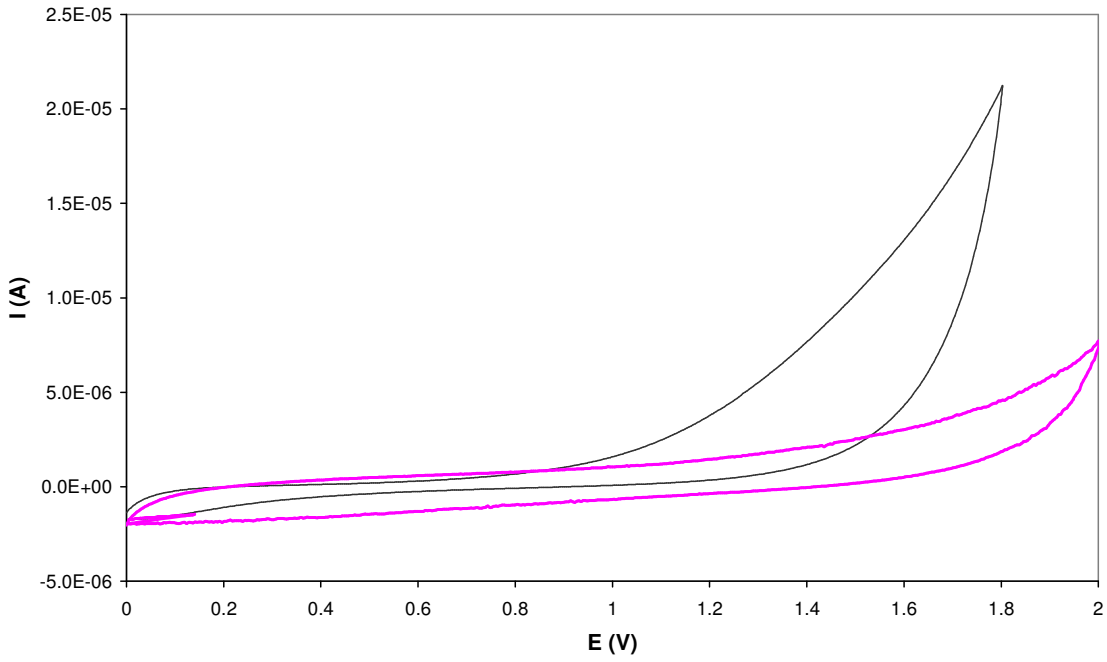

Figure 5.19 Comparison of the background current CV curves recorded in a mixture of acetonitrile and pentanol (1:1) (—) with that recorded in acetonitrile (—).

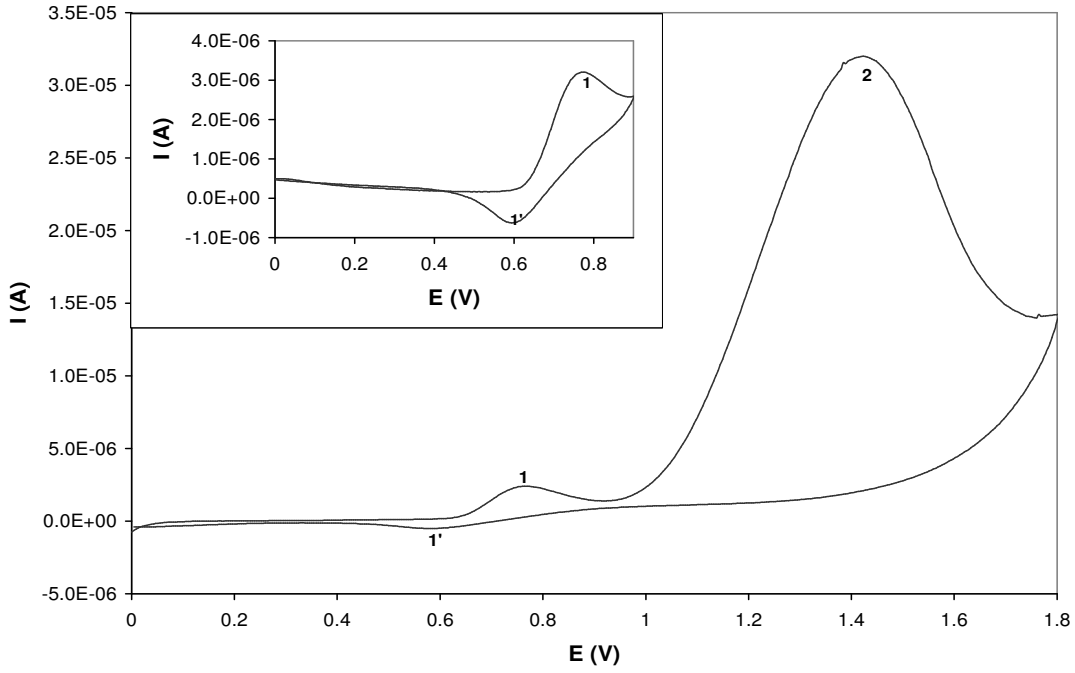

Figure 5.20 CV curves obtained in solutions containing TEACl at a Pt disk WE. CV curve obtained at short potential range up to 1.15 V is shown as an insert.

CV was also recorded in cobalt-free media, using tetraethyl ammonium chloride (TEACl) as a chloride source, to confirm the assignment of the oxidation peak 2 of $CoCl_2(PPh_3)_2$ in a mixture of acetonitrile and pentanol in Figure 5.10.

Voltammograms of TEACl revealed two oxidation peaks 1 and 2 at E_p = 0.75 and 1.40 V and one cathodic peak at E_p = 0.6 V (Figure 5.20). The oxidation peak at E_p ~ 1.40 V agreed exactly in position and shape with the oxidation peak 2 observed in $CoCl_2$ solutions. The oxidation peak 1 at E_p = 0.75 V was assigned to chloride oxidation since chloride was the only electroactive species present in this salt. But from the peak intensity, it appears that the oxidation peak 1 obtained from solutions of $CoCl_2$ was higher than the oxidation peak 1 obtained in TEACl solutions. This proves that the oxidation peaks 1 obtained from CV of $CoCl_2$ arisen due to oxidation of both cobalt and chloride ligand. In conclusion, TEACl cannot be used as a supporting electrolyte because it contained a chloride ion which can be easily oxidized at a Pt WE.

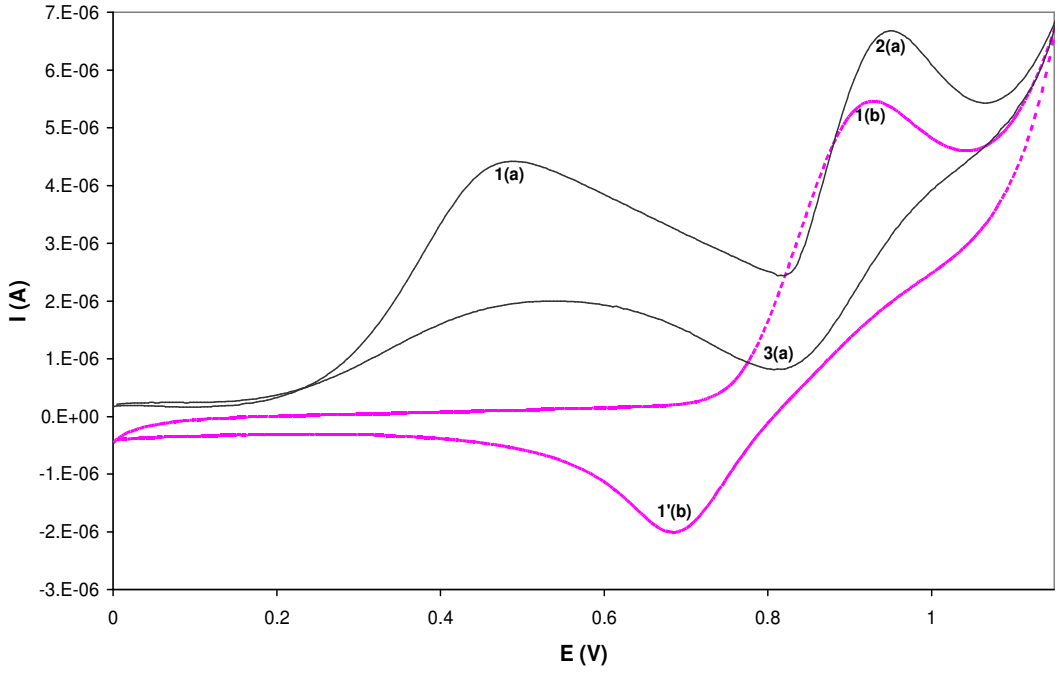

Figure 5.21 Comparison of the CV curve of $CoCl_2(PPh_3)_2$ (—) with that of $CoCl_2$ (—).

To further confirm the assignment of the oxidation peak 2 of $CoCl_2(PPh_3)_2$, we compared the CV curve of $CoCl_2(PPh_3)_2$ with that of $CoCl_2$ and that of PPh_3 obtained in a mixture of acetonitrile and pentanol (1:1). Figure 5.21 shows comparison of the CV curve of $CoCl_2(PPh_3)_2$ with that of $CoCl_2$. The oxidation peak 2(a) of the complex, $CoCl_2(PPh_3)_2$

agreed in position, shape and height with the oxidation peak 1(b) of $CoCl_2$. We suggested that the oxidation peak 2(a) of $CoCl_2(PPh_3)_2$ might have arisen due to oxidation of a chloride ligand from the complex. Comparison of the CV curve of $CoCl_2(PPh_3)_2$ with that of PPh_3 revealed no similarities between the two voltammograms (Figure 5.22).

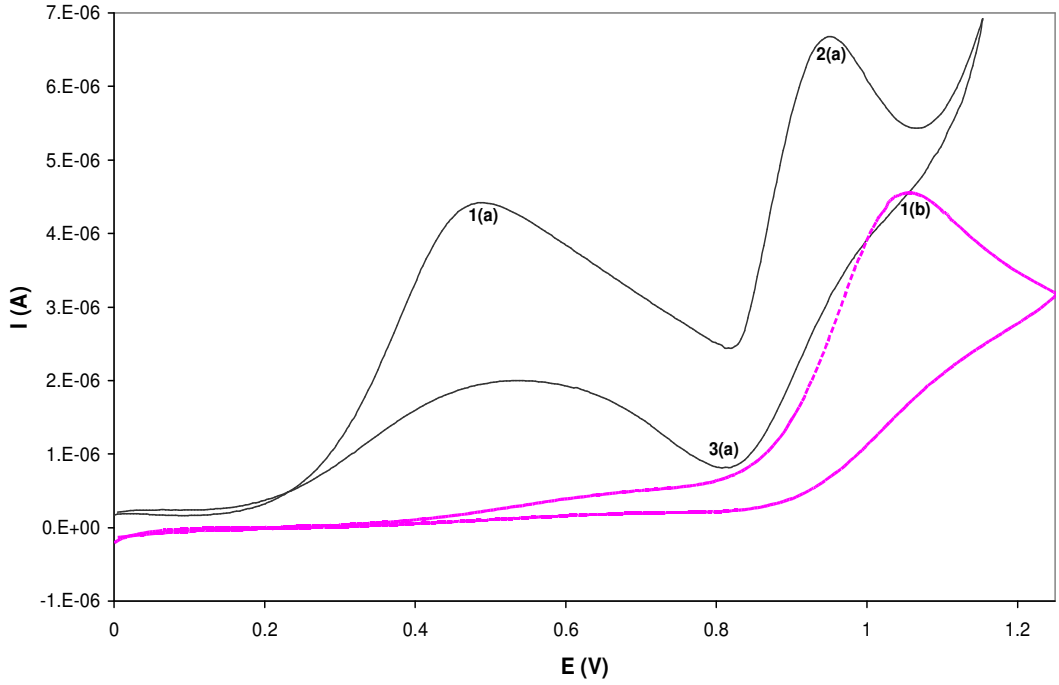

Figure 5.22 Comparison of the CV curves of $CoCl_2(PPh_3)_2$ (—) with that of PPh_3 (—).

The oxidation peak 2(a) of the complex occurred at less positive potentials and had a coupled reduction peak 3(a), whilst the oxidation peak 1(b) of PPh_3 occurred at more positive potential and had no coupled reduction peak. Similar results were also obtained from comparison of the CV curve of $CoCl_2$ with that of PPh_3 (Figure 5.23).

We also compared the oxidation peak 1 of $CoCl_2$ with that of TEACl (Figure 5.24) [Note: the CV curve of $CoCl_2$ and that of TEACl were recorded on the same day using the same solution of background electrolyte, starting with a $CoCl_2$ experiment]. The oxidation peak 1(b) obtained from a TEACl solution was observed at almost the same potential as that of $CoCl_2$ peak 1(a) shown as an insert of Figure 5.24 and the reduction peaks 1'(a and b) were at exactly the same position.

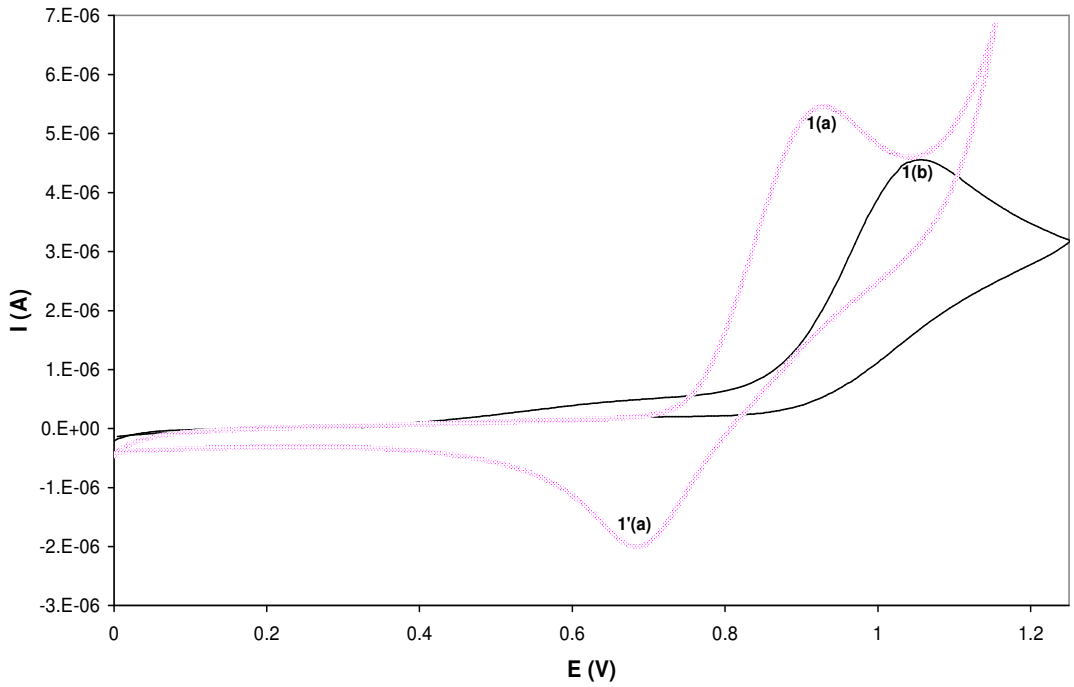

Figure 5.23 Comparison of the CV curve of PPh_3 (—) with that of $CoCl_2$ (....).

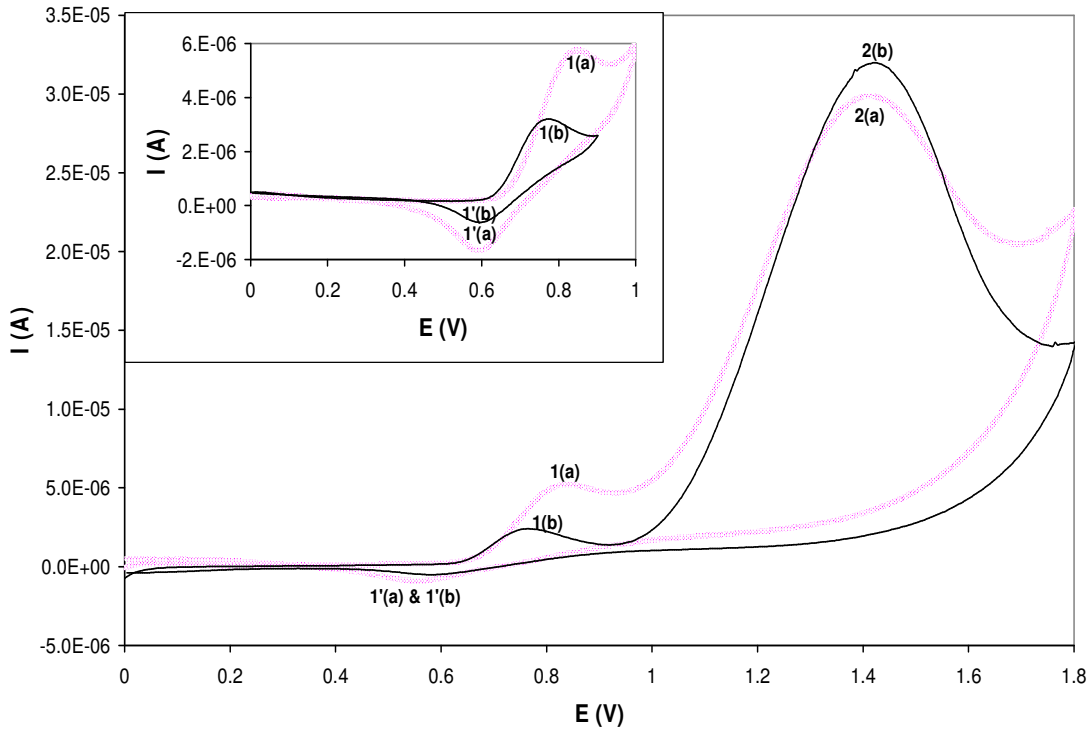

Figure 5.24 Comparison of the CV curves of TEACl (—) with that of $CoCl_2$ (....). CV curves obtained at short potential range up to 1.15 V are shown as an insert.

The peak current of the oxidation peak 1(a) obtained from a $CoCl_2$ solution and its coupled reduction peak 1'(a) are about a factor of two times higher than the peak current obtained for the oxidation peak 1(b) and its coupled reduction peak 1'(b) obtained from a TEACl solution. As it is well known that the peak current depends on the concentration of the oxidized species, an increase in oxidation peak 1(a) of $CoCl_2$ might have arisen due to two chloride ions present in $CoCl_2$ since only one chloride ion was present in TEACl.. Furthermore, the little shift in peak potentials might be related to different solvation energies present in solutions of TEACl and $CoCl_2$ or most likely due to an irreversible nature of the electrochemical reactions.

The oxidation peak 2 in both salts did not show any relation to the concentration of the chloride ion, but seemed to be related to the amount of water present in background solutions (Figure 5.24). The peak current of the oxidation peak 2 increased slightly in TEACl solutions in comparison to that obtained in $CoCl_2$ solutions, due to different amounts of water present in background solutions, as shown by different background current curves of TEACl and $CoCl_2$ in Figure 5.25.

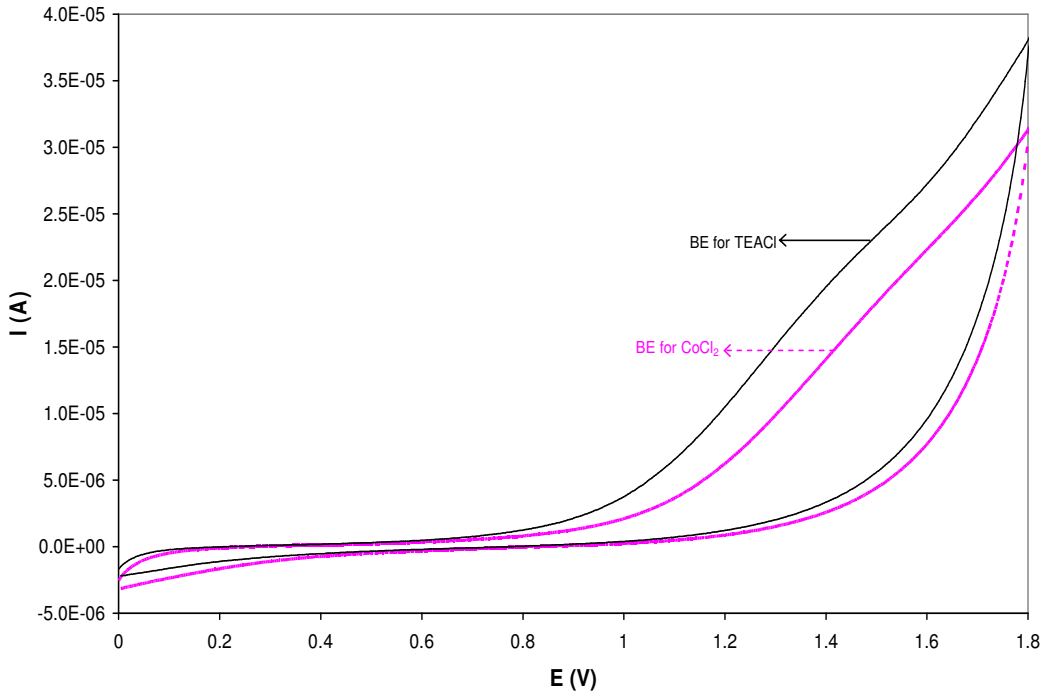

Figure 5.25 Influence of water on the background current CV curves obtained before CV measurements of TEACl and $CoCl_2$ at a Pt disk WE.

In conclusion, the anodic voltammetric studies of $CoCl_2(PPh_3)_2$ revealed three oxidation peaks, the first one involving oxidation of the metal centre, Co^{II} to Co^{III} which was followed by oxidation of chloride ligand from $CoCl_2(PPh_3)_2$ (peak 2) and this was complicated by a catalytic reaction of chloride with water present in the background solvent (peak 3) which caused a diffusion current enhancement.

5.1.3 Electrochemically Monitored Titration of $CoCl(PPh_3)_3$ With Chloride

In this section we focused on titration of the complex $CoCl(PPh_3)_3$ with chloride electrochemically, to investigate the binding ability of the chloride ions to $CoCl(PPh_3)_3$. TEACl was used as a chloride source. We synthesized the complex $CoCl(PPh_3)_3$ and characterised it using elemental analysis and infrared spectroscopy (the results obtained are presented in Experimental Section, Chapter 3).

CV curves of 7.7 x 10^{-4} mol/l $CoCl(PPh_3)_3$ before (solid-line curve) and after (dotted-line curve) addition of an equivalent concentration of TEACl are shown in Figure 5.26. Two oxidation peaks labelled peak 1(a) and 2(a) which had a coupled reduction peak 3(a) were observed from the CV of $CoCl(PPh_3)_3$ (Figure 5.26(a)).

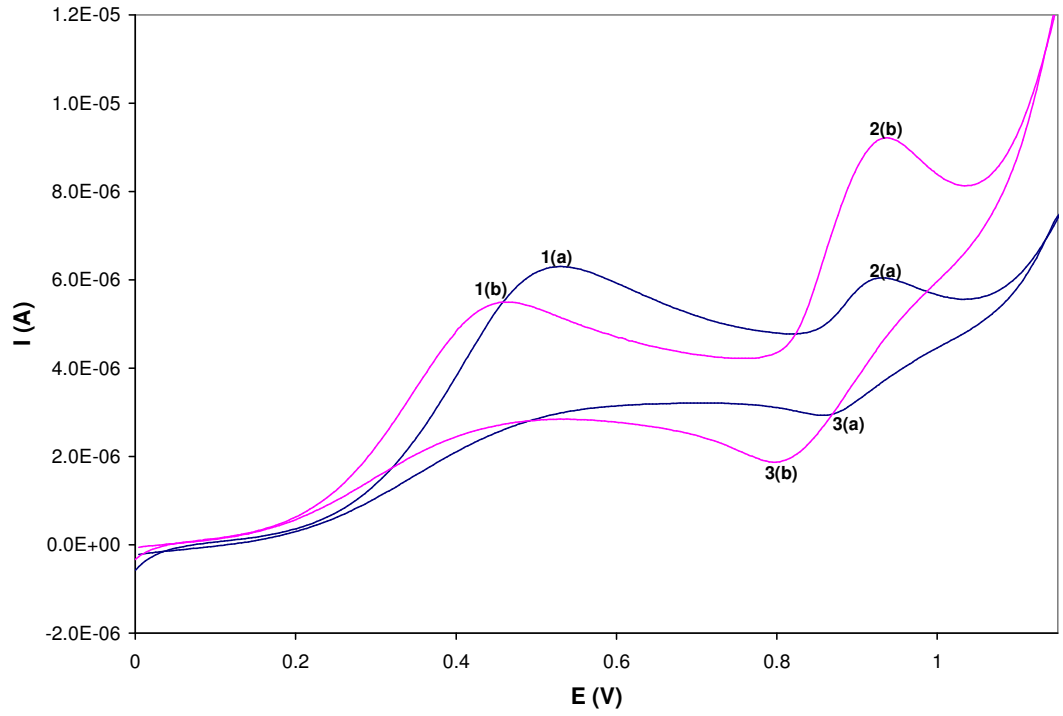

Figure 5.26 Effect of added chloride on the CV curve of $CoCl(PPh_3)_3$. CV curves of $CoCl(PPh_3)_3$ before (—) and after (—) addition of an equivalent concentration of TEACl are presented.

Addition of an equivalent concentration of TEACl to a $CoCl(PPh_3)_3$ solution resulted in a small decrease in the peak current of oxidation peak 1(a) (peak 1(b)) and an increase in current of oxidation peak 2(a) (peak 2(b)) and its coupled reduction peak 3(a) (Peak 3(b)) [Figure 5.26(b)]. An increase in current of oxidation peak 2(a) was assumed to be related to an increase in concentration of added chloride ion to a $CoCl(PPh_3)_3$ complex. Note that peak 1(b) appeared at a less positive potential, whilst peak 2(b) remained at the same potential. An increase in current of peak 2(b) after addition of chloride must indicate formation of another compound (most likely $CoCl_2(PPh_3)_2$).

Comparison of the CV curve of $CoCl_2(PPh_3)_2$ with that of $CoCl(PPh_3)_3$ after addition of an equivalent concentration of TEACl revealed similarities between the oxidation peak 1 and 2; in terms of the peak height, position and shape (Figure 5.27). It appears that electrochemical reactions occurring at peak 2(a) and (b) are the same or are electrochemically reversible whilst electron transfer reactions at peak 1(a) and (b) are irreversible. From this similarity we attributed the oxidation peak 2 of the complexes $CoCl_2(PPh_3)_2$ and $CoCl(PPh_3)_3$ to occur due to oxidation chloride ligand. In conclusion, it appears that chloride is capable of binding to $CoCl(PPh_3)_3$ resulting in replacement of one PPh_3 ligand by a chloride ligand.

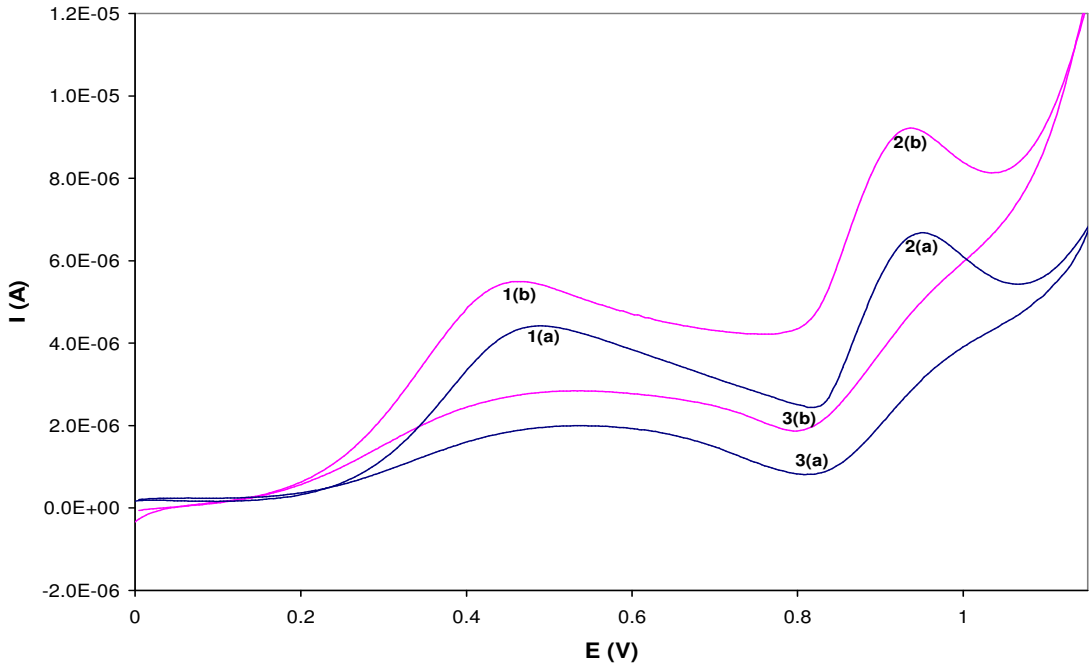

Figure 5.27 Comparison of CV curves of $CoCl_2(PPh_3)_2$ (—) with that of $CoCl(PPh_3)_3$ after addition of an equivalent concentration of TEACl (—).

From the above results, we concluded that addition of chloride (as TEACl) to a solution containing $CoCl(PPh_3)_3$ resulted in addition of a chloride ion to this complex which displaced one PPh_3 molecule from the complex. This was shown by an increase in current of oxidation peak 2(b) (see Figure 5.26(b)) which was previously assigned to chloride ligand oxidation and is evidence of formation of the complex $CoCl_2(PPh_3)_2$ since oxidation peak currents of 2(a) and (b) are equal (see Figure 5.27). Since free PPh_3 was oxidized at E_p = 1.0 V, one would expect its oxidation peak to appear after its replacement by a chloride ligand from $CoCl(PPh_3)_3$ but this was not the case. The explanation to the above statement will be given in the next section (Section 5.1.4) during analysis of CV curves obtained in an experiment involving titration of $CoCl_2(PPh_3)_2$ with PPh_3.

In Figure 5.28 we compared the CV curve of $CoCl(PPh_3)_3$ (b) with that of $CoCl_2(PPh_3)_2$ (a) to further confirm that the oxidation peak 2 arisen due to oxidation of chloride ligand.

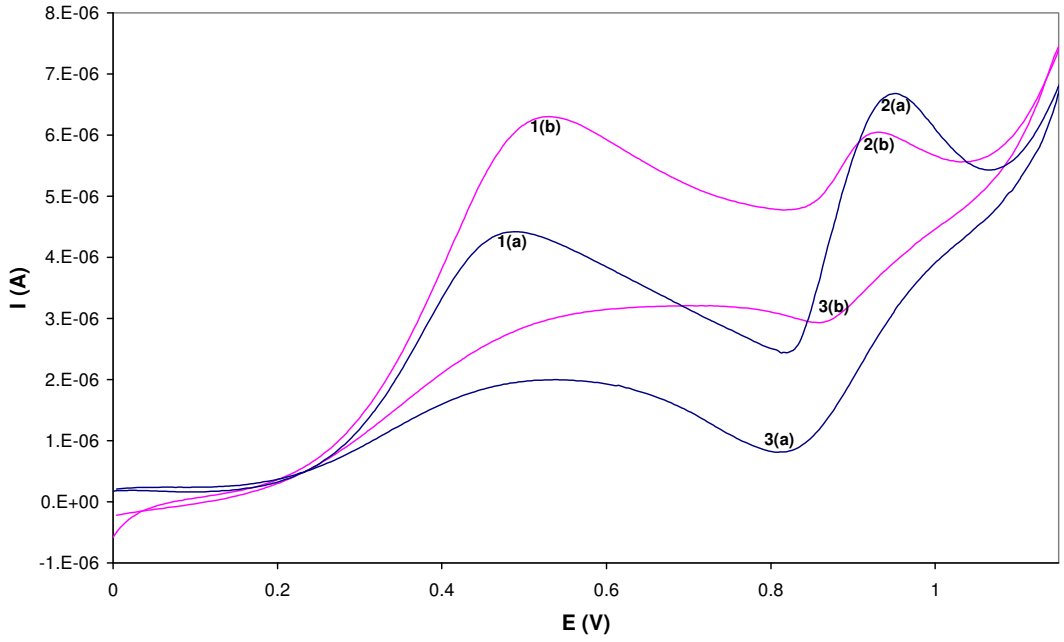

Figure 5.28 Comparison of CV curve of $CoCl_2(PPh_3)_2$ (—) with that of $CoCl(PPh_3)_3$ (—).

It is important to note that when only one chloride ion is attached to a complex molecule i.e. $CoCl(PPh_3)_3$, the current of oxidation peak 2(b) appears lower than for the one obtained from a complex containing two chloride ions i.e. $CoCl_2(PPh_3)_2$ (Figure 5.28). The above result suggests that oxidation peak 2 depends on the concentration of chloride ions attached

to the complex. This further supports the assignment that the oxidation peak 2(a) of $CoCl_2(PPh_3)_2$ arises due to oxidation of chloride ligand. The current of the metal oxidation peak 1(b) of the complex $CoCl(PPh_3)_3$ occurring at E_p = 0.50 V was higher and steeper than that of $CoCl_2(PPh_3)_2$ which we interpreted as involving liberation of two electrons from the complex $CoCl(PPh_3)_3$ [Co^I] to form a Co^{III} complex. We proposed the following overall electrochemical reactions:

Peak 1(b), Figure 5.29: $Co^{I}Cl(PPh_3)_3 \rightarrow [Co^{III}Cl(PPh_3)_3]^+ + 2e^-$ (5.1)

Peak 2(b), Figure 5.28: $Co^{I}Cl(PPh_3)_3 \xrightarrow{TEACl} [Co^{II}Cl_2(PPh_3)_2]^+ + PPh_3 + e^-$ (5.2)

Addition of three (—) and six (**....**) equivalent concentrations of TEACl to a solution containing $CoCl(PPh_3)_3$ resulted in splitting of the oxidation peak 2 into two processes (Figure 5.29). The reduction peaks 3(a) and (b) became broad and shifted to less negative potentials. The metal oxidation peak 1 remained unchanged and shifted only minutely to less negative potentials. The most interesting feature observed from the voltammograms was the appearance of a new oxidation peak 5 at E_p = 0.80 V, which increased in intensity with an increase in concentration of added TEACl.

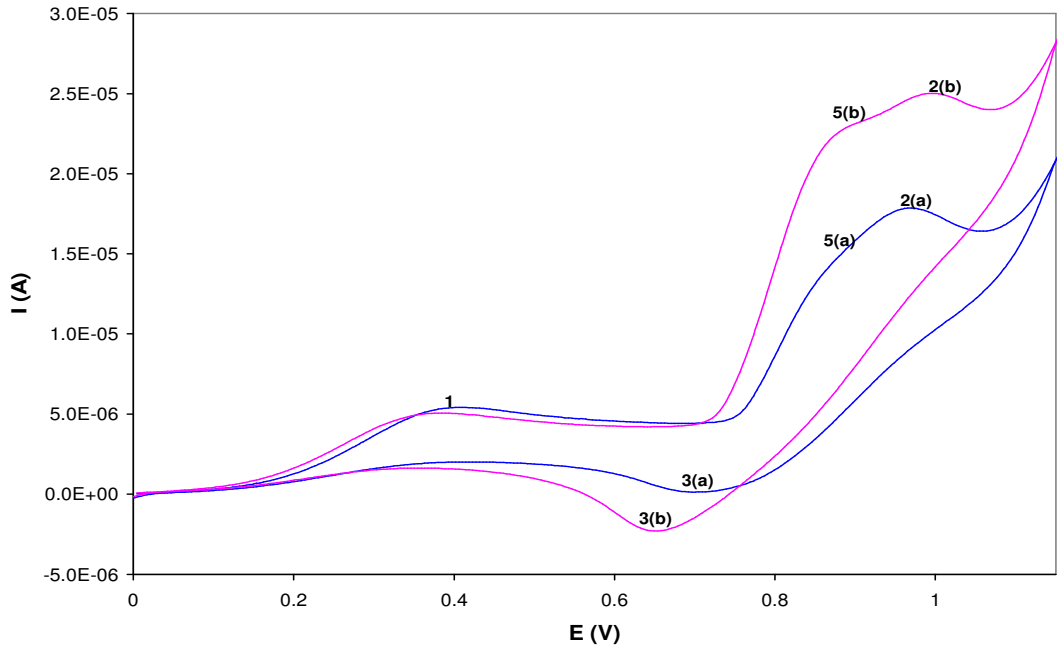

Figure 5.29 CV curves of $CoCl(PPh_3)_3$ after addition of 2.31×10^{-3} mol/l (—) and 4.62×10^{-3} mol/l (—) TEACl.

The appearance of the oxidation peak 5, led us to a conclusion that the broadness and shift to less negative potential of i.e. peak 3(b) was a result of an overlap between this peak and peak 5(b). And from this we concluded that the oxidation peak 5 was due to the oxidation of unbound chloride ion from TEACl present in solution in excess. Also the oxidation peak 5 was at almost the same position as that obtained from a solution containing free TEACl as shown in Figure 5.20.

From the above observation we concluded that the complex $CoCl_2(PPh_3)_2$ is the most stable since addition of excess chloride to $CoCl(PPh_3)_3$ resulted in formation and oxidation of free chloride in solution, thus no further substitution of PPh_3 by chloride could occur.

5.1.4 Monitored Titration of $CoCl_2(PPh_3)_2$ with PPh_3.

5.1.4.1 Cyclic Voltammetry

In this section, the binding ability and the electrocatalytic property of PPh_3 towards the complex $CoCl_2(PPh_3)_2$ is investigated in detail. In the previous section we investigated the binding ability of chloride towards the complex $CoCl(PPh_3)_3$. We found that chloride is capable of binding to $CoCl(PPh_3)_3$ with release of one PPh_3 ligand resulting in formation of $CoCl_2(PPh_3)_2$. CV of $CoCl_2(PPh_3)_2$ before addition of PPh_3 is shown in Figure 5.30.

The oxidation peak 4 was not investigated because an increase in background current was observed at potentials above 1.2 V due to oxygen evolution from traces of water present in the background solvents. As previously assigned, the oxidation peak 1 involved metal oxidation, Co^{II} to Co^{III} whilst oxidation peak 2 involved oxidation of chloride ligand from the complex, $CoCl_2(PPh_3)_2$ (Figure 5.30).

Figure 5.31 shows the CV curve of $CoCl_2(PPh_3)_2$ after addition of 2.5 and 5 equivalent concentration of PPh_3. Addition of 2.5 equivalent concentration of PPh_3 to a $CoCl_2(PPh_3)_2$ solution resulted in an increase in current of oxidation peak 1(a) and a decrease in current of the oxidation peak 2(a) and its coupled reduction peak 3(a) [Figure 5.31(a)]. Addition of 5 equivalent concentration of PPh_3 to a $CoCl_2(PPh_3)_2$ solution resulted in a further increase in peak current of an oxidation peak 1(b) and a further decrease in peak current of an oxidation peak 2(b) [Figure 5.31(b)].

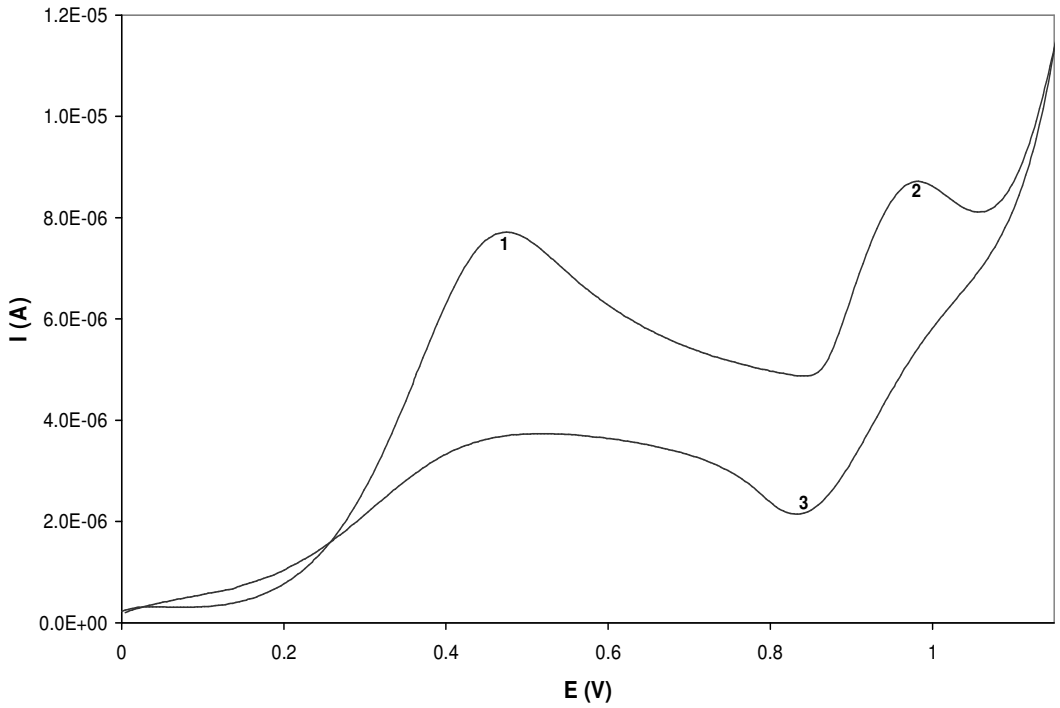

Figure 5.30 CV curves obtained in solutions containing $CoCl_2(PPh_3)_2$ at a Pt disk WE.

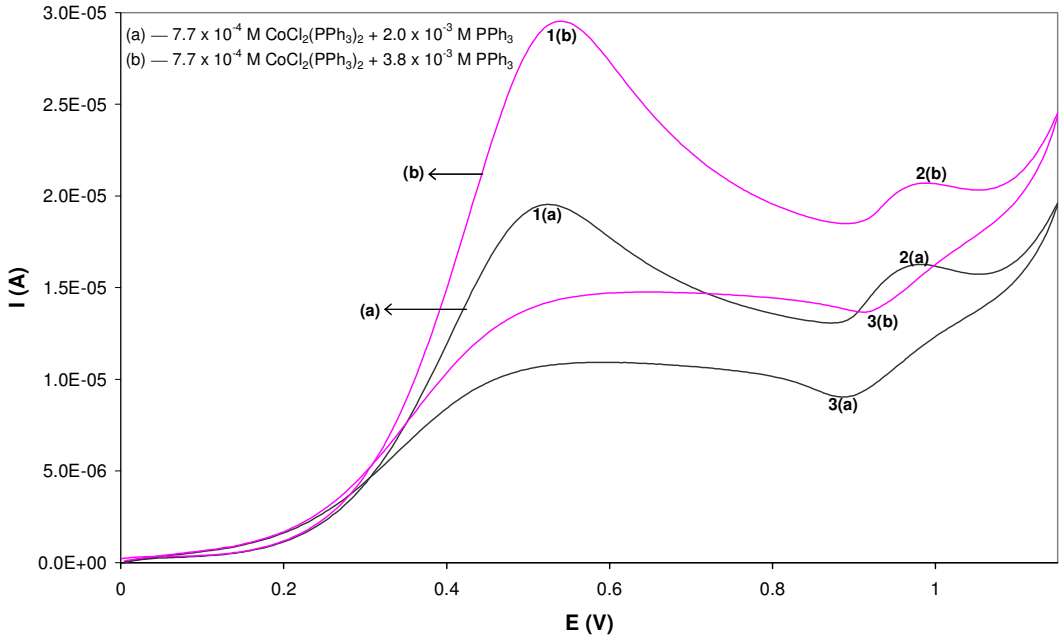

Figure 5.31 CV curves obtained from a solution of $CoCl_2(PPh_3)_2$ after addition of 2.5 (—) and 5 (—) equivalent concentration of PPh_3.

Addition of 15 equivalent concentration of PPh_3 to a $CoCl_2(PPh_3)_2$ solution resulted in an even further increase in current of an oxidation peak 1 and disappearance of an oxidation peak 2 (Figure 5.32).

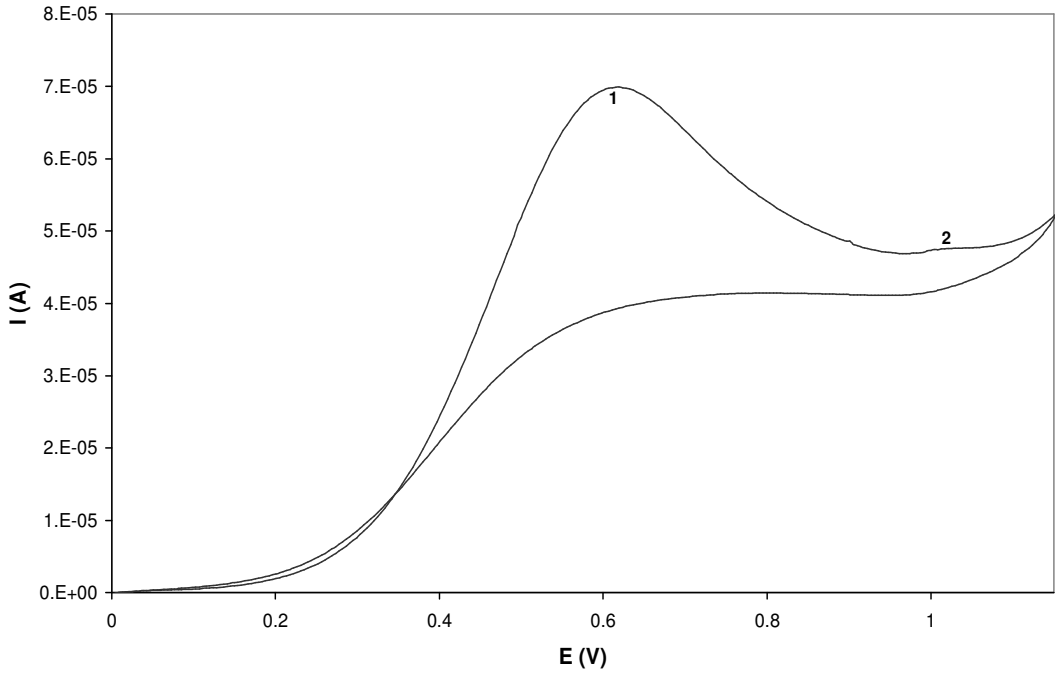

Figure 5.32 CV curve obtained from a solution of $CoCl_2(PPh_3)_2$ after addition of 15 equivalent concentration of PPh_3.

An oxidation peak 2 disappeared either because it is masked by a large oxidation peak 1 or because the species that is oxidized at peak 2 was depleted away from an electrode surface by the added PPh_3. In order to interpret the above results we looked at some literature review on titration of metal complexes with PPh_3.

Switzer and co-workers [72], have studied a CV behaviour of $MeCpMn(CO)_2(CH_3CN)$ in the presence of added PPh_3 in 0.1 M tetraethyl ammonium perchlorate (TEAP) in acetonitrile. They have found that the presence of PPh_3 led to a drastic alteration of the well-behaved, reversible CV of $MeCpMn(CO)_2(CH_3CN)$ which appeared at E_p = 0.22 V. After addition of an equal concentration of PPh_3, another reversible oxidation wave appeared at E_p = 0.55 V, the CV oxidation wave of $MeCpMn(CO)_2(CH_3CN)$ at E_p = 0.22 V became irreversible and decreased in magnitude in proportion to the concentration of PPh_3.

After addition of nine times equivalent concentration of PPh_3 the anodic peak current I_{pa} of $MeCpMn(CO)_2(CH_3CN)$ decreased further in magnitude in proportion to the concentration of PPh_3 and the diffusion current fallen to near zero. This behaviour requires that $MeCpMn(CO)_2(CH_3CN)$ be removed from the vicinity of the electrode by some alternative process that does not require net flow of current. Such a process simultaneously led to the substitution product [P = $MeCpMn(CO)_2(PPh_3)$], which was clearly shown by its reversible CV wave at the higher potential of E_p = 0.55 V. This was confirmed by measuring the CV of the synthesized $MeCpMn(CO)_2(PPh_3)$ and similar results were obtained [72].

The CV behaviour of $CoCl_2(PPh_3)_2$ in the presence of added PPh_3, was explained using the above explanation by Switzer and co-workers [72]. Therefore, we concluded that the disappearance of oxidation peak 2 was a result of depletion of chloride oxidized at this potential away from the electrode surface. This might have resulted in formation of $Co(PPh_3)_4$ in large amounts at the electrode surface, which might explain a large increase in current of oxidation peak 1.

In order to prove that a $Co(PPh_3)_4$ complex is formed, one will have to synthesize this complex using an independent method and record its voltammogram. If the voltammogram can show one irreversible oxidation peak at E_p ~ 0.50 V then we will know for sure that addition of excess PPh_3 results in substitution of all chloride ions from $CoCl_2(PPh_3)_2$ to form $Co(PPh_3)_4$. This behaviour is characteristic of electrocatalysis of ligand exchange.

The CV of $CoCl_2(PPh_3)_2$ after addition of 75 equivalent concentration of PPh_3 is shown in Figure 5.33. Addition of 75 equivalent concentration of PPh_3 to a $CoCl_2(PPh_3)_2$ solution, resulted in an appearance of a new irreversible oxidation peak labelled peak 4 at E_p = 1.0 V (Figure 5.33). The oxidation peak 1 of the complex appeared as a shoulder as it was masked by this new oxidation peak 4 with a very large diffusion current, which appeared when the solution contained large concentration of PPh_3 (Figure 5.33). An irreversible oxidation peak 4 was assigned to oxidation of a free PPh_3, since the CV curve was similar to that of a free PPh_3; and it had no coupled reduction peak. We can conclude that, only when the amount of cobalt from the complex was insufficient to consume all the added PPh_3 was then that the peak for oxidation of free PPh_3 was observed (which happened after addition of ~ 30 equivalent concentration of PPh_3).

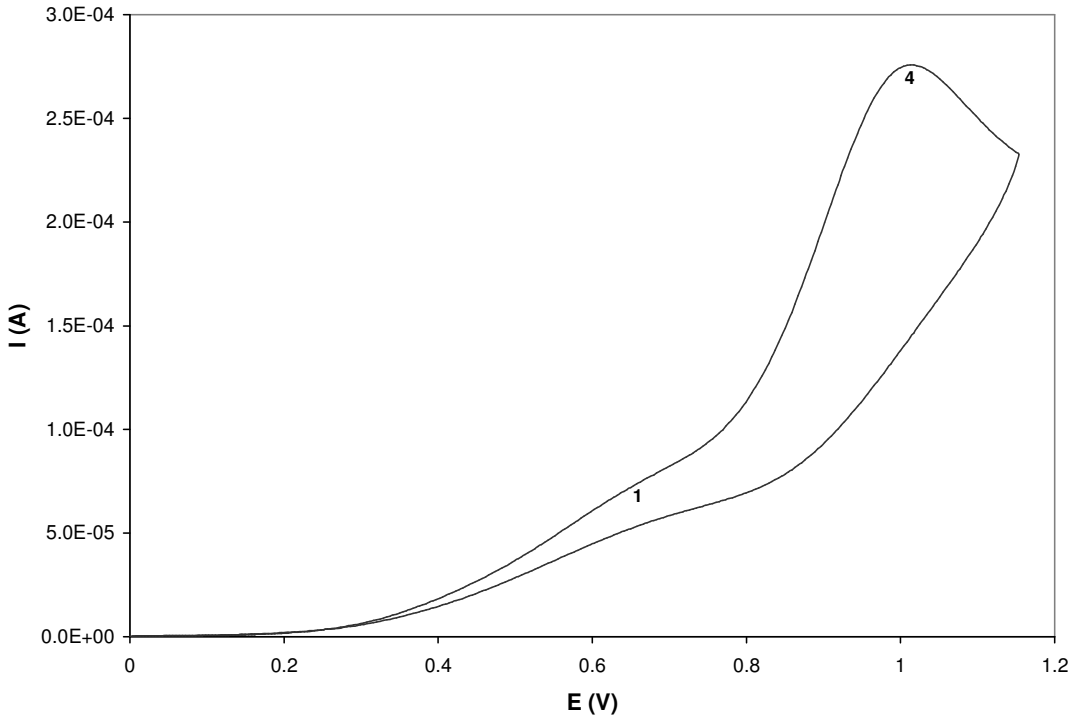

Figure 5.33 CV curve obtained from a solution of $CoCl_2(PPh_3)_2$ after addition of 75 equivalent concentration of PPh_3.

This also explains why we did not observe the oxidation peak of a free PPh_3 in solutions containing $CoCl(PPh_3)_3$ after addition of an equivalent concentration of chloride (Section 5.1.3). Since we concluded that addition of chloride ion to $CoCl(PPh_3)_3$ resulted in replacement of one PPh_3 ligand by a chloride ligand which in turn resulted in formation of a $CoCl_2(PPh_3)_2$ complex.

5.1.4.2 Ultraviolet-Visible Spectroscopy

UV-Visible spectrometry was also used to determine the fate of the bound PPh_3 ligand on the complex $CoCl_2(PPh_3)_2$, by titration of the complex with PPh_3 and comparing the UV-Visible spectrum of a free triphenylphosphine with that of $CoCl_2(PPh_3)_2$.

A UV-Visible spectrum was recorded first from a background solution to check if there is any absorption of the solvent impurities or the supporting electrolyte (Figure 5.34). There was no evidence of absorption of any of the background components from the UV-Vis spectra of the background solution. Nevertheless there is a negative dip in the spectrum of the background solution which might have arisen due to impurities or other substances present in the background solution. The UV-Visible spectrums of PPh_3, $CoCl_2$ and

$CoCl_2(PPh_3)_2$ in a mixture of acetonitrile and pentanol (1:1) containing 0.05 M TBAHFP are presented in Figures 5.35, 5.36 and 5.37.

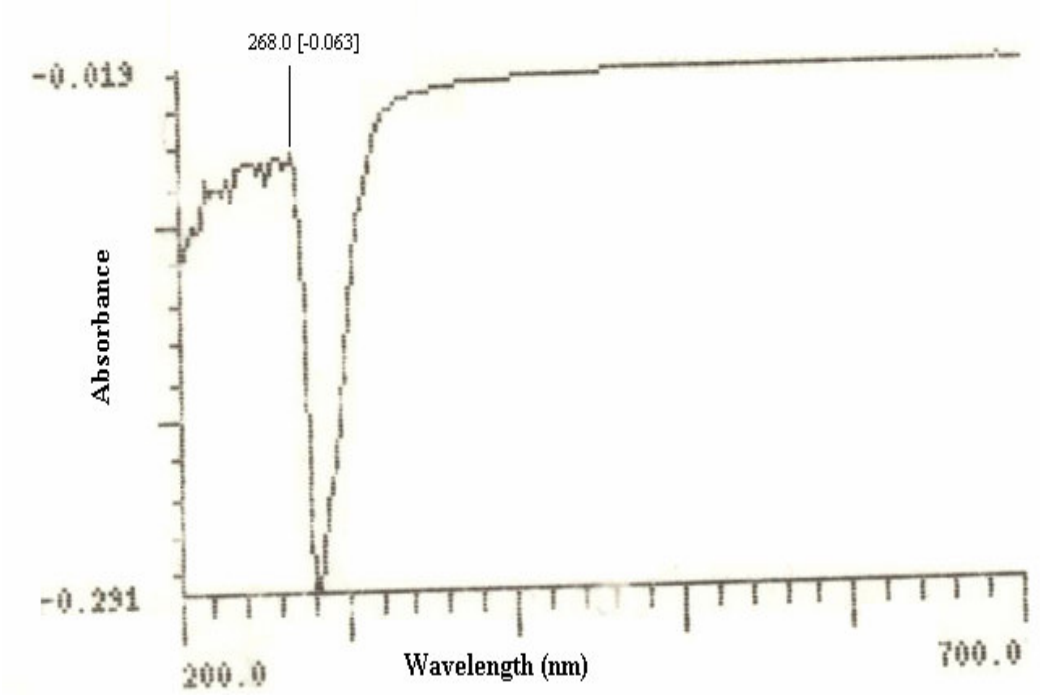

Figure 5.34 UV-Visible spectrum recorded in an acetonitrile background solution containing 0.05 M TBAHFP.

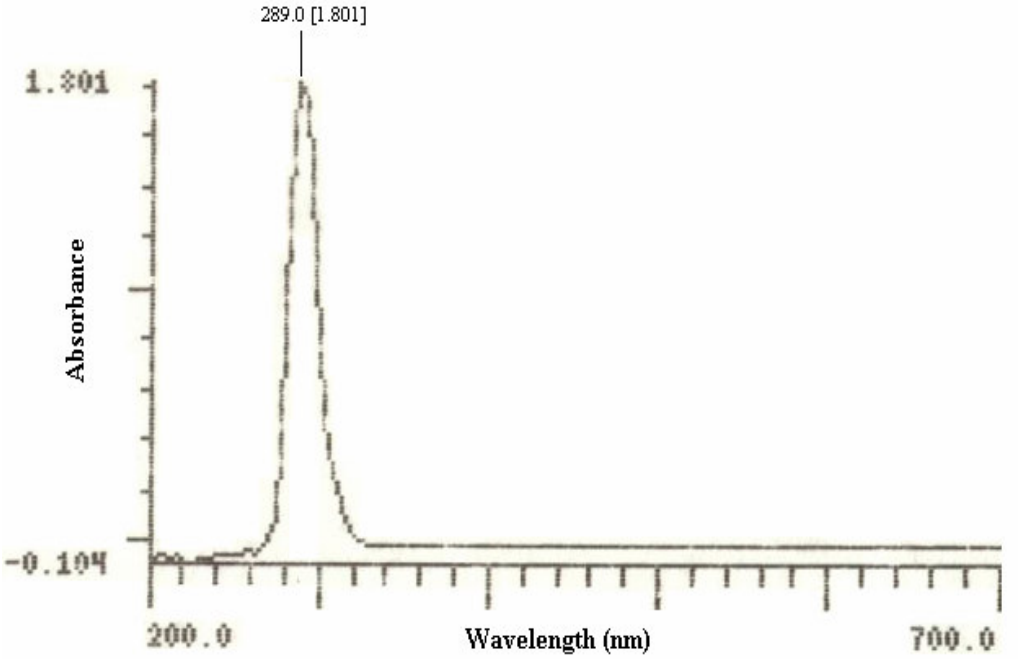

Figure 5.35 UV-Visible spectrum of a 7.7×10^{-4} mol/l PPh_3.

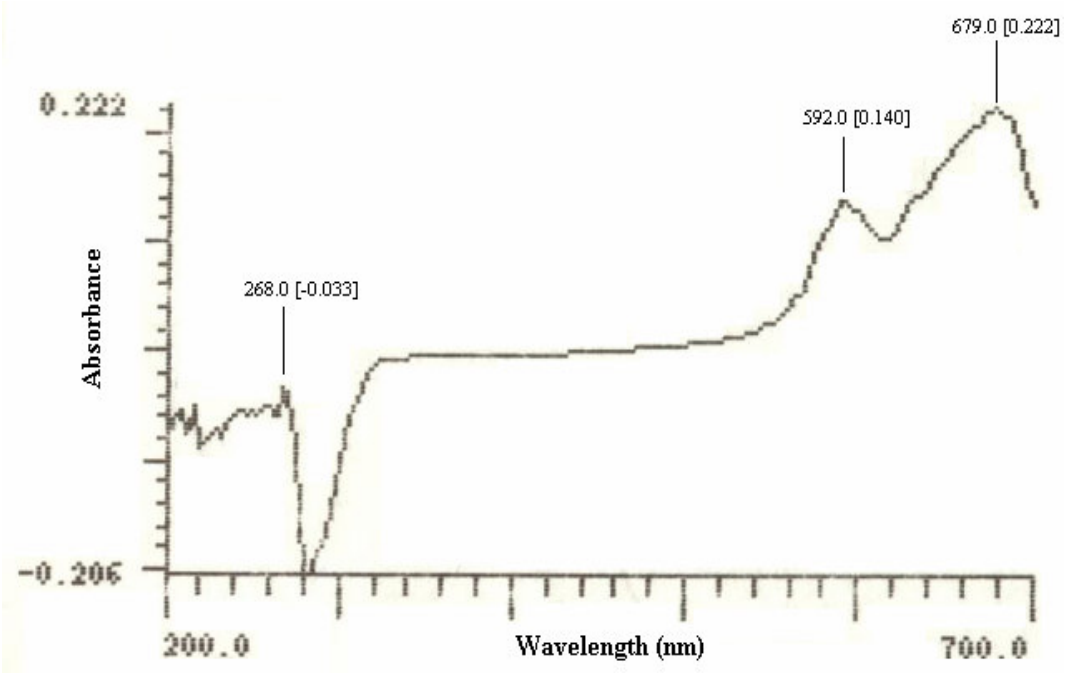

Figure 5.36 UV-Visible spectrum of a 7.7×10^{-4} mol/l $CoCl_2$.

A spectrum of PPh_3 revealed one major intense absorption band at 289 nm; with no bands appearing at higher wavelengths in reasonable agreement with a literature value of 261 nm [73] and 260 nm in acetonitrile, DMF and ethyl alcohol [74] (Figure 5.35). A negative dip observed from the spectrum of the background solution was not observed during measurement of PPh_3 or it was suppressed by a huge peak of PPh_3 absorption at 289 nm. A spectrum of $CoCl_2$ revealed two absorption bands at 592 and 679 nm (Figure 5.36), which are in reasonable agreement with literature values of 600 and 690 nm observed in DMF [75]. A negative dip in spectrum was also observed from the spectrum of $CoCl_2$ and it is at the same position as the one observed from the spectrum of the background solution. The observation of the negative dip might be due to the fact that the absorption peak of $CoCl_2$ are observed at a wavelength far away from were the dip occurs and also because the absorption peaks are very weak. From these results it follows that UV-Visible spectroscopy is very sensitive to PPh_3 since it can be detected easily with a very high absorption signal, but insensitive to cobalt present in $CoCl_2$, as shown by small absorption bands. One can, however, distinguish the UV-Visible spectrum of $CoCl_2$ from that of PPh_3.

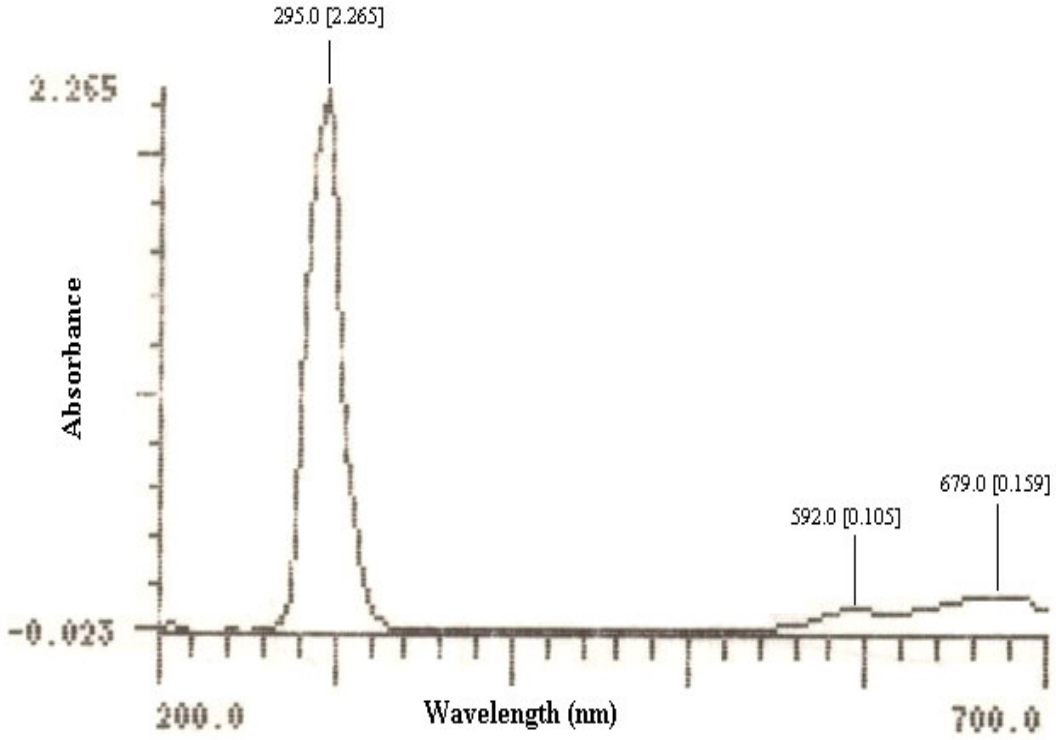

Figure 5.37 UV-Visible spectrum of a 7.7×10^{-4} mol/l $CoCl_2(PPh_3)_2$.

$CoCl_2(PPh_3)_2$ complex on the other hand revealed a major broad absorption band at 295 nm and other two small bands at higher wavelengths of 592 and 679 nm (Figure 5.37). Three absorption bands were found in the literature for a $CoCl_2(PPh_3)_2$ complex in ethyl acetate ($CH_3COC_2H_5$) as 581, 638 and 682 nm and another broad, weak absorption band appeared at ~ 100 to 160 nm [61].

It was mentioned that an absorption band at ~ 100 to 160 nm was so broad that no precise energy values could be ascertained from them, although in truly tetrahedral complexes they provide fairly precise information [61]. Broadening of the UV-Vis spectroscopy of the ligands in $CoCl_2(PPh_3)_2$ (band at 295 nm) indicates a dynamic ligand exchange in both bis- and tris-phosphorus complexes [76]. It is shown from the UV-Visible spectrum of $CoCl_2(PPh_3)_2$ and PPh_3, that one cannot distinguish between the two since they both have a large absorption band at shorter wavelength ~ 290 nm.

In order to assign this band at 297 nm from the UV-Visible spectrum of the complex, we recorded a UV-Visible spectrum of $CoCl_2$ alone in solution and then after addition of 2 equivalent moles of PPh_3 as we have done with cyclic voltammetry.

A UV-Visible spectrum of $CoCl_2$ shown in Figure 5.36, revealed two absorption bands at longer wavelengths of ~ 592 and 679 nm.

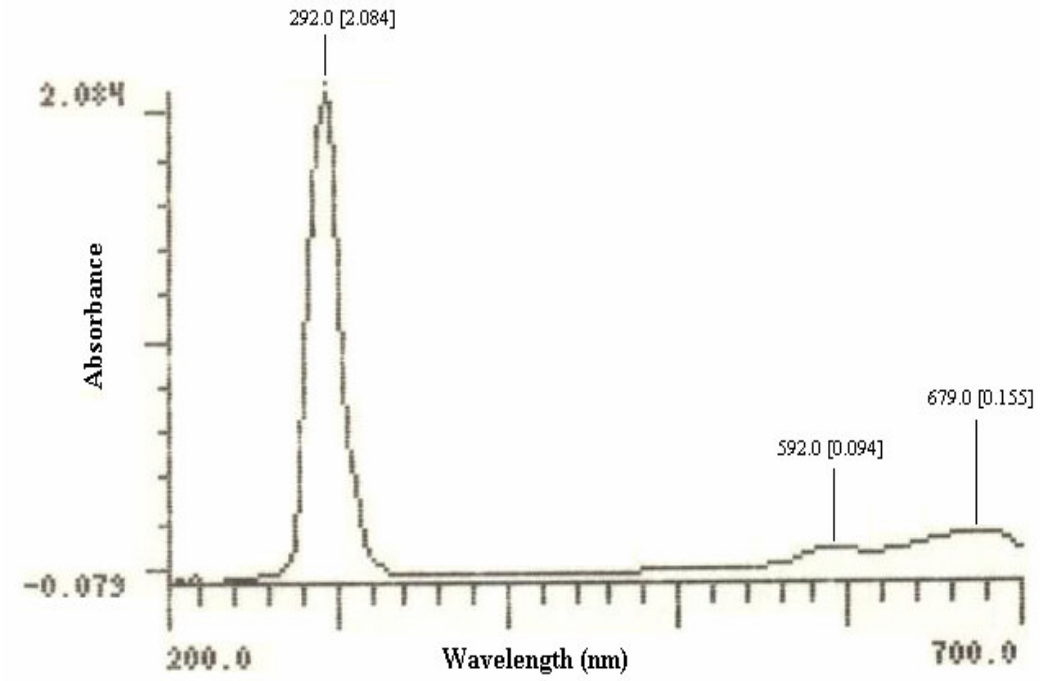

Figure 5.38 UV-Visible spectrum of 7.7×10^{-4} mol/l $CoCl_2$ after addition of 1.54×10^{-3} mol/l (2 equivalent concentration) of PPh_3.

After addition of 2 equivalent moles of PPh_3, another absorption band of large intensity appeared at 292 nm (Figure 5.38). The absorption band at 292 nm agrees in position, shape and height with the one observed from a UV-Visible spectrum of $CoCl_2(PPh_3)_2$. Since this band appeared only after mixing of the two starting materials it was assigned to cobalt absorption from the complex.

Titration of the complex $CoCl_2(PPh_3)_2$ with PPh_3 did not give us any additional information, meaning we did not observe an appearance of a peak for a free PPh_3 even after addition of 75 equivalent moles of PPh_3. This might have arisen due to overlap of the cobalt absorption band from the complex and that of PPh_3 and also no significant change was observed on the absorption bands that appeared at longer wavelengths. The UV-Visible curves for the titration are presented in an Appendix B 2 (Figure B.5 to B.8).

5.1.4.3 ^{31}P Nuclear Magnetic Resonance Spectroscopy

NMR spectroscopy was also used to investigate the effect of added PPh_3 on the NMR spectra of $CoCl_2(PPh_3)_2$. An NMR spectrum of a free triphenylphosphine was recorded first for convenience (Figure 5.41). An NMR spectrum of PPh_3 in $CDCl_3$ shows a main peak at – 4.0465 ppm, in reasonable agreement with a literature value of – 4 ppm recorded in the same solvent $CDCl_3$ [76] and another minor peak appeared at + 31.0421 ppm (Figure 5.39).

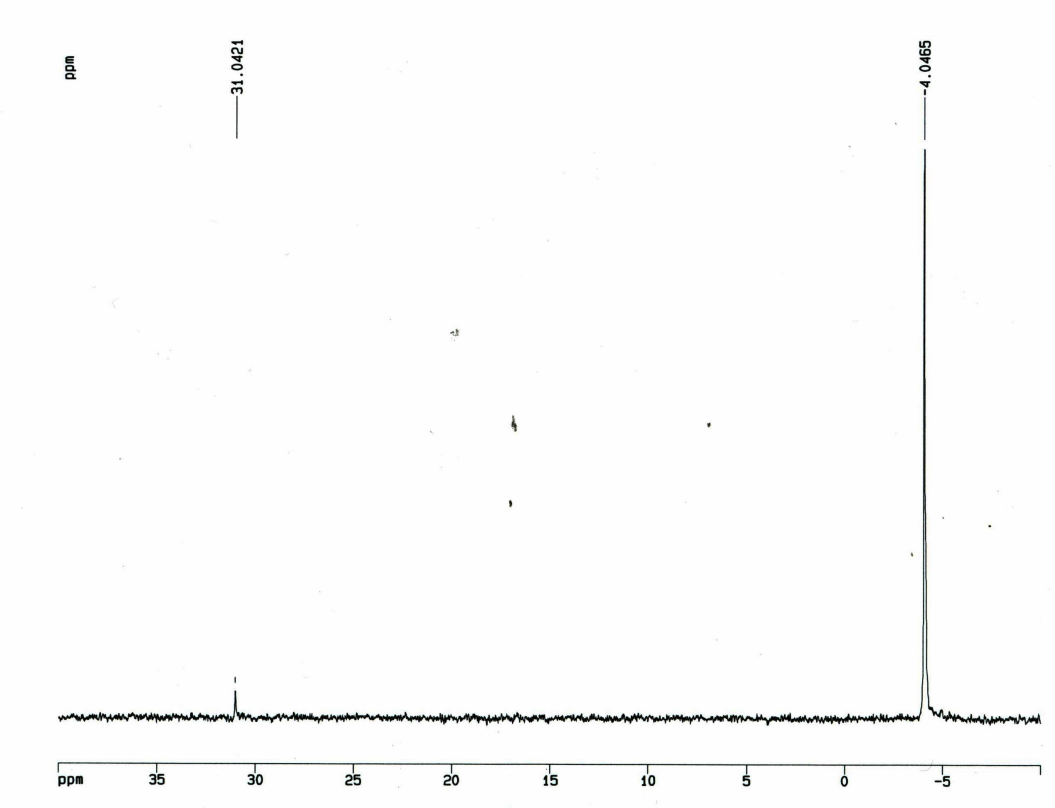

Figure 5.39 ^{31}P NMR signals of triphenylphosphine (PPh_3).

Figure 5.40 shows an NMR spectrum of the complex $CoCl_2(PPh_3)_2$ which revealed a broad peak at – 4.0063 ppm. This peak is at around the same position as that for a free triphenylphosphine. The difference is that the peak shifted downfield and became broad. The broadening of an NMR peak of $CoCl_2(PPh_3)_2$ and the roughness of an NMR baseline arisen due to the presence of paramagnetic ions from cobalt. Furthermore, the peak that appeared up field at + 31.0421 ppm from an NMR spectrum of PPh_3 did not appear from an NMR spectrum of $CoCl_2(PPh_3)_2$. The broadening of the resonance peak of the complex

$CoCl_2(PPh_3)_2$ indicates rapid ligand exchange on the NMR time scale [76]. Most of the phosphorus resonances are also broadened upon complexation [76].

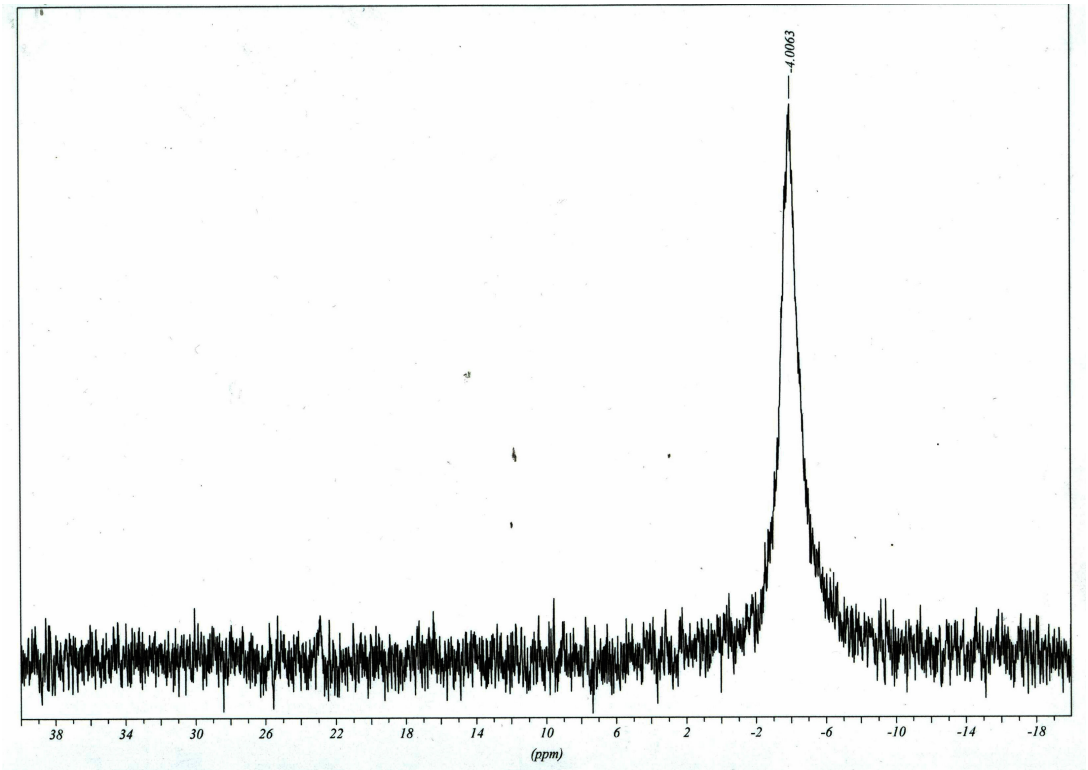

Figure 5.40 ^{31}P NMR signals of $CoCl_2(PPh_3)_2$.

Titration of the complex $CoCl_2(PPh_3)_2$ with PPh_3 resulted in an appearance of a new peak resonance at ~ + 30 ppm, which appeared only after addition of 15 equivalent moles of PPh_3 and increased with an increase in concentration of PPh_3. The peak at ~ – 4 ppm shifted to more negative resonance with an increase in concentration of PPh_3. The shift in peak position for a peak that appears downfield at ~ – 4 ppm to more negative resonance and the appearance of another peak up field at ~ + 30 ppm, indicates the formation of a free PPh_3 in solution. The NMR curves obtained during titration are presented in Appendix B 3 (Figure B.9 to B.12).

5.2 FERROCENE AS AN INTERNAL STANDARD FOR ELECTROCHEMICAL MEASUREMENTS

In this section we will focus on the electrochemical behaviour of cobalt compounds in the presence of added ferrocene as an internal standard. Ferrocene was chosen as it is oxidized reversibly with transfer of one-electron and because like cobalt it is a transition metal

compound. After the electrochemistry attributed to the compound of interest has been identified, ferrocene was added to the working compartment of the cell. The electrochemical experiment (a CV scan) was repeated, and the position of the CV peaks were directly compared to the potential of ferrocene. If ferrocene is used as an internal standard the reversible oxidation peaks of it must be observed at an appropriate position. It is also worth noting that the $Fe^{2+}Cp/Fe^{3+}Cp$ couple may be inappropriate as an internal standard for some systems due to overlapping signals. In these cases other compounds like cobaltocene or any of a variety of aromatic compounds, can be used as internal standards [77].

Employing a redox couple as an internal standard in electrochemical experiments can be compared to the use of internal standards in nuclear magnetic resonance spectroscopy. For example, in proton NMR spectroscopy tetramethylsilane is commonly used to reference chemical shifts of other protons but is sometimes replaced by chloroform or other materials to avoid overlapping signals. As with NMR standards, an ideal electrochemical internal standard should not interact with any species in solution [77]. Also comparing the CV curves of cobalt compounds and those of mixture of cobalt compounds and ferrocene, we should be able to detect from the spectra if we can distinguish the oxidation potentials of different metals present in the same solution. This experiment was performed in a mixture of acetonitrile and pentanol (1:1) containing 0.05 M $TBAPF_6$.

5.2.1 Investigations involving $CoCl_2(PPh_3)_2$, $CoCl_2$ and PPh_3.

In this sub-section we focussed on the analysis of the CV curves of $CoCl_2(PPh_3)_2$, $CoCl_2$ and PPh_3 in the presence of added ferrocene as an internal standard. Figure 5.41 presents a CV of $CoCl_2(PPh_3)_2$ before and after addition of equivalent concentration of ferrocene. CV of ferrocene in the same solvent mixture is also shown for reference. CV of $CoCl_2(PPh_3)_2$ reveals two oxidation peaks labelled 1(a) and 2(a) at E_p = 0.55 V and 1.0 V and one reduction peak labelled 3(a) at E_p = 0.80 V (Figure 5.41). Addition of an equivalent concentration of ferrocene resulted in an appearance of a reversible oxidation peak of ferrocene labelled peak 4(b) at E_p = 0.19 V. Oxidation peak 1(a) of $CoCl_2(PPh_3)_2$ shifted to more positive potentials and became broad (peak 1(b)). The oxidation peak 2(a) and reduction peak 3(a) disappeared. Comparison with the CV curve of ferrocene showed that the current of a reversible oxidation peak 4(c) of ferrocene became 2 times higher after

addition to $CoCl_2(PPh_3)_2$ (peak 4(b)). An increase in a reversible oxidation process of ferrocene and a disappearance of a chloride oxidation peak 2(a) might suggest that ferrocene is oxidizing chloride. The most interesting feature observed from the voltammogram was an appearance of another rather small, ill-defined reduction peak at less negative potentials of ~ – 0.10 V.

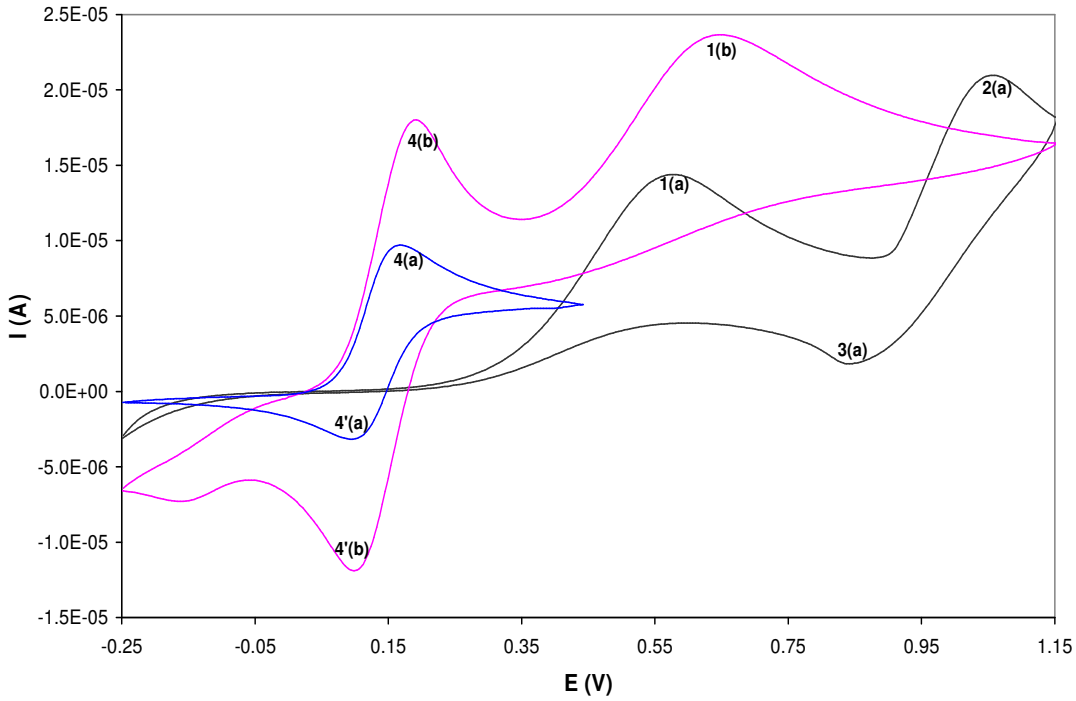

Figure 5.41 CV curve of a 2.0×10^{-3} mol/l $CoCl_2(PPh_3)_2$ before (—) and after (—) addition of an equivalent concentration of ferrocene as an internal standard. CV of a 2.0×10^{-3} mol/l ferrocene (—) is shown for reference.

To further verify the above observations, we analysed the CV curve of $CoCl_2$ before and after addition of an equivalent concentration of ferrocene (Figure 5.42). CV of $CoCl_2$ reveals one oxidation peak labelled 1(a) at E_p = 1.0 V and one reduction peak labelled 1'(a) at E_p = 0.65 V (Figure 5.42). Addition of an equivalent amount of ferrocene resulted in appearance of one broad oxidation peak 2(b) at E_p = 0.35 V and reduction peak 2'(b) at E_p = 0 V. The oxidation peak 1(a) and its coupled reduction peak 1'(a) for the oxidation of $CoCl_2$ disappeared. A new reduction peak was also observed at less negative potentials of ~ – 0.20 V. These results are similar to those observed from the CV of $CoCl_2(PPh_3)_2$ where oxidation peak 2 disappeared and a ferrocene oxidation peak current increased.

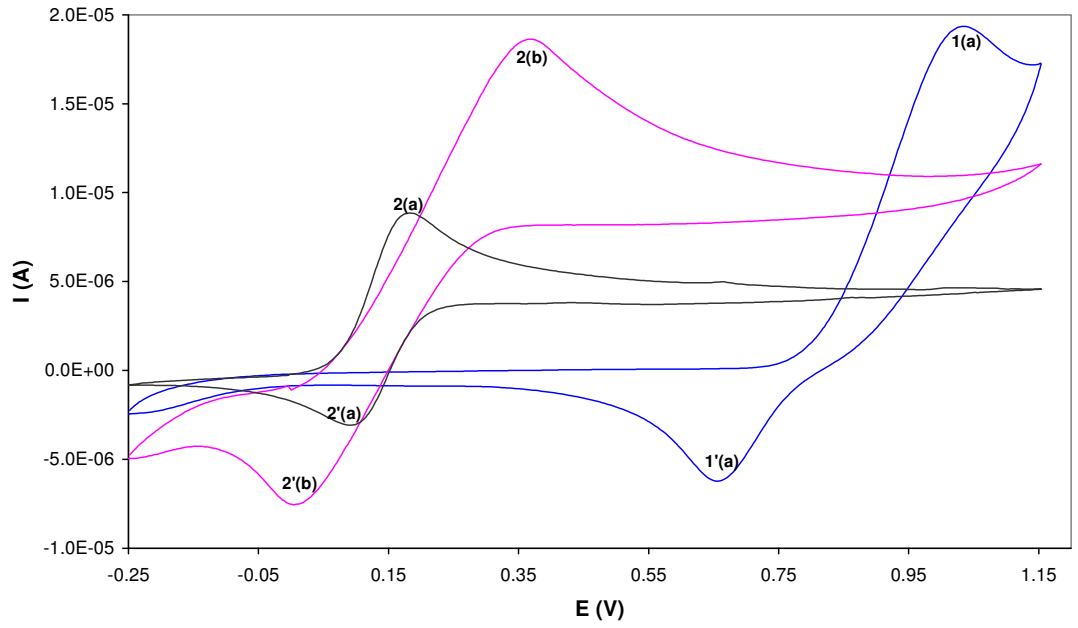

Figure 5.42 CV curve of a 2.0×10^{-3} mol/l $CoCl_2$ before (—) and after (—) addition of an equivalent concentration of ferrocene as an internal standard. CV of a 2.0×10^{-3} mol/l ferrocene (—) is shown for reference.

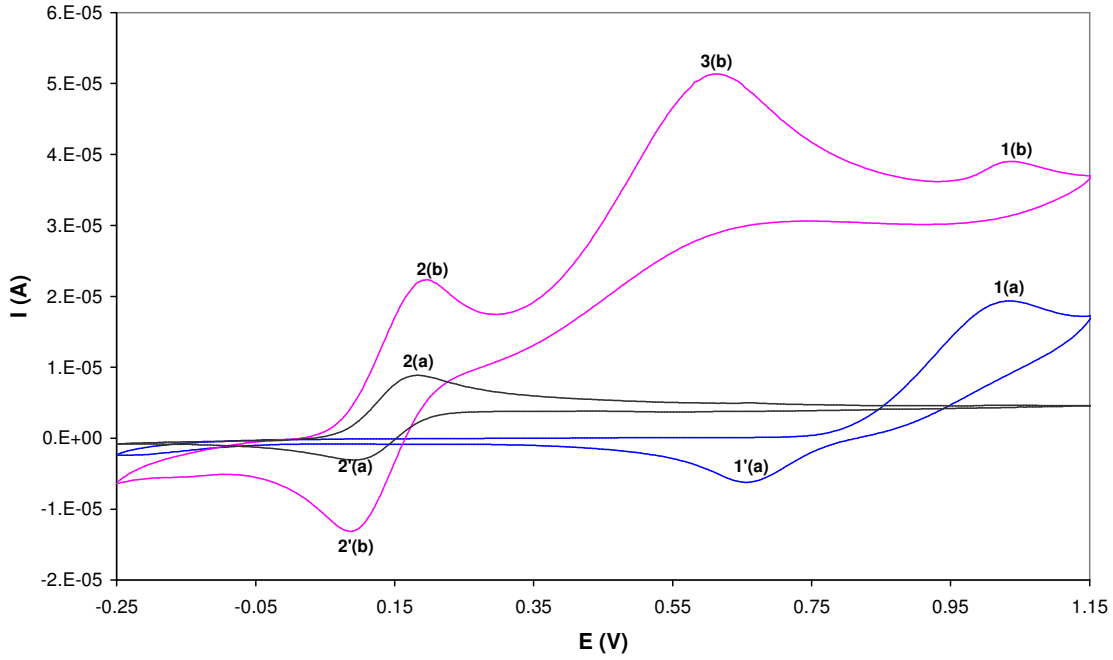

Figure 5.43 CV curve of a 2.0×10^{-3} mol/l $CoCl_2$ before (—) and after (—) addition of an equivalent concentration of ferrocene as an internal standard and 4.0×10^{-3} mol/l PPh_3. CV of a 2.0×10^{-3} mol/l ferrocene (—) is shown for reference.

This result verifies the assignment made above that ferrocene oxidize chloride resulting in formation of another species since the oxidation peak of ferrocene was also not observed. It appears that ferrocene can only oxidize chloride (the species oxidized at peak 2(a) Figure 5.41), but it cannot oxidize Co^{II} (a species oxidized at peak 1(a)) from the CV of $CoCl_2(PPh_3)_2$. To further confirm this two equivalent concentrations of PPh_3 were added to a solution containing both ferrocene and $CoCl_2$ (Figure 5.43).

It can be seen from Figure 5.43 that addition of two equivalent concentrations of PPh_3 resulted in a appearance of another irreversible oxidation peak of cobalt at E_p = 0.6 V due to the formation of a complex $CoCl_2(PPh_3)_2$. The oxidation peak 1(a) of $CoCl_2$ decreased tremendously in height and its reduction peak 1'(a) disappeared. Electrochemically oxidized ferrocene resulted in formation of redox couple $Fe^{2+}Cp_2/Fe^{3+}Cp_2$ that in turn oxidized chloride leading to a tremendous increase in height of the ferrocene peaks. This result supports the above conclusion that ferrocene oxidized chloride but did not oxidize Co^{II} from the complex.

In principle, the reversibility of the ferrocenium couple suggests that the ferrocenium ion can be used only with compounds with negative formal oxidation potentials [78]. Ferrocene has the ability to interact with other compounds and may catalyze electron-transfer reactions normally occurring at more positive potentials [78]. In such cases use of substituted ferrocenes with electron withdrawing substituents is permitted as potential mediators of the electron-transfer-catalyzed oxidation of compounds with $E_{1/2}$ more positive than 0.0 V. The substituted ferrocenium ions themselves need not be isolable, and a catalytic cycle would be sustained if the redox couple is reversible and its members are both inert to side reactions [78]. From this literature studies it appears that ferrocene caused catalyzed electron-transfer reactions of $CoCl_2(PPh_3)_2$ and $CoCl_2$ since these compounds in the absence of ferrocene are oxidized at more positive potentials.

To further confirm the conclusion that there is an interaction between ferrocene and the studied cobalt compounds, we analysed the CV of PPh_3, in the presence of added ferrocene since PPh_3 is also oxidized at more positive potentials. CV curve of PPh_3 before and after addition of an equivalent concentration of ferrocene is presented in Figure 5.44. CV of PPh_3 reveals one irreversible oxidation peak labelled 1(a) at E_p = 1.0 V (Figure 5.44). Addition of an equivalent concentration of ferrocene resulted in an appearance of a reversible oxidation

peak of ferrocene labelled peak 2(b) at E_p = 0.19 V, an irreversible oxidation peak 1(b) of PPh_3 remained at the same position and retained its current intensity. Surprisingly, peak currents of a reversible ferrocene couple increased by a factor of 2 after addition to PPh_3. Also a reduction peak observed at less negative potentials of – 0.10 V and – 0.20 V from the CV of $CoCl_2(PPh_3)_2$ and that of $CoCl_2$ was not observed from the CV of PPh_3 after addition of ferrocene. This suggests that a new reduction peak might be related to the reduction peak of chloride ion at 0.85 V for the complex $CoCl_2(PPh_3)_2$ and at 0.65 V for $CoCl_2$ since it disappeared after addition of ferrocene.

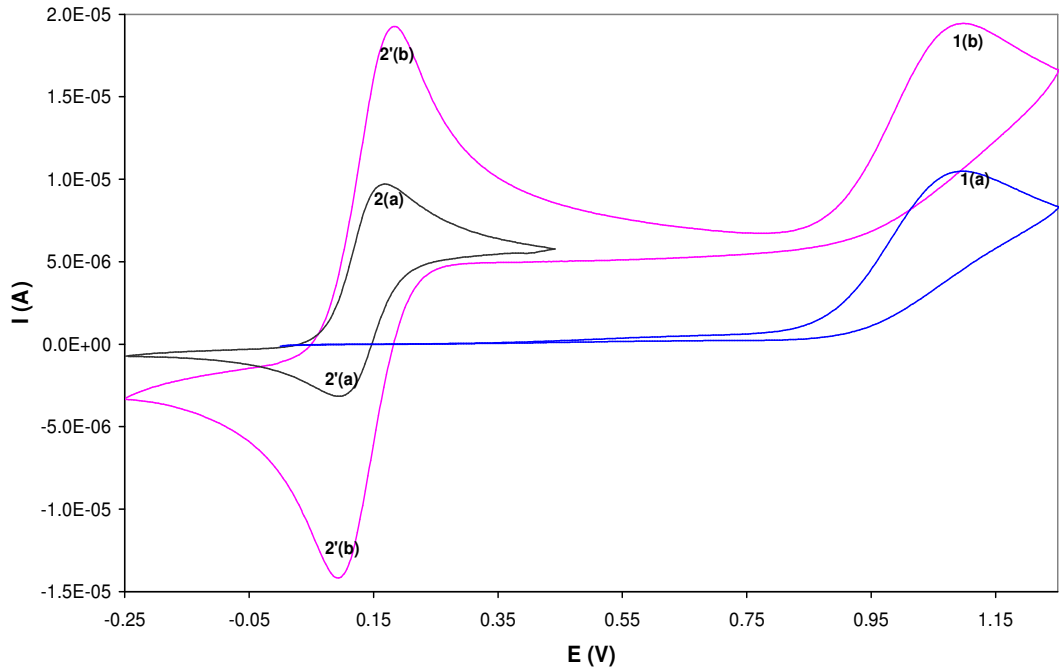

Figure 5.44 CV curve of a 2.0×10^{-3} mol/l PPh_3 before (—) and after (—) addition of an equivalent concentration of ferrocene as an internal standard. CV of a 2.0×10^{-3} mol/l ferrocene (—) is shown for reference.

From the above results we concluded that an increase in peak current of the ferrocene couple arisen due to interaction or catalytic reaction of ferrocene with $CoCl_2(PPh_3)_2$, $CoCl_2$ and PPh_3 since they are all oxidized at more positive potentials. And a disappearance of a chloride oxidation peak 2(a) and 1(a) from the complex $CoCl_2(PPh_3)_2$ and from $CoCl_2$ arisen because they were oxidized by ferrocene. Moreover, a disappearance of a reduction peak 3(a) and 1'(a) from $CoCl_2(PPh_3)_2$ and $CoCl_2$ and an appearance of new reduction peaks at less negative potentials might also be related to oxidation of chloride by ferrocene. This

then led to a shift in oxidation peak potentials to more positive and a shift in reduction peak potentials to less negative.

In order to verify that chloride is oxidized by ferrocene, we recorded the CV curves starting with ferrocene alone in solution and then adding an equivalent concentration of $CoCl_2(PPh_3)_2$ (Figure 5.45).

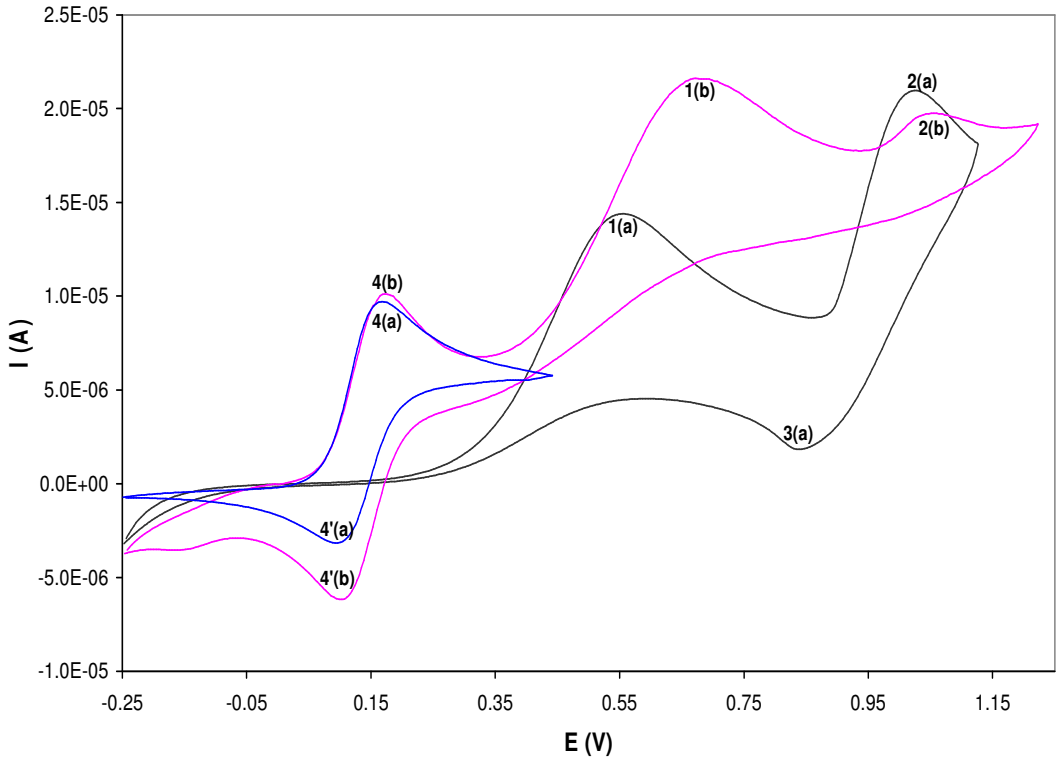

Figure 5.45 CV curve of a 2.0×10^{-3} mol/l ferrocene before (—) and after (—) addition of an equivalent concentration of $CoCl_2(PPh_3)_2$. CV of a 2.0×10^{-3} mol/l $CoCl_2(PPh_3)_2$ (—) is shown for reference.

If we start recording the CV with ferrocene in solution, and then add an equivalent concentration of $CoCl_2(PPh_3)_2$, peak 4(a) for the oxidation of ferrocene remains unchanged but the reduction peak 4'(a) slightly increases in current. Peak 1(a) shifted to more positive potentials as before but retained its shape and height. Peak 2(a) decreased tremendously in current and its coupled reduction peak 3(a) disappeared and a new reduction peak was observed at less positive potentials of ~ – 0.10 V. Before analysis of the above we performed a similar experiment using $CoCl_2$.

The same behaviour was observed from a CV of ferrocene after addition of $CoCl_2$ (Figure 5.46). No significant change was observed from the oxidation peak of ferrocene, whilst peak 1(a) for the chloride oxidation decreased tremendously to almost zero current and its coupled reduction peak 1'(a) disappeared. A new reduction peak was also observed at less negative potentials of ~ – 0.20 V.

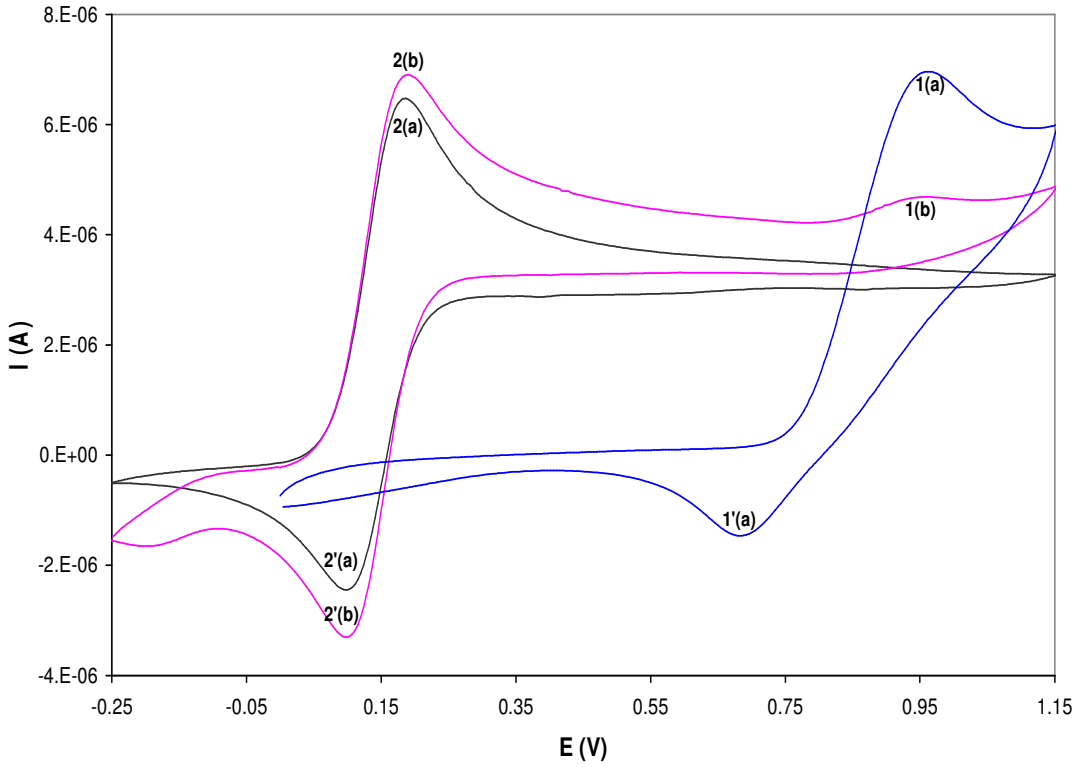

Figure 5.46 CV curve of a 7.7 × 10^{-4} mol/l ferrocene before (—) and after (—) addition of an equivalent concentration of $CoCl_2$. CV of a 7.7 × 10^{-4} mol/l $CoCl_2$ (—) is shown for reference.

Addition of 2 equivalent concentrations of $CoCl_2$ (Figure 5.47) resulted in an increase in peak current of an oxidation peak 1(a). The reduction peak 1'(a) is still absent and a new reduction peak at less negative potentials of ~ – 0.20 V increased in height. From these results we can conclude that ferrocene is capable of oxidizing chloride ion resulting in a shift in the chloride oxidation peak to less positive potentials. In conclusion, we cannot recommend the use of ferrocene as an internal standard for compounds containing chloride so one will have to choose other compounds like substituted ferrocene that can be used as internal standards that are inert to side reactions.

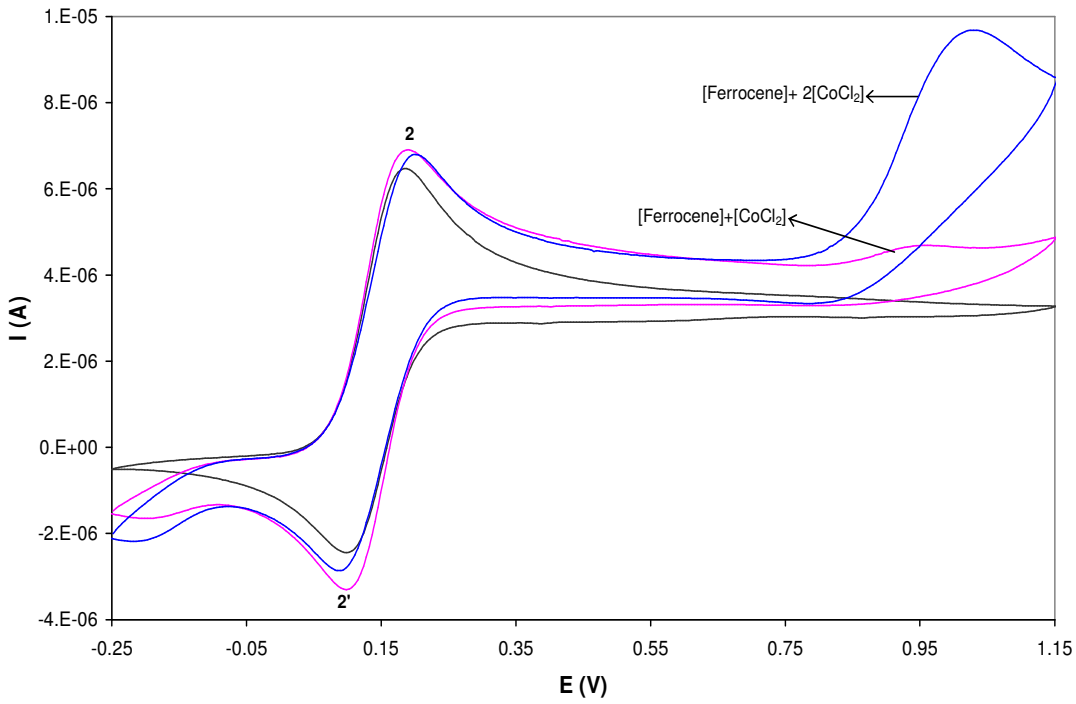

Figure 5.47 CV curve of a 7.7 × 10^{-4} mol/l ferrocene before and after addition of several concentrations of $CoCl_2$.

5.3 DETERMINATION OF PHYSICAL PARAMETERS USING CHRONOAMPEROMETRY

This subsection will focus on determination of the diffusion coefficient (D, in cm^2/s), electrochemical surface area (A, in cm^2) of the working electrode (WE) and number of electrons (n, in mol^{-1}) involved during oxidation of the studied cobalt compounds. Chronoamperometry has proven useful for the measurement of diffusion coefficients of electroactive species. An average value of $it^{1/2}$ over a range of time is determined at an electrode with an area which is accurately known and with a solution of known concentration. The diffusion coefficient can then be calculated from $it^{1/2}$ via the Cottrell equation. Although the electrode area can be physically measured, a common practice is to measure it electrochemically by performing the chronoamperometric experiment on a redox species whose diffusion coefficient is known (because a physically measured A does not take into account other factors like surface area roughness). The value of A is then calculated from $it^{1/2}$. Such an electrochemically measured surface area takes into account

any unusual surface geometry that may be difficult to measure geometrically [2]. The Cottrell equation is given as:

$$i_t = {nFACD^{1/2}}/{\pi^{1/2}t^{1/2}} \quad (5.3)$$

where C is a concentration of the electroactive species (mol/cm^3), F is the Faraday's constant (96485 A.s), i_t is a current at time t (A) and t is the time (s).

Ferrocene was used to measure the electrochemical surface area of the WE, since it is a well-studied reversible redox active species, which involves transfer of one-electron and its diffusion coefficient is known in many non-aqueous solvents. In this section we will first show the data obtained with ferrocene to determine the electrochemical surface area and the diffusion coefficient of ferrocene in a mixture of acetonitrile and pentanol. We will then use the electrochemically determined electrode area to determine the diffusion coefficient and number of electrons involved in the oxidation of the studied cobalt compounds.

Figure 5.48 presents the voltammograms of ferrocene obtained, in acetonitrile and in a mixture of acetonitrile and pentanol. CV was recorded first to determine the applied potentials that can be used in chronoamperometric experiments. A potential of 0.20 V was applied for ferrocene solutions in acetonitrile whilst 0.25 V was applied for ferrocene solutions in a mixture of acetonitrile and pentanol, the corresponding chronoamperometric plots are shown in Figure 5.49. And from these plots a current versus square root of time curve, known as a Cottrell plot, was constructed (Figure 5.50).

The slope was obtained using a linear regression analysis and was used to calculate the electrochemical surface area as follows:

$$i_t = {nFACD^{1/2}}/{\pi^{1/2}t^{1/2}}$$

Therefore, slope for Cottrell plot = $it^{1/2}$

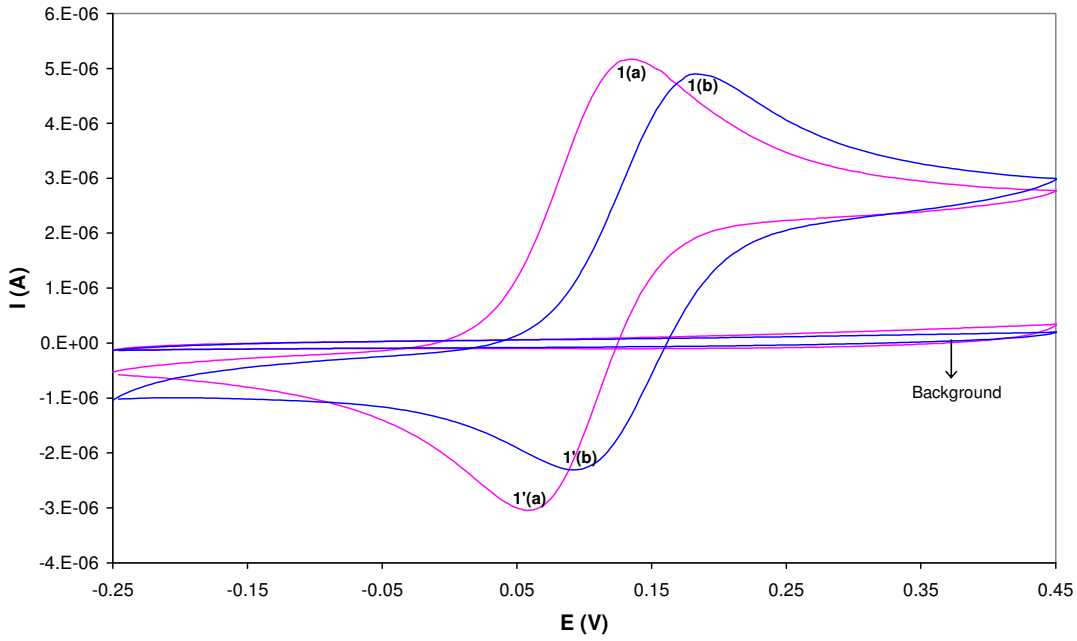

Figure 5.48 CV curves of ferrocene obtained in (—) acetonitrile and in (—) a mixture of acetonitrile and pentanol (1:1).

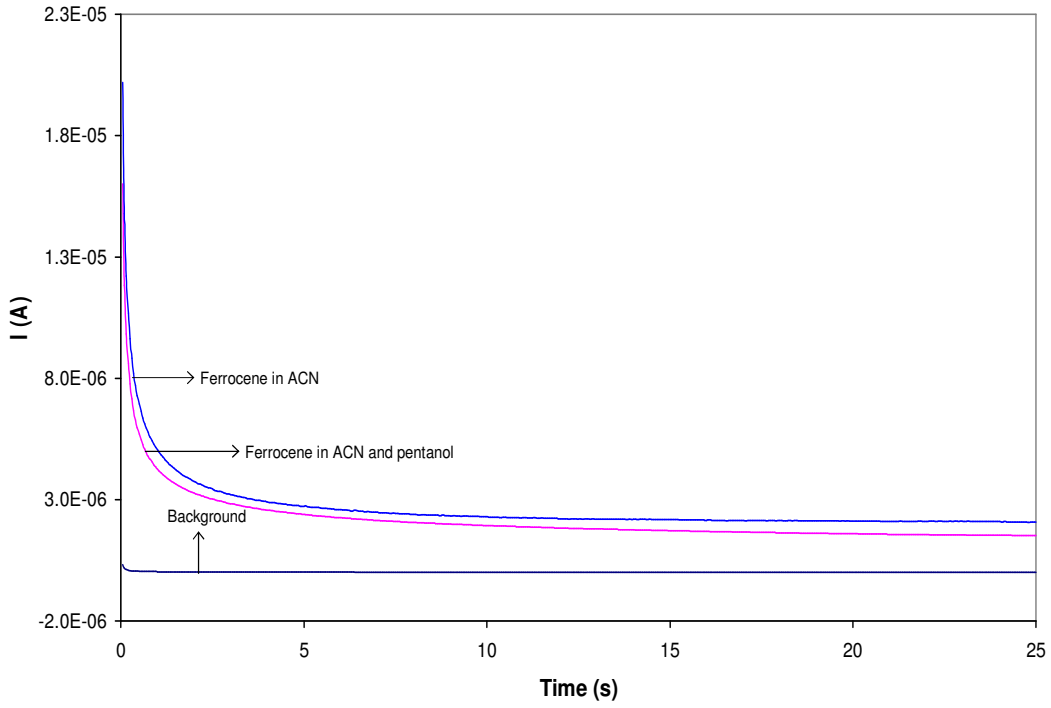

Figure 5.49 Chronoamperometric plots for Ferrocene obtained in acetonitrile ($E_{applied}$ = 0.2 V) and in a mixture of acetonitrile and pentanol ($E_{applied}$ = 0.25 V).

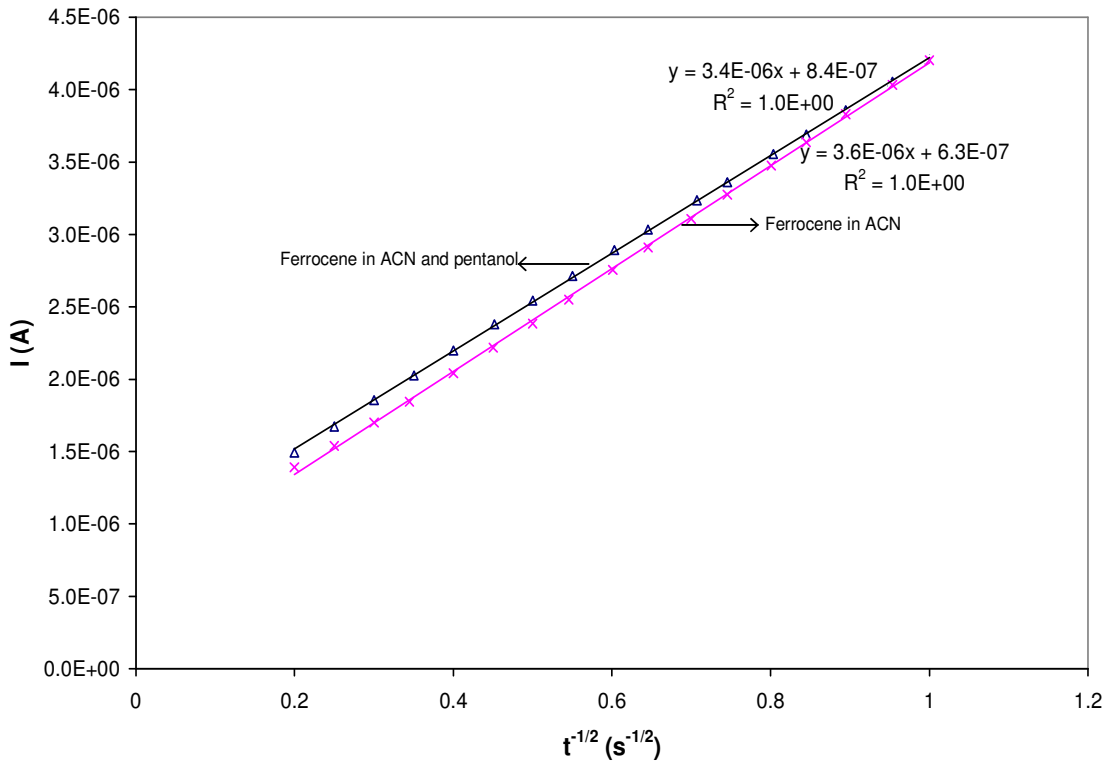

Figure 5.50 Cottrell plots obtained from data in Figure 5.49.

Hence, Slope = $nFAC(D/\pi)^{1/2}$

Area $= it^{1/2} / nFC(D/\pi)^{1/2}$

Slope $= 3.6 \times 10^{-6}$ A.s$^{1/2}$

D $= 2.37 \times 10^{-5}$ cm^2/s [63]

C $= 7.7 \times 10^{-7}$ mol/cm^3

F $= 96485$ A.s

n $= 1$ mol^{-1}

$$A = \left[3.6\times10^{-6}\ As^{1/2} \Big/ (1\ mol^{-1})(96485\ A.s)(7.7\times10^{-7}\ mol/cm^3)\left(\sqrt{2.37\times10^{-5}\ cm^2/s/\pi}\right) \right]$$

$$= 0.0176\ cm^2$$

We used the measured electrochemical surface area of the working electrode to determine the diffusion coefficient of ferrocene in a mixture of acetonitrile and pentanol. A current

versus time curve of ferrocene in a mixture of acetonitrile and pentanol is shown in Figure 5.49 and the corresponding Cottrell plot is shown in Figure 5.50. From the Cottrell plot a slope was found using a linear regression analysis. From the value of slope the diffusion coefficient was calculated as follows:

Slope = 3.4×10^{-6} A.s$^{1/2}$

$A = 0.0176$ cm^2

$C = 7.7 \times 10^{-7}$ mol/cm^3

$F = 96485$ A.s

$n = 1$ mol^{-1}

Slope = $nFAC(D/\pi)^{1/2}$

$$D^{1/2} = \left[3.4\times10^{-6}\ A.s^{1/2} \Big/ \left((1\ mol^{-1})(96485\ A.s)(0.0176\ cm^2)(7.7\times10^{-7}\ mol/cm^3)/\sqrt{\pi}\right)\right]$$

$$D = (4.61\times10^{-3}\ cm.s^{-1/2})^2$$

$$= 2.12\times10^{-5}\ cm^2/s$$

We attempted to determine the number of electrons involved during oxidation of cobalt (peak 1) from a CV of $CoCl_2(PPh_3)_2$. In order to do this a compound was required that had a diffusion coefficient very similar to $CoCl_2(PPh_3)_2$. $CoCl_2$ was chosen as it was found to be one of the products formed during oxidation of $CoCl_2(PPh_3)_2$ and was oxidized at peak 2. Studies involving reduction of cobalt bromides are well documented in the literature and one one-electron reduction peak was found to arise due to reduction of both Co^{II} and a bromide ligand [14]. In order to confirm that indeed oxidation of $CoCl_2$ involved transfer of one electron, we compared the slopes obtained from the Cottrell plots of $CoCl_2$ with that of ferrocene in acetonitrile. First we plotted a Cottrell curve of I vs. $t^{-1/2}$ and obtained the slope which was the best fit value of $it^{1/2}$. From the slope we calculated the value of D of $CoCl_2$ using the Cottrell equation.

A Chronoamperometric plot of $CoCl_2$ obtained applying a potential of 1.3 V is shown in Figure 5.51, with the corresponding CV curve shown as an insert. The corresponding Cottrell plot obtained from data in Figure 5.51 is shown in Figure 5.52.

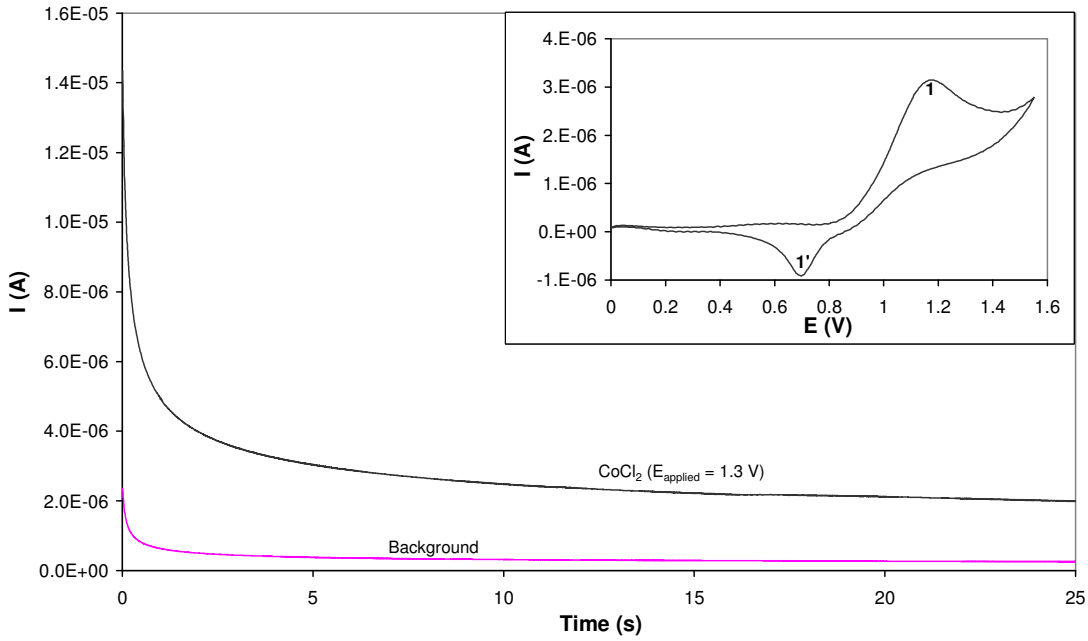

Figure 5.51 Chronoamperometric plot of $CoCl_2$ in acetonitrile. A CV curve of $CoCl_2$ is shown as an insert.

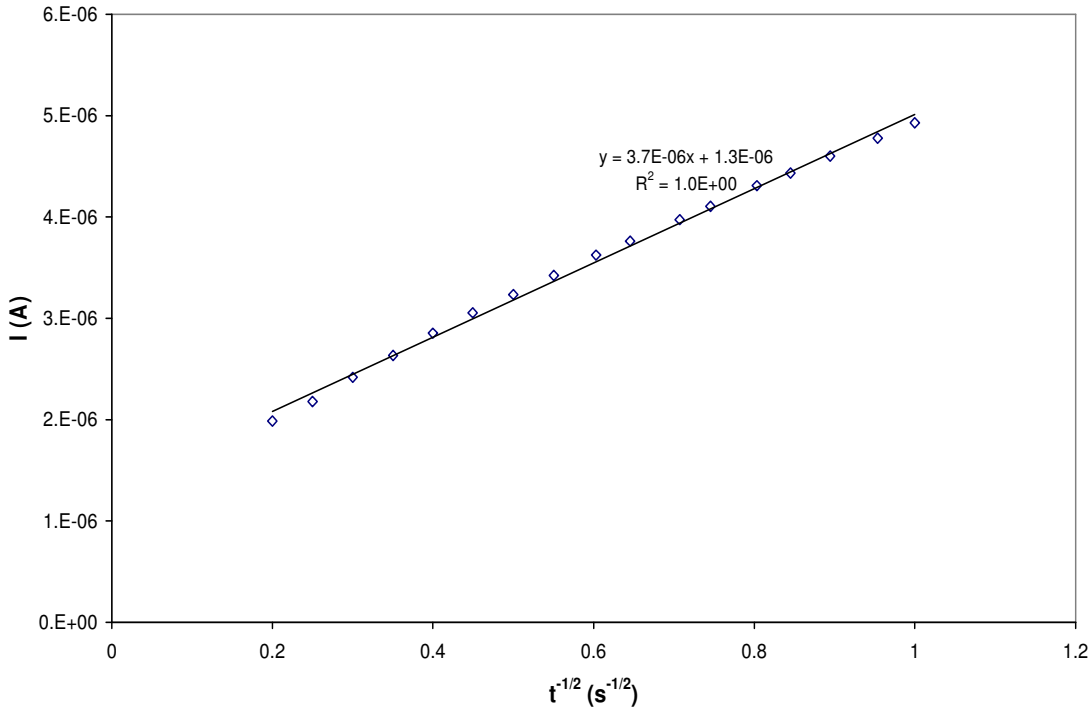

Figure 5.52 Cottrell plot obtained from data in Figure 5.51.

From a value of slope the diffusion coefficient was calculated as follows:

Slope = 3.7×10^{-6} A.s$^{1/2}$

$A = 0.0176$ cm^2

$C = 7.7 \times 10^{-7}$ mol/cm^3

$F = 96485$ A.s

$n = 1$ mol^{-1}

Slope = $nFAC(D/\pi)^{1/2}$

$$D^{1/2} = \left[3.7\times10^{-6}\ A.s^{1/2} \Big/ \left((1\ mol^{-1})(96485\ A.s)(0.0176\ cm^2)(7.7\times10^{-7}\ mol/cm^3)/\sqrt{\pi}\right)\right]$$

$$D = (5.01\times10^{-3}\ cm.s^{-1/2})^2$$

$$= 2.52\times10^{-5}\ cm^2/s$$

After obtaining a diffusion coefficient of $CoCl_2$, we plotted a Cottrell plot $i\pi^{1/2}/FACD^{1/2}$ vs. $t^{-1/2}$ in order to confirm the number of electrons involved during its oxidation (Figure 5.53).

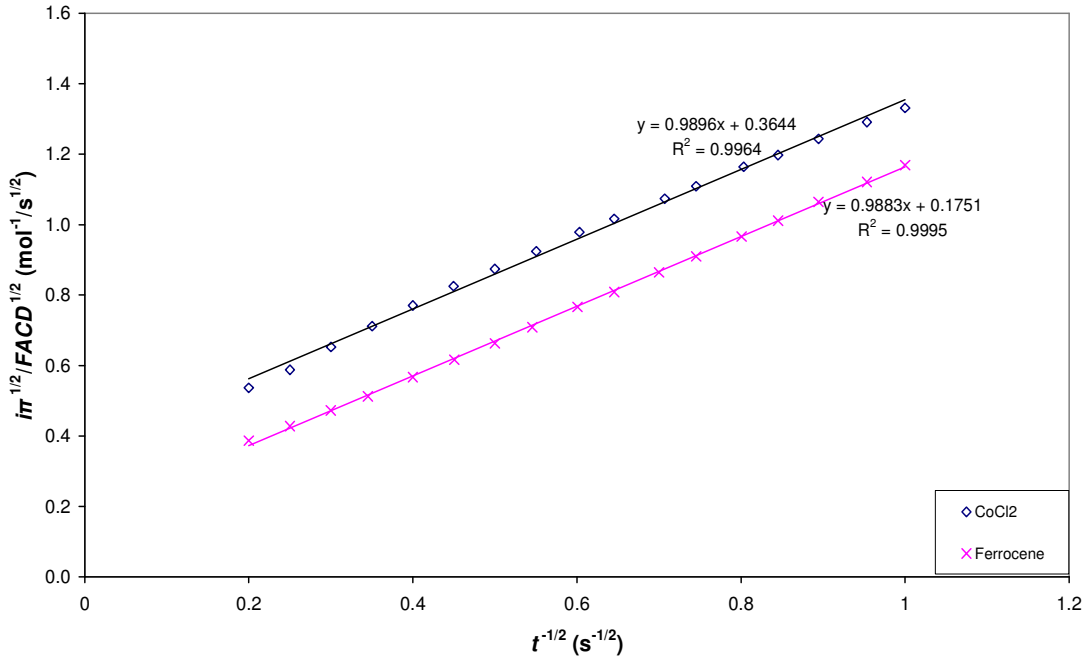

Figure 5.53 Data plotted as $i\pi^{1/2}/FACD^{1/2}$ vs. $t^{-1/2}$ for comparison of slopes obtained from ferrocene and $CoCl_2$ data in acetonitrile, for the determination of number of electrons.

From comparison of the slopes we immediately concluded that one electron was involved during oxidation of $CoCl_2$. The above experiment was repeated for $CoCl_2$ in a mixture of acetonitrile and pentanol. As we have done above we first determined a diffusion coefficient of $CoCl_2$ in a mixture of acetonitrile and pentanol. Figure 5.54 presents a typical current time response of $CoCl_2$ following a potential step from 0.4 to 1.0 V. CV of $CoCl_2$ is also shown as an insert in Figure 5.55. From this data, a Cottrell plot was constructed and the slope was determined using linear regression analysis (Figure 5.55) and was a best fit value of $it^{1/2}$.

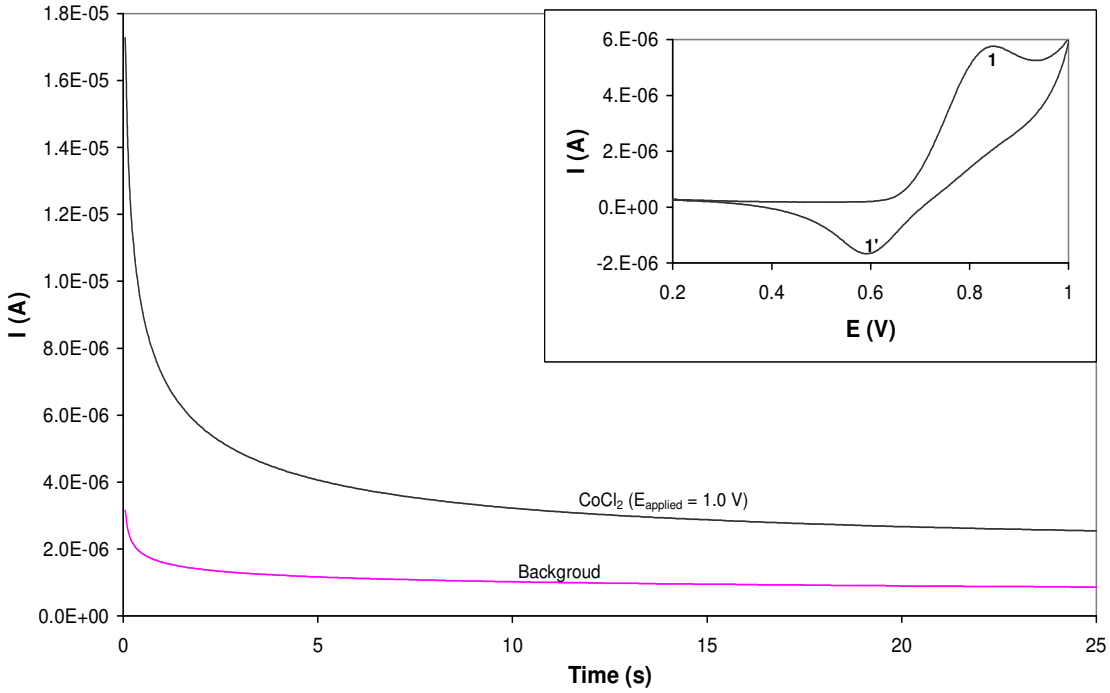

Figure 5.54 Chronoamperometric plot of $CoCl_2$ in a mixture of acetonitrile and pentanol (1:1). A CV curve of $CoCl_2$ is shown as an insert.

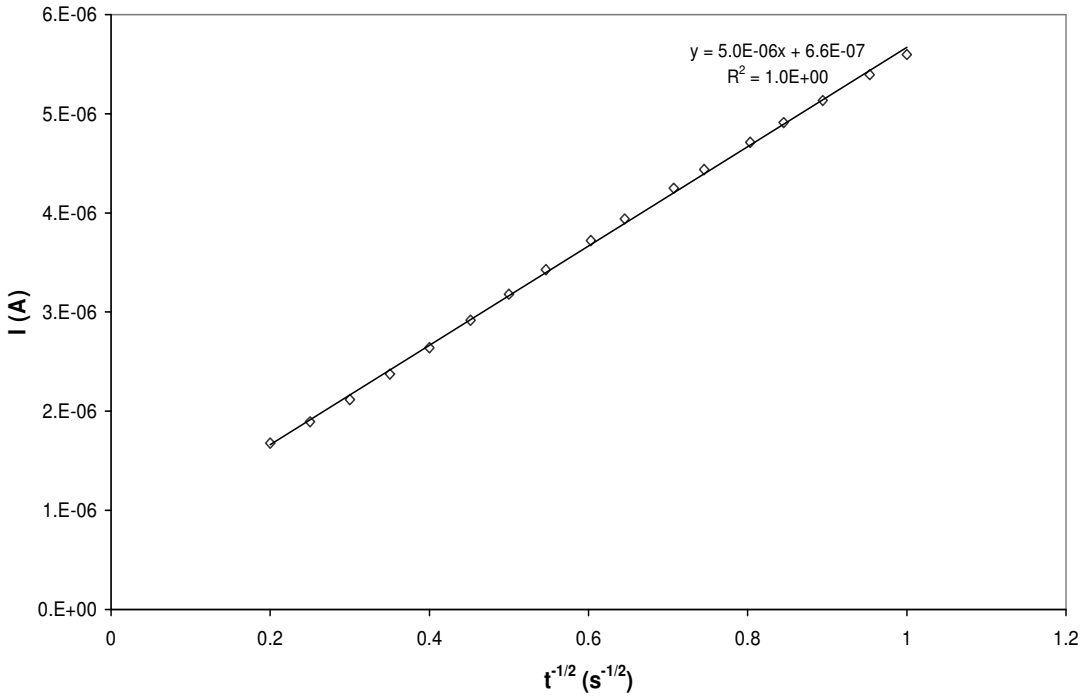

Figure 5.55 Cottrell plot obtained from data in Figure 5.54.

From the value of slope the diffusion coefficient of $CoCl_2$ in a mixture of acetonitrile and pentanol was calculated as follows:

Slope = 5.0×10^{-6} A.s$^{1/2}$

A = 0.0176 cm^2

C = 7.7×10^{-7} mol/cm^3

F = 96485 A.s

n = 1 mol^{-1}

Slope = $nFAC(D/\pi)^{1/2}$

$$D^{1/2} = \left(5.0\times10^{-6}\ A.s^{1/2} \Big/ (1mol^{-1})(96485A.s)(0.0176cm^2)(7.7\times10^{-7}\ mol/cm^3)/\sqrt{\pi} \right)$$

$$= 6.78\times10^{-3}\ cm.s^{-1/2}$$

$$D = (6.78\times10^{-3}\ cm.s^{-1/2})^2$$

$$= 4.59\times10^{-5}\ cm^2/s$$

After obtaining a diffusion coefficient of $CoCl_2$, we plotted a Cottrell plot of $i\pi^{1/2}/FACD^{1/2}$ vs. $t^{-1/2}$ in order to confirm the number of electrons involved during its oxidation (Figure 5.56).

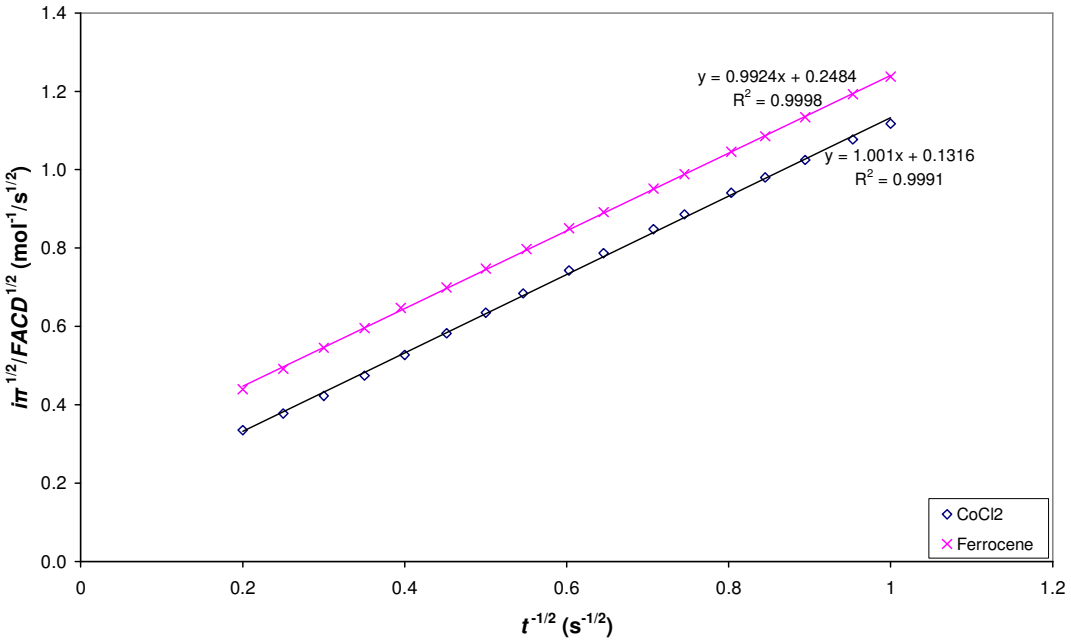

Figure 5.56 Data plotted as $i\pi^{1/2}/FACD^{1/2}$ vs. $t^{-1/2}$ for comparison of slopes obtained from ferrocene and $CoCl_2$ data in a mixture of acetonitrile and pentanol, for the determination of number of electrons.

From comparison of the slopes we immediately concluded that one electron was involved during oxidation of $CoCl_2$. But the slopes obtained from $CoCl_2$ in a mixture of acetonitrile and pentanol deviated a little from one when comparing it with that obtained in acetonitrile. This might have occurred due to involvement of an oxidation peak 2 for the catalytic reaction of chloride with water which complicates the electrode reaction; we applied a potential of 1.0 V and at this potential an increase in current was already observed as the catalytic reaction already starts at this potential. For best results one will have to apply a potential of ~ 0.9 V. The suggested overall electrochemical reaction is as follows:

$$CoCl_2 \leftrightarrow [CoCl]^{2+} + Cl^- + e^- \quad [79] \qquad (5.4)$$

In order to determine the number of electrons involved during oxidation of Co^{II} from $CoCl_2(PPh_3)_2$ we assumed that this complex had the same diffusion coefficient as $CoCl_2$. The number of electrons was determined from comparison of the slopes obtained from the Cottrell plot of $CoCl_2$ with that of $CoCl_2(PPh_3)_2$ in a mixture of acetonitrile and pentanol. A Chronoamperometric plot of $CoCl_2(PPh_3)_2$ is shown in Figure 5.57. In this experiment (refer to Figure 5.57), a potential was stepped abruptly from 0.2 V, where $CoCl_2(PPh_3)_2$ is

electroinactive, to 1.1 V a potential where both $CoCl_2(PPh_3)_2$ and $CoCl_2$ are oxidized concurrently. CV curve of $CoCl_2(PPh_3)_2$ is shown as an insert in Figure 5.57.

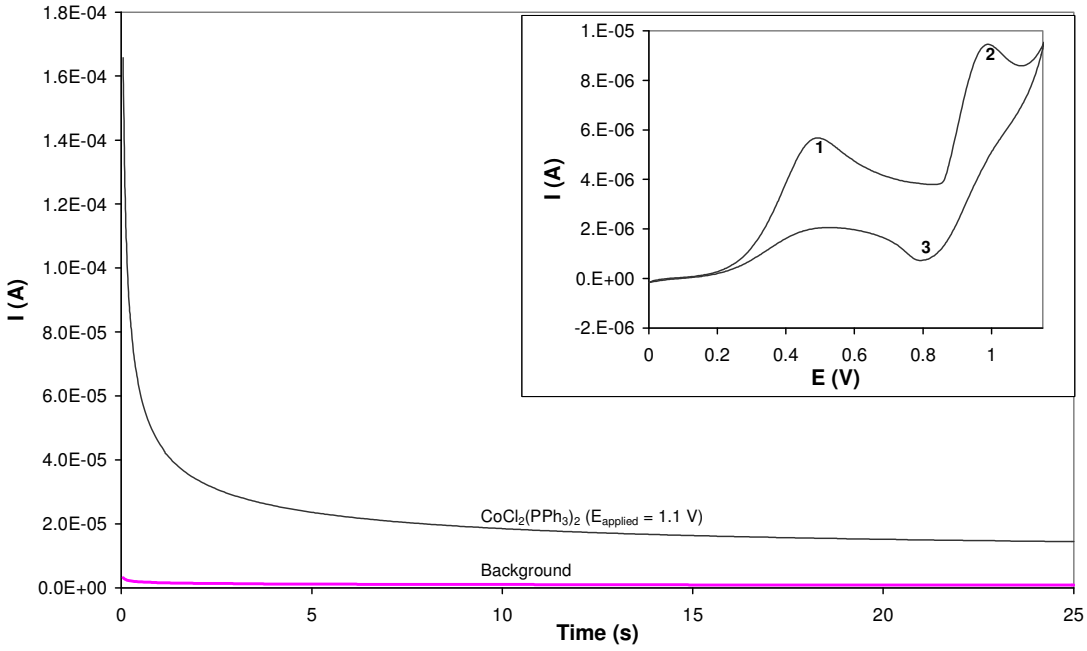

Figure 5.57 Chronoamperometric plot of $CoCl_2(PPh_3)_2$ in a mixture of acetonitrile and pentanol (1:1). A CV curve of $CoCl_2(PPh_3)_2$ is shown as an insert.

A Cottrell plot of $i\pi^{1/2}/FACD^{1/2}$ vs. $t^{-1/2}$ was constructed for the determination of number of electrons involved during oxidation of Co^{II} from $CoCl_2(PPh_3)_2$ (Figure 5.58). From Figure 5.58 we concluded that since a one-electron process from $CoCl_2$ gave a slope of 1.001 mol^{-1}, the corresponding slope of 2.0196 mol^{-1} for the oxidation of $CoCl_2(PPh_3)_2$ must represent an overall two-electron process. When we subtract the one electron that is required to oxidize $CoCl_2$ from this total, we immediately conclude that one electron is required to oxidize Co^{II} to Co^{III} in $CoCl_2(PPh_3)_2$ complex. A little deviation of slopes from one might be due to involvement of some catalytic or chemical reactions of the species oxidized after peak 2 (i.e. a catalytic reaction of chloride with water observed at peak 3 from the CV of the complex, Figure 5.10).

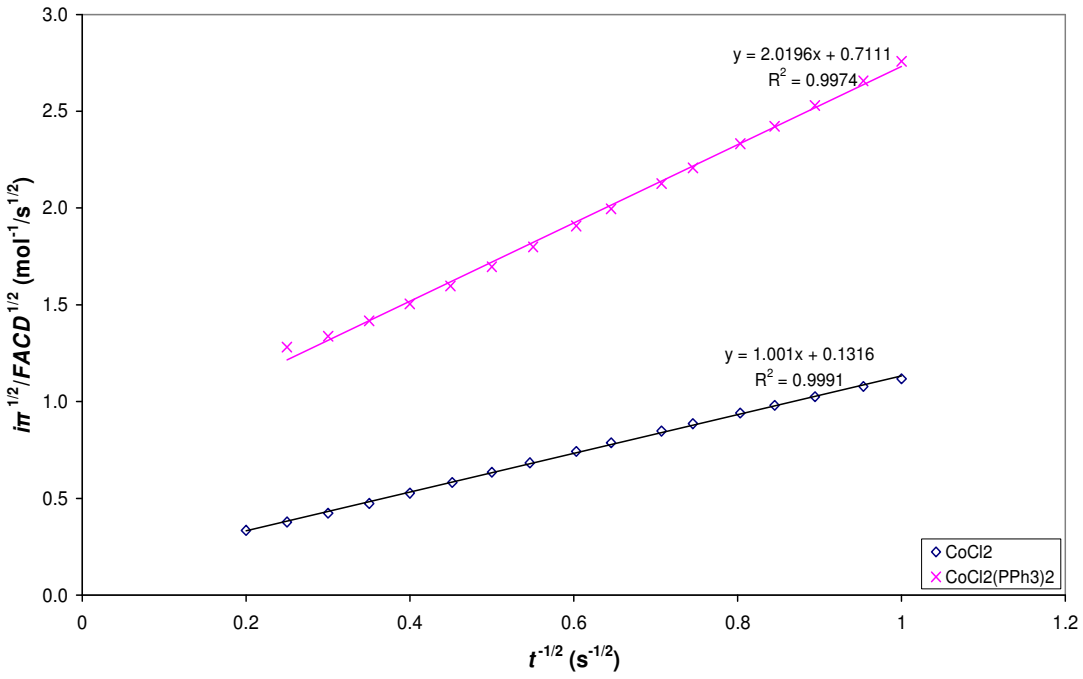

Figure 5.58 Cottrell plot of the data shown in Figure 5.57. The Cottrell plot for $CoCl_2$ is also shown for comparison.

The suggested overall electrochemical reactions are as follows:

Oxidation peak 1: $Co^{II}Cl_2(PPh_3)_2 \rightarrow [Co^{III}Cl_2(PPh_3)_2]^+ + e^-$ [this work] (5.5)

Oxidation peak 2: $CoCl_2 \leftrightarrow [CoCl]^{2+} + Cl^- + e^-$ [79] (5.6)

5.4 QUANTITATIVE ANALYSIS

In this section we will present the voltammograms obtained in solutions containing different concentrations of $CoCl_2(PPh_3)_2$ in a mixture of acetonitrile and pentanol, after IR drop correction (Figure 5.59) and the corresponding calibration plot was also constructed for quantitative analysis (Figure 5.60).

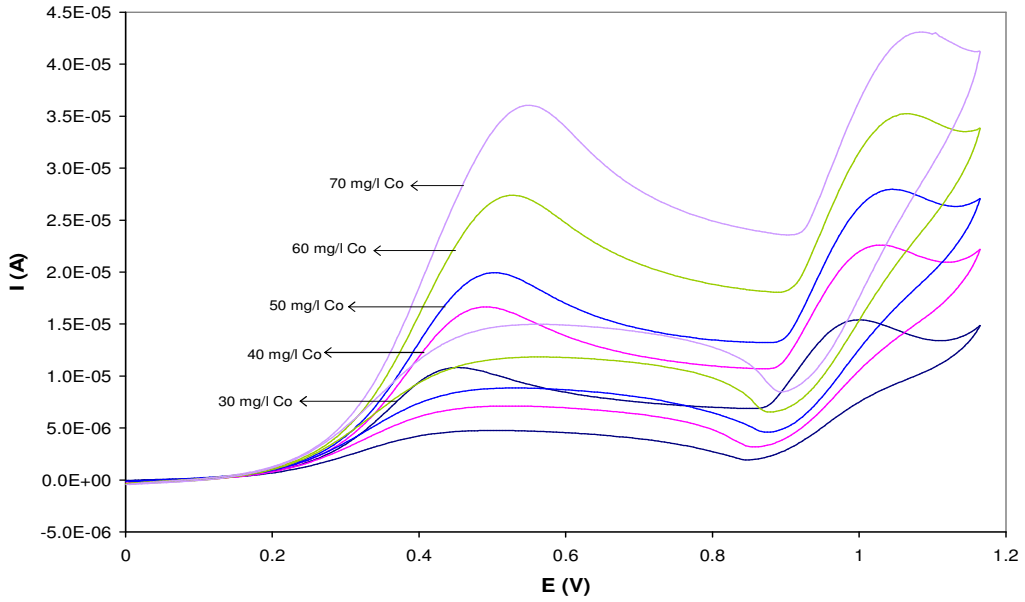

Figure 5.59 CV curves obtained in solutions containing different concentrations of Co from $CoCl_2(PPh_3)_2$.

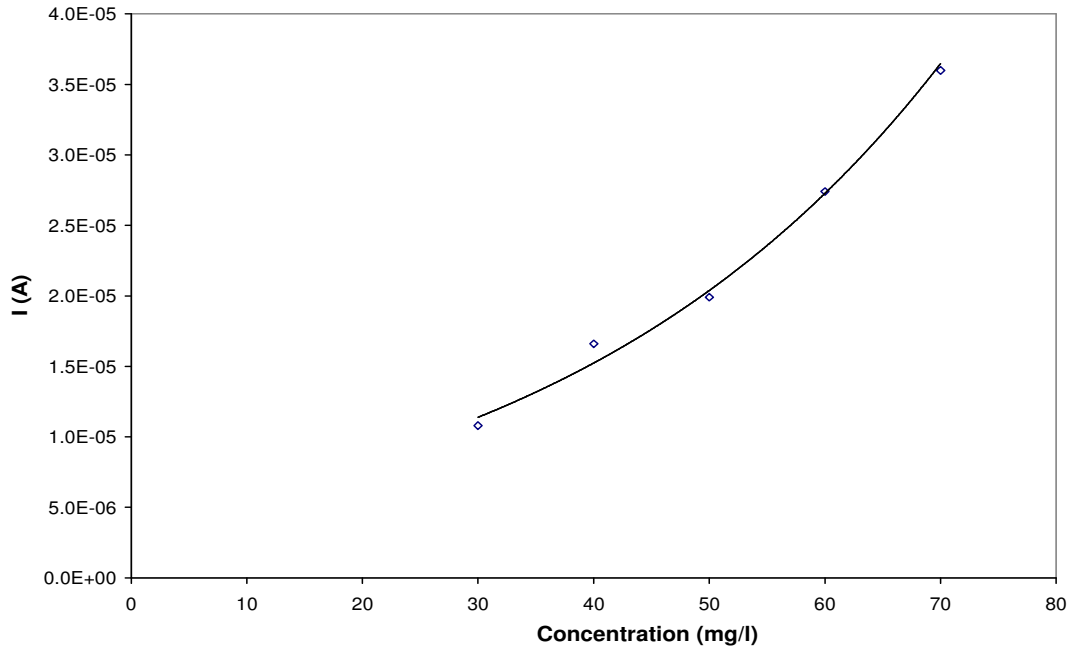

Figure 5.60 Calibration plot obtained using the oxidation peak at ~ 0.5 V shown in Figure 5.59.

The peak height increases with an increase in concentration, giving a non-linear relationship between current and concentration. The non-linearity might be due to the presence of complicated chemical reactions, occurring during oxidation of chloride occurring at E_p ~

0.95 V. For better quantitative analysis, we measured the voltammograms of $CoCl_2(PPh_3)_2$ scanning up to 0.9 V, to exclude the chloride oxidation peak observed at more positive potentials.

Figure 5.61 shows cyclic voltammograms of $CoCl_2(PPh_3)_2$ for the anodic peak obtained at ~ 0.50 V for various concentrations, when scanning to potential of 0.9 V, and the corresponding calibration plot is shown in Figure 5.62. The peak height increases with increase in concentration, giving a linear relationship between current and concentration. This proves that the non-linearity observed in Figure 5.60 was due to the presence of chloride oxidized at more positive potentials which complicated an electrode process occurring at E_p ~ 0.50 V.

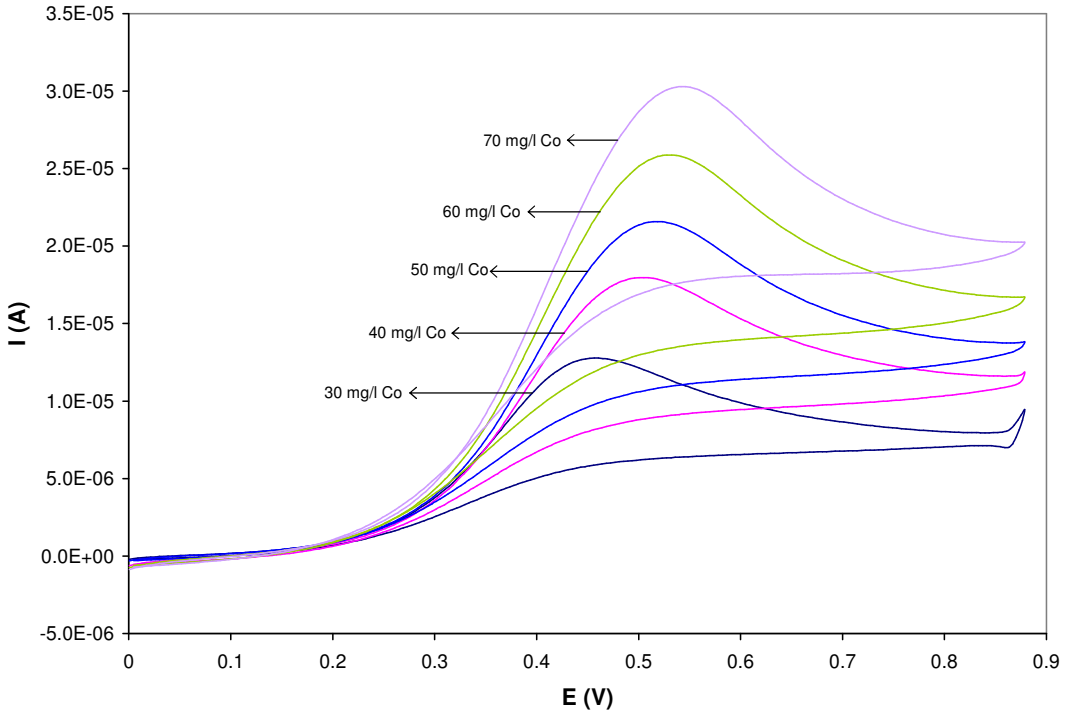

Figure 5.61 CV curves obtained in solutions containing different concentrations of Co from $CoCl_2(PPh_3)_2$ at a short potential range excluding the chloride oxidation peak.

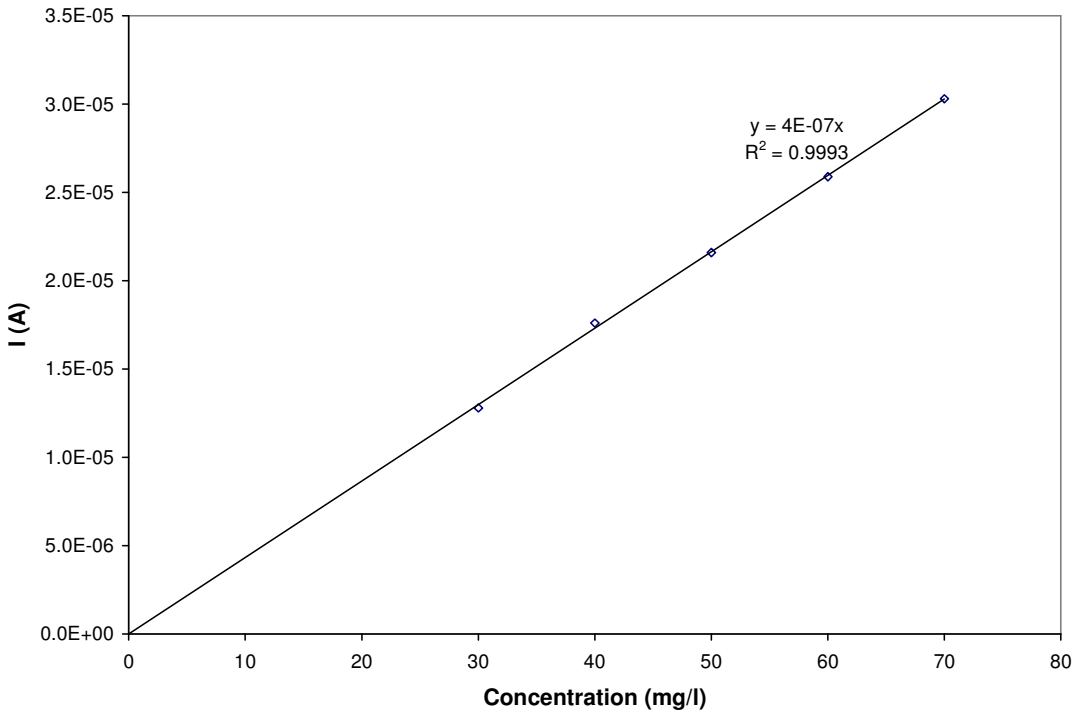

Figure 5.62 Calibration plot of the data shown in Figure 5.61.

In conclusion, chloride modifies the electrode surface resulting in a change in the chemistry of the compound which is evident from an exponential calibration plot observed for the metal oxidation peak when the CV was scanned to a potential after oxidation of chloride.